

**SEMMELWEIS EGYETEM**  
**DOKTORI ISKOLA**

**Ph.D. értekezések**

**3169.**

**GÓG ISTVÁN**

**Klinikai és kísérletes angiológiai kutatások**  
című program

Programvezető: Dr. Sótonyi Péter, egyetemi tanár

Témavezető: Dr. Sótonyi Péter, egyetemi tanár

# NOVEL CLINICAL INDICATIONS FOR DIGITAL VARIANCE ANGIOGRAPHY (DVA) AND THE CLINICAL USABILITY OF COLOR-CODED DVA

PhD thesis

**István Góg**

Doctoral College of Semmelweis University

Cardiovascular Medicine and Research Division



Supervisor: Péter Sótónyi, MD, D.Sc

Official reviewers: Arnold Tóth, MD, Ph.D  
Miklós Vértes MD, Ph.D

Members of the Complex Examination Committee: György Wéber, MD, D.Sc  
Pál Ákos Deák, MD, Ph.D  
Rudolf Ménesi, MD, Ph.D

**Budapest**

**2025**

## TABLE OF CONTENTS

I. List of abbreviations.....	3
II. Introduction.....	5
II/1. History of vascular imaging and intervention .....	5
II/2. Digital Variance Angiography (DVA) .....	5
II/3. Parametric angiography .....	9
III. Objectives .....	15
IV. Materials and methods .....	17
IV/1. TACE study materials .....	17
IV/2. PAE study materials .....	17
IV/3. Contrast-to-Noise Ratio (CNR).....	19
IV/4. Visual surveys .....	19
IV/5. CcDVA study .....	21
IV/6. Summary of applied statistical tests .....	23
V. Results .....	25
V/1. TACE study .....	25
V/2. PAE study .....	29
V/3. CcDVA study .....	33
VI. Discussion .....	36
VI/1. TACE study.....	36
VI/2. PAE study.....	38
VI/3. CcDVA study .....	39
VII. Conclusions.....	41
VIII. Summary.....	42
IX. References .....	43
X. Bibliography of the candidate's publications .....	52
XI. Funding statement .....	54
XII. Acknowledgements.....	55

## **I. LIST OF ABBREVIATIONS**

2D-PA – Two-dimensional parametric angiography.

AUC – Area under the curve.

BMI – Body mass index.

CARE - Combined applications to reduce exposure.

ccDVA – Color-coded digital variance angiography.

CLI – Critical limb-threatening ischaemia.

CNR – Contrast-to-noise ratio.

CT – Computed tomography.

DSA – Digital subtraction angiography.

DVA – Digital variance angiography.

FPS – Frames per second.

GFR – Glomerular filtration rate.

IQR – Interquartile range.

IVUS – Intravascular ultrasound.

KMIT – Kinect Medical Imaging Tool.

MRI – Magnetic resonance imaging.

NEQ – Noise equivalent quanta.

PA – Peak attenuation.

PAD – Peripheral artery disease.

PAE – Prostatic artery embolization.

POBA – Plain old balloon angioplasty.

PTA – Percutaneous transluminal angioplasty.

ROI – Region of interest.

SD – Standard deviation.

SEM – Standard error of mean.

SNR – Signal-to-noise ratio.

TACE – Transarterial chemoembolization.

TIC – Time-intensity curve.

TTP – Time-to-peak.

TURP – Transurethral resection of the prostate.

## **II. INTRODUCTION**

### **II/1. History of vascular imaging and intervention**

The origins of vascular imaging can be dated to the 1920s [1], Hascheks and Lindenthals's idea of intravasal contrast agent administration lead to the development of several clinical applications [2]. In 1953, Seldinger described his technique of transfemoral arterial access for selective catheterisation, which revolutionised many medical disciplines and established the field of interventional radiology [3]. In the 1970s, Dotter introduced percutaneous transluminal angioplasty (PTA), which laid the foundation for minimally invasive vascular therapies [4]. With the introduction and development of real-time ultrasound, computed tomography (CT), and magnetic resonance imaging (MRI), the diagnosis of vascular diseases has become primarily non-invasive [5]. However, during vascular interventions, invasive angiography remained the primary form of intraprocedural imaging.

### **Digital subtraction angiography**

The gold standard algorithm in the last 40 years was digital subtraction angiography (DSA), which was described in 1935 but was not commercially available until the 1980s, when digital flat panel detectors and faster computers made DSA a practical clinical tool. Several advancements have been made regarding image quality, dose management, and computational time, but the basics of the method remained the same, which is the subtraction of a mask image from the post-injection image series. This subtracted sequence can be further processed into a stacked opacification image, which can be used as a roadmap during vascular intervention. The mask image can also be post-processed to eliminate noise originating from patient movement [6].

### **II/2. Digital Variance Angiography (DVA)**

DVA is a novel method developed by Szigeti and Osváth [7] that claimed to be able to produce an angiographic image very similar to DSA. The technology was originally named "kinetic imaging," and it is based on the calculation of mean, standard error of mean (SEM), standard deviation, and standard error of standard deviation from image sequences acquired through some type of penetrating radiation, which is most commonly X-ray radiation in medical and non-medical fields also.

The four types of images were intended to serve different purposes according to the original paper describing the patented method. The “mean image” is almost identical to the summation image, which is used, e.g. during routine medical X-ray examinations of the chest. The advantage of this method is that the inevitable quantum noise is minimised; therefore, it serves as a basic noise cancellation method. The two “standard error” type images were supposed to be used for optimising image acquisition parameters, but no further research has been conducted to provide evidence for these claims.

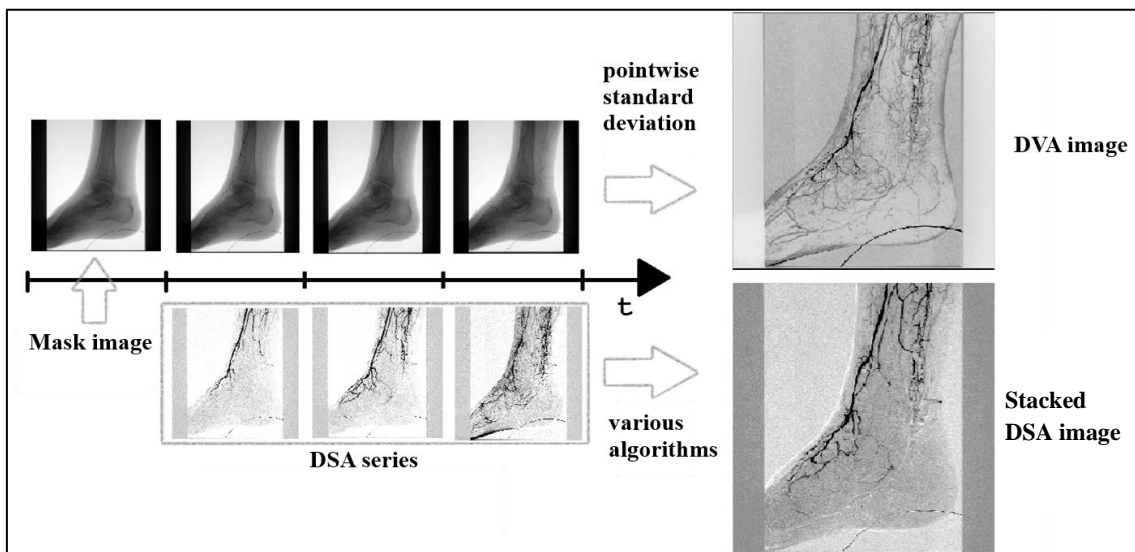


**Figure 1. The algorithms for DSA series, stacked DSA image and DVA image calculations. Both image types are calculated from the same series and both processes end in similar still-images. (Source: own work.)**

The last type, “standard deviation image,” is what the DVA technology was based on. By calculating the pointwise standard deviation of the image sequence, the most intensely changing regions can be made more visible, whereas the most stable regions or objects can create the least intensity. In the case of imaging moving objects, the moving parts appear brightest, and the background intensity remains close to zero. The calculation method of DVA and DSA images is presented in Figure 1.

Kinetic imaging has been tested for non-medical purposes [7], such as border control, device testing, and pest control, but the usability of this method in industrial practice remains questionable as it has not been studied further. However, the use of kinetic imaging for creating angiographies has been more researched, from the level of in silico studies to prospective clinical studies.

### **In silico studies**

Although no peer-reviewed publications mention these preliminary investigations, we must mention them to introduce the idea of dose management through DVA. Pre-clinical studies provided the idea of visualising moving objects inside living creatures, such as the beating heart of a frog [7]. Since the “standard deviation image” was known to be sensitive to motion, it was hypothesised that the motion of the contrast agent inside the vessel might be visualised more effectively with kinetic imaging. To prove this, a simple model was created that included a pixel with two possible states: the “contrast agent” and “no-contrast” states [8]. It was assumed that the more stationary the motion (flow) of the contrast agent inside the vessel, the less image contrast would appear on the “standard deviation image,” and inversely, the less stationary the flow, the higher the image contrast it generates on the “kinetic image”, which we call digital variance angiography (DVA). Background noise and image contrast were calculated for hypothetical DVA and DSA images, and then the signal-to-noise ratio (SNR) was calculated as a simple measure of the image quality. The SNR is not the only parameter contributing to the image quality, but it has a strong connection with the radiation and contrast agent dose. Since the model indicated that DVA may have a significant advantage over DSA in terms of SNR, it was assumed that DVA may have the potential to provide the clinical standard image quality but at a lower radiation or contrast agent dosage.

### **Retrospective studies**

In 2018, the results of a retrospective study published by Gyánó et al. showed that the SNR benefit of DVA is also observable in a clinical setting [9]. The study involved 42 patients, and the methods included visual comparison in addition to SNR measurement. The compared images were standard DVA images and “postprocessed DSA” images, which is analogous to “stacked DSA image”. The images were generated from the same X-ray image sequence so that they could be paired for comparison. The SNR measurements revealed a 2.1 to 2.4 times advantage in favour of DVA SNR, with a slightly higher SNR ratio in the femoral region (2.4 median value) and a slightly lower SNR advantage in the abdominal region (2.1). The outcome of the visual questionnaire revealed a visual preference for the DVA, which was more prominent in the femoral and popliteal regions. In conclusion, our results indicated a quality reserve that could be utilised for dose management [9].

In the following years, other retrospective studies aimed at comparing DSA and DVA resulted in similar results (by using similar study designs and methods) and similar conclusions. In 2019, Óriás et al. presented the benefits of using DVA during carbon-dioxide angiography [10]. Since in this type of imaging, the number of captured images is several times higher than during a normal DSA procedure, and the motion of contrast agent “bubbles” cannot be captured on a single frame, the effectiveness of image combination is of key importance. In this study, the advantage of DVA was more pronounced regarding SNR ratios (DVA vs. DSA SNR 3.5 to 4.5 higher) and visual comparison (DVA was chosen as better in 78 to 90% of cases) [10]. In 2021, Bastian et al. investigated the use of DVA in patients with metal implants and concluded that the 1,84 times higher medial SNR values and 84.5% visual preference (83% agreement) over DSA verified the superiority of DVA in this indication [11]. It is important to mention the work of Rohit et al, 2021, which was a publication of a retrospective study that involved 28 patients [12]. In the two-cohort investigation, one group received iodinated contrast media, and the other (nephropathy group) received carbon dioxide. SNR measurements and visual comparisons were carried out, and the results were very similar to previous outcomes: an at least 2-fold increase in SNR and significantly higher visual evaluation scores favouring DVA [12].

### **Prospective studies**

To provide evidence of dose management capabilities, Óriás et al. studied the effects of 50% contrast media dose reduction while using DVA [13]. 26 patients were enrolled who underwent carotid percutaneous transluminal angioplasty. Half of the patients who underwent intervention received the mandatory angiography at the end of the procedure with 50% reduced contrast agent volume and normal flow. SNR measurements revealed a significant advantage over standard-dose DSA versus both normal- and reduced-dose DVA, and an almost two-fold increase in SNR was measured. Regarding visual comparison (which was done by using a 5-grade Likert scale visual quality questionnaire), normal-dose DVA was superior to normal-dose DSA, and low-dose DVA was able to provide the same visual quality as standard DSA, which agreed with previous results [13].

The radiation dose-reducing potential of DVA was also studied in 2021 by Gyánó et al. in a prospective study involving 30 patients who underwent lower-limb invasive angiography using a standard protocol [14]. By signing informed consent, a 68% reduced-dose angiography was also performed in three regions, and images were further processed into DSA and DVA images for SNR measurement and visual comparison. The SNR measurements resulted in similar results as the previously mentioned carotid study; the low-dose DVA group provided a two-fold higher SNR than the standard-dose DSA. The visual comparison validated the non-inferiority of reduced-dose DVA images to standard-dose DSA images [14].

The research group continued to investigate the same issue by performing a randomised controlled trial that enrolled 57 patients who underwent standard-dose angiography (control group) and 57 patients underwent invasive angiography with a 70% reduced radiation dose [15]. In this study, the comparison was based only on visual evaluation. Two vascular surgeons and four interventional radiologists conducted a blind evaluation of the images, and the images were evaluated using a 5-grade rating scale ranging from poor (“1”) to outstanding (“5”) image quality. The key findings of the study were that the DSA-related radiation dose reduction was 61%, low-dose DVA provided at least similar or better image quality than standard-dose DSA, and it was also revealed that a novel DVA algorithm (DVA2) is even more capable of producing higher quality angiograms, an advantage that is more prominent in the crural region [15].

The presented works validated the ability of DVA to enable dose reduction in lower-limb and carotid regions, but its usability in other regions remained in question. The other studies mentioned in the following sections of this thesis aimed to investigate other indications of DVA technology.

### **II/3. Parametric angiography**

Another question regarding imaging technologies is: what else can be calculated from the image sequences besides morphological information? It is well known that DSA provides a two-dimensional image, which often gives inadequate information on vascular lesions, especially in cases of complex geometries [16]. If functional data could be acquired from an already recorded image sequence, decision-making would be much easier in difficult instances, resulting in safer and more effective work in the catheter lab. The evolution of

computers has paved the way for complex calculations to be performed at an almost real-time speed, making modern technologies usable in the catheter lab or in the operating room.

### **General concept**

Technologies utilising such calculations are based on the same concept: converting conventional greyscale DSA images into color-coded representations to provide a more comprehensive and intuitive understanding of vascular dynamics. The colours code different parameters of the time-intensity curve (TIC), which can be (but not exclusively) acquired through the selection of regions of interest (ROIs). This process is called quantitative analysis, in which several parameters are calculated.

The most important is Time to Peak (TTP), which is basically the time (in seconds) for the contrast intensity to reach its maximum value measured at a specified point (ROI). Color-coding of this parameter allows the visualization of hemodynamic conditions in a single still image. The principles of the calculation of ccDVA are shown in Figure 2.

Some additional parameters are also calculated; however, their interpretation is less straightforward, and they can be useful only in specific settings (e.g. when the overall blood supply of an area, rather than a single vessel's blood flow is evaluated). These are:

- Peak value, peak attenuation (PA) or peak ratio: intensity value or the ratio of the maximum intensity value of a specified ROI to a reference ROI,
- Area Under the Curve (AUC) or AUC ratio (AUCr): area under the time-intensity curve or ratio of the AUC of an ROI to the reference.

The reference ROI is typically selected in a region without pathology. The software can also visualise these parameters as a colour-coded map, allowing for instant presentation of blood flow patterns without requiring ROI selection. In the case of TTP, specific colours are assigned to different TTP values ranging from red (early maximum intensity) to blue (late maximum intensity).

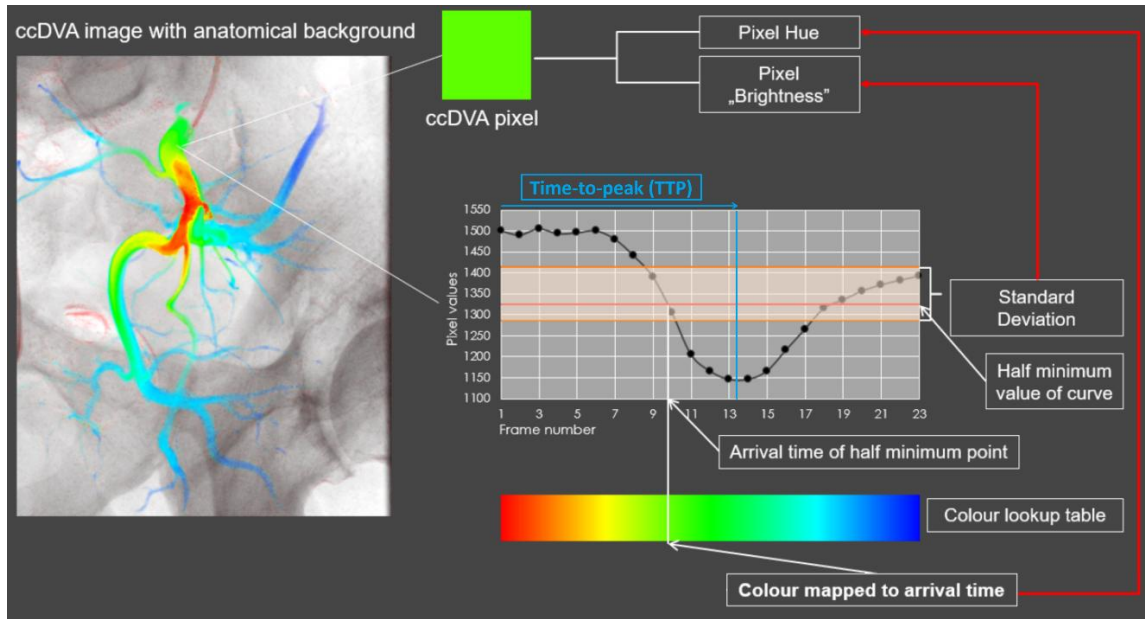


**Figure 2. Generation of ccDVA image. Parameters are calculated from the time-intensity curve, similarly to ccDSA, but the pixel brightness is defined by the standard deviation of the given pixel values, instead of the pixel intensity. (Source: own work.)**

### Available technologies

All major manufacturers developed its own color-coded imaging technology. The literature mostly mentions the Siemens iFlow product [17–22], followed by Philips's Smart Perfusion or 2D perfusion technology [23–27]. “Color Coded Circulation” technology from Canon and General Electric’s “Angioviz” must also be mentioned; however, the available data regarding these methods are very limited [28–30]. Some publications have reported manufacturer-independent solutions that are fundamentally similar to the previously mentioned techniques [31,32]. Recently a new color-coded technology has also been developed, which is, in contrast to the previously mentioned DSA-based methods, entirely based on DVA, and thereby brings the advantages of DVA technology in the parametric imaging field. These technologies are summarized in Table 1.

**Table 1. Comparison of available color-coded angiography technologies. (Source: own work.)**

Name of technology	Manufacturer	Basis of technology	Disadvantages	Platform dependency	Published clinical applications	Current status
“iFlow”	Siemens Healthineers	DSA	higher framerate and radiation dose required	Only available as part of the manufacturer's angiographic suite	peripheral interventions [33] neurointerventions [33] aortic dissection[34]	available
“2D-Perfurison Angiography (2D-PA)” or “Smart Perfusion	Philips Medical Systems				neurointerventions [35] peripheral interventions[27]	not available[36]
“Angioviz”	General Electric HealthCare				neurointerventions[37]	available
“Color Coded Circulation”	Canon Medical Systems				peripheral interventions[29,38]	available
“Color-coded DVA” (ccDVA)	Kinepict Health Ltd.	DVA		independent	prostatic artery embolization [39]	available

### **Siemens Syngo iFlow**

Syngo iFlow has demonstrated potential in various medical fields. In peripheral artery disease (PAD), this technology has shown promise in assessing the technical success of post-endovascular procedures and prognosticating clinical outcomes [20,22]. In aortic diseases, it has shown promise in evaluating renal artery haemodynamics in endovascular aortic repair [34]. The most studied indication of iFlow is neuroendovascular intervention, where the software has been used to analyse fluid dynamics in various pathologies and procedures [40–42]. It has also been reported that Syngo iFlow has practical value in evaluating treatment success in tumour embolisation [43,44].

### **Philips Smart Perfusion (also known as 2D Perfusion Angiography, 2D-PA)**

As with other technologies, the 2D-PA software also analyses the time-density curves generated during the first pass of the contrast agent through the tissue of interest, then produces colour-coded maps and calculates several key parameters, including TTP and AUC.

2D-PA appeared to show promise for interventions targeting the lower limbs, given the apparent improvements in perfusion curves following successful endovascular interventions among patients with critical limb ischaemia (CLI) [25,27,45]. For instance, a study involving five bypass surgery patients indicated that 2D-PA managed to provide detailed information that could not be achieved through conventional angiography, thus leading to re-anastomosis due to unexpected findings [46]. Philips Smart Perfusion was an advanced form of 2D-PA technology within the Philips suite of angiographic systems that allowed better visualisation with advanced analytical tools to assess tissue perfusion. Although the modality promised real-time feedback during procedures and claimed to be a potentially effective decision-aid tool, it was recalled in 2023, due to “technical issues related to signal generation and processing, which could lead to inaccurate presentations [36].”

### **Clinical experience with color-coded parametric imaging**

Color-coded parametric imaging was tested in several clinical studies in the last 15 years [20,45,47–55]. Certain ccDSA parameters showed strong correlation with the clinical outcome in stroke treatment [48,50], and helped the evaluation of carotid cavernous fistulas better than grey-scale DSA videos [49]. In comparison with DSA videos, color-

coded images significantly improved diagnosis and treatment planning in cerebrovascular disorders, and the positive effect was greater for less experienced readers [47]. Parametric imaging proved to be useful in other endovascular procedures as well, including lower limb inter-ventions [20,51], intraprocedural evaluation of type B aorta dissections in thoracic endo-vascular aortic repair [52], identification of bleeding points [53], intraprocedural evaluation of genicular embolization [54], spleen embolization [55], evaluation of hemodynamic changes during the endovascular treatment of brain arteriovenous malformations [56] and prediction of brain aneurysm occlusion after embolization [57,58].

### **General concerns and limitations**

In addition to its indisputable advantages, color-coded angiography has several limitations, which contributes to the fact that it did not become an every-day tool in the catheter labs. The most important one is that the accuracy of parametric angiography depends on the time resolution, which can be improved by increasing the number of images acquired over time (frames per second, FPS), but this also substantially increases the radiation dose. Since the color-coded technologies require at least 4 FPS, while conventional angiography can be performed with 1-2 FPS, parametric imaging can increase radiation dose by at least 2 to 4 times compared to regular burden [59]. It seems to be a great challenge to find the optimal FPS with assessable image quality, which gave the idea of combining image quality enhancement technology, such as the introduced DVA, with parametric imaging. As DVA was proven to effectively lower radiation dose, we hypothesised that it could solve this major limitation of parametric angiography. Another crucial drawback is the lack of standardisation. Protocols and interpretation guidelines must be established across different clinical scenarios, which requires appropriately designed large-scale clinical trials. It should also be mentioned that color-coded methods require specialised software and training, which can increase the cost of therapy. According to some reports, interpretation may also vary between observers, and patient movement may significantly affect image quality and analysis accuracy due to motion artefacts [22,25,45].

### **III. OBJECTIVES**

From the questions expressed in the introduction regarding the future of DVA technology, the following research objectives were set:

1. The advantages of DVA were proved in lower limb interventions. **Can DVA be used in other therapeutic indications?**

The aim is to assess the potential advantages of DVA in TACE and PAE procedures.

2. **What are the qualitative advantages of color-coded DVA in other therapeutic indications?**

The aim is to evaluate the potential benefits of ccDVA in PAE.

3. **Is the DVA-based color-coded imaging is a reliable tool for the measurement of time-related parameters?**

The aim is to compare the calculated parameters of ccDVA with Syngo iFlow, a commercially available parametric angiographic method.

Three different smaller-scale retrospective proof-of-concept studies were conducted to complete these objectives. The first referenced paper is “Possible Use of Digital Variance Angiography in Liver Transarterial Chemoembolisation: A Retrospective Observational Study” by Lucatelli et al. The objective of this investigation was to determine whether the previously described improvement in image quality could also be observed during liver transarterial chemoembolisation (TACE). We will call this study the “TACE study” in the upcoming parts [60].

The second, which is presented in the publication called “Initial Experience Using Digital Variance Angiography in Context of Prostatic Artery Embolisation in Comparison with Digital Subtraction Angiography,” written by Alizadeh et al., aimed to examine whether DVA possesses a comparable quality reserve in prostatic artery embolisation (PAE) and to investigate the possible benefits of color-coded DVA (ccDVA) technology in PAE. We refer to this study as the “PAE study” in the following sections [39].

The third study was “Quantitative Comparison of Color-Coded Parametric Imaging Technologies Based on Digital Subtraction and Digital Variance Angiography: A Retrospective Observational Study” by Góg et al. [61]. The purpose of this analysis was

to compare color-coded DVA with the most common commercially available parametric angiographic method, Syngo iFlow (Siemens Healthineers). We cite this study as the “CcDVA study” in the following chapters. As DSA and DVA methods rely on different algorithms, the assumption was not evident that they produce the same time-related parameters.

## **IV. MATERIALS AND METHODS**

### **IV/1. TACE study materials**

Twenty-five patients with hepatocarcinoma underwent transarterial chemoembolization (TACE) in 2021 at the University Hospital “Policlinico Umberto I” (Rome, Italy). Pre-embolisation angiographies were retrospectively acquired, and DSA and DVA images were generated with separate workstations. The image acquisition was performed on an Artis Zee system, and peak opacification (“stacked”) DSA images were generated on a Syngo XWP VB21N workstation. DVA images were created using KMIT version 5.0. Radial or femoral access was used for the catheterisation of hepatic arteries. Additionally, to find the best site for embolisation, cone-beam CT was also performed. Embolisation was performed using microspheres (LifePearl – Terumo, Japan or DC beads M1 – Boston Scientific, USA).

All procedures were in accordance with the ethical standards of the institutional and/or national research committee and with the 1964 Helsinki declaration and its later amendments. For this type of study informed consent was not required. Because of the retrospective nature of the study, informed consent was not necessary. All indications for treatment were decided in a multidisciplinary tumor board (composed of a surgeon, oncologist, hepatologist and body radiology).

### **IV/2. PAE study materials**

Thirty male patients underwent prostatic artery embolisation (PAE) between May and October 2020 who previously did not receive TURP treatment for prostate hyperplasia. Each patient received PAE with a unilateral transfemoral approach. Both prostatic arteries were superselectively catheterised and embolised shortly thereafter with 1-300 micron spheres. For image acquisition, an Artis Pheno angiography system (Siemens Healthineers, Germany) was used. With “CARE aorta” and “CARE pelvis” protocols, a 1.17  $\mu$ Gy/frame dose (2 fps) provided sufficient DSA image quality. An automated injector and “Ultravist 370” contrast agent were used for injection [39].

Ethical approval was obtained from the Institutional Review Board (IRB no. 467-17) with a waiver for informed consent, which contained a statement on potential anonymous use of images for research purposes. The patients received only the standard-of-care treatment according to the existing institutional protocols.

The images were extracted from the angiographic workstations as unsubtracted image series, which were used for DSA and DVA image generation. DSA images were created with mask subtraction, and the DSA series were summarised into a single “peak opacification” image with the “Syngo” software of Siemens’ workstation. DVA images were created using the Kinepict Medical Imaging Tool (v.4.0; Kinepict Health Ltd., Hungary). Color-coded DVA images were also generated. DSA and DVA images were used for CNR measurements (performed the same way as described previously) and all three image types (DSA, DVA and ccDVA) were used for visual evaluation. The design of the study is detailed in Figure 3.

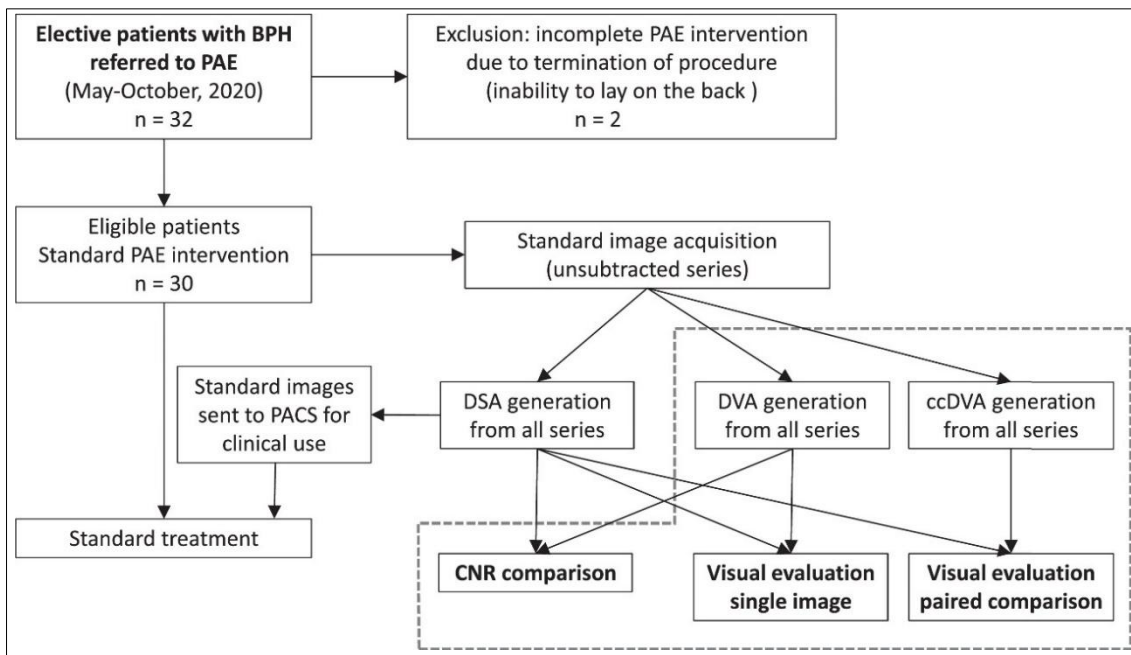


**Figure 3. Flow chart of the study. Elective patients with benign prostatic hyperplasia, referred for prostatic artery embolization (PAE) between May and October 2020, were screened for inclusion. Patients with completed PAE were added in a consecutive manner. All patients received standard treatment, and the observational study was performed retrospectively (dashed rectangle). Digital subtraction angiography (DSA) images were prepared during the intervention by the Siemens Syngo workstation, whereas digital variance angiography (DVA) images (both greyscale and color-coded types) were generated later with the Kinepict Medical Imaging Tool from the same unsubtracted series as DSA images. Contrast-to-noise ratio (CNR) and single image visual score was determined for DSA and DVA images, whereas ccDVA images were compared to DSA images in another blinded and randomised survey. (Source: Alizadeh et al. 2023) [39].**

### **IV/3. Contrast-to-Noise Ratio (CNR)**

To further discuss the methods used in both TACE and PAE studies, we must introduce the theory and technique of signal-to-noise or contrast-to-noise measurement. Perceived image quality, image contrast, and noise are strongly related and this relationship is incarnated in signal-to-noise ratio measurement [62–65]. Image quality depends on other factors, most importantly spatial resolution; however, proper phantom measurements are necessary to acquire such parameters [66–68]. In our research, because phantoms were not available, we were able to calculate only the SNR, which is still an objective measure. Because the signal in angiographies is basically the absolute image contrast, the SNR is often referenced as the contrast-to-noise ratio (CNR). In practice, CNR measurement refers to the selection of the background ROI and adjacent signal ROI (signal, in this case, meant vascular segments). The mean intensity was calculated for each ROI, and for each ROI pair, the intensity differences were calculated, which provided absolute contrast. The noise level was determined as the standard deviation of the intensities measured in the background ROIs. The CNR of a given ROI pair was calculated as the absolute contrast divided by background noise. The simplicity of this method enabled robust measurement of the CNR for numerous DSA and DVA image pairs calculated from the same angiographic sequence. Because the same ROI positions could be used in analogous DSA and DVA images, the difference between CNR values of analogous ROIs could be interpreted as a consequence of lower noise and/or higher contrast caused by the different image processing algorithms.

In both embolization studies, we used ImageJ (v.2.0.0-rc-68/1.52e, NIH) and Microsoft Excel (2016 Microsoft, Redmond, WA, USA) software for the CNR calculation. CNR values were compared, and the results were summarised as the median and interquartile range of the CNR ratios (R). The CNR values were compared using the Wilcoxon signed-rank test (Prism 8.4.2., GraphPad).

### **IV/4. Visual surveys**

The human visual system is a subjective but more complex measure of image quality [64,65]. To use this system for image comparison in TACE study, we created a randomised and blinded web survey involving readers, who were interventional radiologists with at least 15 years of experience in the field. During single-image evaluation, a 4-grade scale was used, which consisted of the following options regarding

image diagnostic value: (1) poor IQ, vascular structures are not distinguishable; (2) low IQ, good visualisation of lobar vessels only; (3) medium IQ, good visualisation of lobar and segmental vessels; and (4) good IQ, good visualisation of lobar, segmental, and subsegmental vessels. The readers also had to determine the visibility of the tumours and their feeding arteries using a 3-option survey: (1) not visible, (2) suspected but not definitive, and (3) clear identification. A paired image comparison was also conducted, where radiologists had to choose a preferred image (DSA or DVA) based on the visibility of the small vessels, lesions, and feeding arteries. The preference was answered according to the following 5-grade list: (1) no difference, (2) slightly better, (3) moderate differences, (4) major differences, and (5) better in every aspect. For statistical analysis, the CNR ratio (R) was calculated, and the median and interquartile range of the CNR values were compared using Wilcoxon's signed-rank test. For single-image evaluation score analysis, the median and interquartile range values (of image scores) were calculated, and image type (DVA vs. DSA) comparison was performed using Wilcoxon's signed-rank test. The paired comparison results were also evaluated using Wilcoxon's test, where the null hypothesis was equality in DVA and DSA image quality. The results of a single-image diagnostic survey questioning feeding artery, tumour, and small artery visibility were evaluated using the two-sided Z test. To assess inter-rater agreement, Kendall's W score was calculated [60].

In PAE study, visual evaluation was also performed using two randomised, blinded web-based surveys. The first was to evaluate DVA and DSA images in a single-image evaluation, where readers graded image quality according to a 5-grade rating scale: ("1") non-diagnostic, ("2") low, ("3") medium, ("4") good, and ("5") outstanding. Readers were four interventional radiologists with 5, 6, 7, and 25 years of experience in the field. The second survey compared DSA and color-coded DVA in a paired manner. Readers were asked to decide which image was better able to visualise large vessels, small vessels, tissue blush, and feeding arteries. The following answer options were provided: ("1") DSA is better, ("2") ccDVA is better, and ("3") no difference. Only images in which all four readers identified and evaluated the tissue blush and feeding arteries were included in the final analysis, which was performed as follows:

1. The median and interquartile range (IQR) were calculated for single-image scores, and the corresponding image scores were compared using the Wilcoxon signed-

rank test. The level of significance was set at  $p < 0.05$  in all tests. An inter-rater agreement analysis was also performed using Kendall's W test.

2. A binomial test was used for the DSA-ccDVA comparison. Inter-rater agreement was analysed using the Fleiss' kappa test.

Table 2. summarizes the design of visual questionnaires in both PAE and TACE studies.

**Table 2. Design of visual questionnaires in embolization studies. The used image types are indicated in parentheses. (Source: own work.)**

	<b>Readers</b>	<b>Single image evaluation</b>	<b>Paired comparison</b>
<b>TACE Study</b>	5 interventional radiologists, with at least 15 years of experience	4-grade scale for image quality assessment <b>(DVA, DSA)</b>	5 -grade preference scale based on the visibility of small vessels, lesions, and feeding arteries. <b>(DVA vs DSA)</b>
		3-option survey for tumor and feeding artery visibility assessment <b>(DVA, DSA)</b>	
<b>PAE Study</b>	4 interventional radiologists, with 5,6,7 and 25 years of experience	4-grade scale for image quality assessment <b>(DVA, DSA)</b>	3-grade preference scale based on the visibility of large vessels, small vessels, tissue blush, and feeding arteries <b>(color-coded DVA vs DSA)</b>

#### **IV/5. CcDVA study**

In 2020, 19 patients with PAD underwent peripheral intervention at a single centre (Heart and Vascular Centre of Semmelweis University, Hungary). A total of twenty-two interventions were performed, and imaging data were used in a retrospective, observational investigation to study colour-coded DVA and compare it with Siemens Syngo iFlow technology, which was available for testing at the site for a limited time. Interventions were performed from either brachial or groin access, and during the

procedures, the iliac, superficial femoral, popliteal, or crural arteries were treated. A Siemens Artis Zee system was used for the image acquisition. Pre- and post-procedural angiographies were recorded, and target lesions were treated by either "plain-old balloon angioplasty" (POBA) or POBA and implantation of a vascular stent. Written informed consent was obtained from all participants, allowing their anonymised data to be used for research purposes. The institutional interventional protocol was not changed for the purpose of the present study, and all the subjects received standard care [61].

The study was conducted in accordance with the Declaration of Helsinki (as revised in 2013). The study was approved by regional ethics board of Semmelweis University (SE RKEB N.o. 161/2020) and individual consent for this retrospective analysis was waived.

Regarding imaging protocols, almost half of the procedures were recorded with an acquisition rate of four frames per second, whereas in other interventions, a rate of seven frames per second was used. DSA image processing was executed using the Syngo Workplace (XWP VD11B and VD11C; Siemens Healthineers, Germany), in which the Syngo iFlow package was installed, enabling the generation of color-coded DSA images. From the same unprocessed image series transported from the imaging suite, color-coded DVA images were created using another workstation with Kinect Medical Imaging Tool (KMIT version 6.0.3, Kinect Health Ltd., Hungary) software.

Both the Syngo iFlow and KMIT software allowed the selection of optionally sized ROIs. The measuring protocol regarding ROI selection was the following: the first selection was called the "reference" ROI, which was selected in the proximal pre-stenotic segment of the treated (or to be treated) vessel; the second ROI was selected right before (proximally) to the stenosis, the third one inside the stenosis if possible (in the case of subocclusion, this selection was not doable and this step was practically skipped), and the last one (third or fourth ROI, depending on the previous step) selected distally to the vascular lesion, as shown in Figure 4.

The ROI selections were performed accordingly in Syngo iFlow, and the ROIs were selected on DVA images using the KMIT software. In order to select ROIs in the exact positions, a freeware mouse-position tracker software was used (MPOS, Blueprint). Time-attenuation data were obtained from both ccDSA and ccDVA images using the corresponding software, and the time-to-peak (TTP) parameter was calculated from curve

data. Other parameters, such as area under curve (AUC) and peak attenuation (PA), were not used, as they were considered more suited for parenchymal flow analysis, which was not part of this study. To statistically compare data, correlation analysis was performed using Pearson's R test, and Wilcoxon's test was used to investigate the significance of differences.

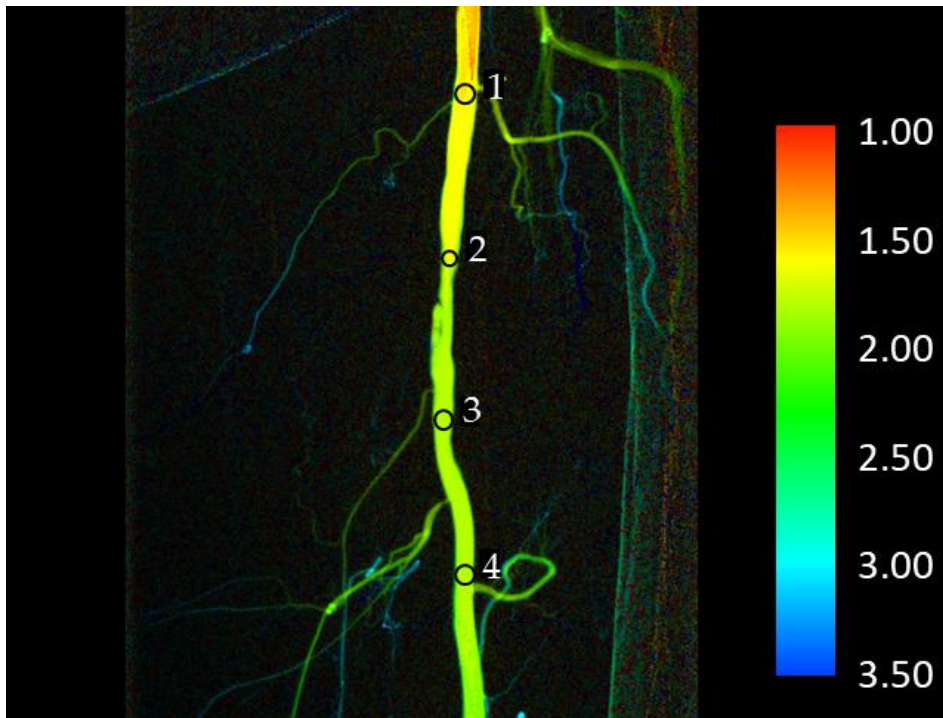


**Figure 4. Typical placement of region of interests (ROIs) on a color-coded DVA image. The colour bar shows the connection between the colours and the elapsed time (in seconds) measured from the injection of contrast media. (Source: Góg et al. 2024) [61].**

#### **IV/6. Summary of applied statistical tests**

**Wilcoxon signed-rank test** is a non-parametric statistical test used to compare two related samples or repeated measurements of a single sample. It was assumed that the data pairs were randomly and independently drawn. The null hypothesis of this test is that the median difference between paired observations is zero. It is best to use it in the evaluation of the effects of a treatment or intervention on the same subjects. We used this test in PAE and TACE studies for the comparison of CNR values, single-image evaluation scores, TACE “DSA vs DVA” paired comparison scores and in the “CcDVA” study, it was used for the comparison of time-derived parameters.

**Two-sided Z test** is a statistical hypothesis test used to determine whether there is a significant difference between a sample mean and a known or hypothesised population mean. The two-sided z-test is used when the population standard deviation is known, the sample size is not small ( $n > 30$ ), and we want to test if there's a significant difference in either direction (higher or lower) from the population mean. Z test was used in TACE study for the comparison of diagnostic ability scores.

**Kendall's W test** is a non-parametric statistical method used to measure the degree of agreement among multiple raters or judges and evaluate interrater agreement. Kendall's W test is a non-parametric test suitable for ordinal data. It can be used with two or more raters and is particularly useful when traditional parametric methods are not applicable. Kendall's test result in W, which ranges from 0 (no agreement) to 1 (complete agreement). The significance of W can also be specified by a formula using a chi-squared distribution. This test was used in both TACE and PAE studies for the assessment of inter-rater agreement in "DVA vs DSA" single-image questionnaires.

**A binomial test** is used when dealing with dichotomous variables in a fixed number of trials. It is a parametric hypothesis test that is used to determine if the proportion of one of the two categories in a population is equal to a specified value. We used this test in the PAE study for DSA versus ccDVA comparison.

**Fleiss' kappa test** is used to assess the reliability of agreement between multiple raters when assigning categorical ratings to items or classifying items. It can be used when there are more than two raters present, which means that it extends Cohen's kappa test's limitations. It can be used with nominal or ordinal data, although other measures may be more appropriate for ordinal data. We also used this test in the PAE study for DSA versus ccDVA comparison, especially for the assessment of inter-rater agreement.

**Pearson's R test** is a statistical method used to measure the strength and direction of the linear relationship between two continuous, normally distributed, independent variables. This test was used in the "CcDVA" study for the correlation analysis of iFlow and ccDVA related time-derived parameters.

## V. RESULTS

### V/1. TACE study

From the image data of twenty-five patients (65% male, mean  $\pm$  SD age:  $67.5 \pm 11.2$  years), fifty DSA and DVA image pairs were created. For CNR measurements a total of 686 ROI pairs were selected on both image types. The median of DSA CNR was 13.34 (IQR: 9.21), whereas DVA measurements resulted in a 16.02 median value (IQR: 14.89), and the derived ratio of CNR pairs was 1.24 (median, IQR: 0.69). According to the Wilcoxon signed-rank test, this difference was significant ( $p < 0.05$ ) (See Table 3.)

**Table 3. Results of contrast-to-noise ratio (CNR) analysis. Data are expressed as mean  $\pm$  standard error of mean (SEM), and as median and interquartile range (IQR). Wilcoxon signed-rank test was used for statistical comparison, significance level was set at  $p < 0.05$ . DVA: digital variance angiography and DSA: digital subtraction angiography. (Source: Lucatelli et al. 2023) [60].**

	CNR		R	Wilcoxon signed-rank test
	DSA	DVA	DVA/DSA	DSA vs. DVA
Mean $\pm$ SEM	15.01 $\pm$ 0.30	20.14 $\pm$ 0.58	1.34 $\pm$ 0.02	$p < 0.001$
Median (IQR)	13.34 (9.21)	16.02 (14.89)	1.24 (0.69)	

The visual survey, which involved the single image evaluation of 50 DSA and 50 DVA images, resulted in a median Likert score of 3.0 (IQR: 1.2) for DSA and 3.34 (IQR: 0.55) for DVA. The difference was significant according to the Wilcoxon signed-rank test ( $p < 0.001$ ). Kendall's  $W$  test was also performed to assess interrater agreement. In the case of DSA-related answers, the agreement was strong ( $W: 0.610$ ,  $p < 0.001$ ), and in the case of DVA, the agreement was moderate but still significant ( $W: 0.423$ ,  $p < 0.001$ ). These results are shown in Figure 5.

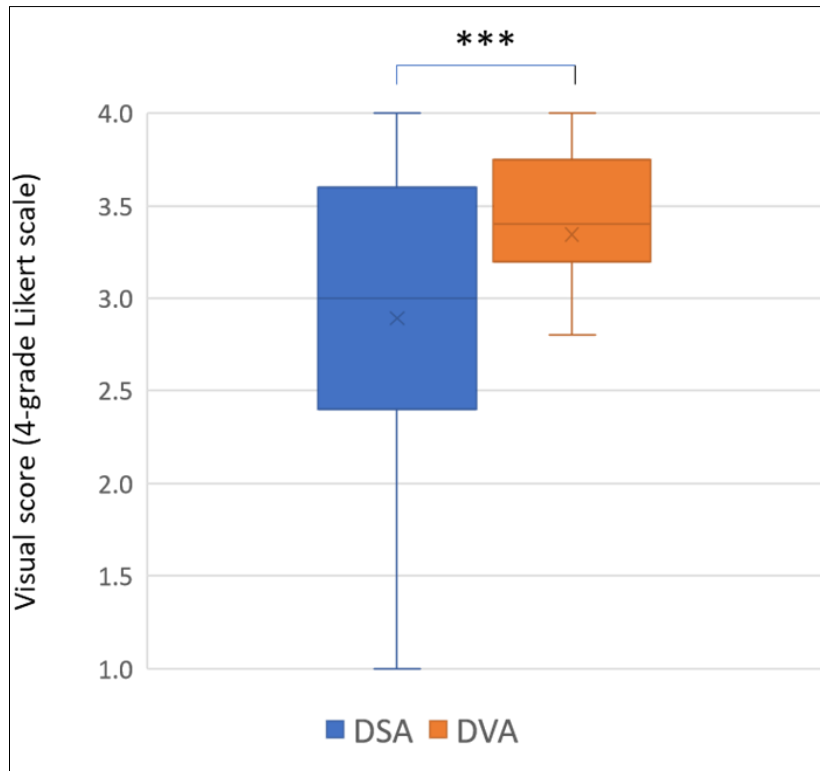


**Figure 5. Single image evaluation results. A 4-grade Likert score was used in the blinded, randomized survey to evaluate the image quality of DSA and DVA images. The box and whisker plots show the median (line), mean (x), interquartile range (box) and internal fences (whiskers) of single image scores values in each group. Data sets were analysed by the Wilcoxon signed-rank test (\*\*\*)  $p < 0.001$ . DVA: digital variance angiography and DSA: digital subtraction angiography. (Source: Lucatelli et al. 2023) [60].**

The survey focusing on diagnostic abilities determined that readers failed to visualise feeding arteries and lesions in only 8% of DVA images, whereas in the case of DSA, 28% of images were not able to visualise lesions. This difference was significant according to the two-sided Z-test ( $p > 0.01$ ). The results for the question regarding feeding artery detection were 16% (DVA) and 32% (DSA) failure of detection. A two-sided Z-test verified a significant difference ( $p < 0.05$ ) in this case also. The inter-rater agreement evaluation indicated moderate agreement for both questions. For feeding artery detection, Kendall's W for DSA was 0.541 ( $p < 0.001$ ), and for DVA was 0.551 ( $p < 0.001$ ), and for lesion detection, the W of DSA was 0.564 ( $p < 0.001$ ), and that of DVA was 0.561 ( $p < 0.001$ ). Results are presented in Figure 6.

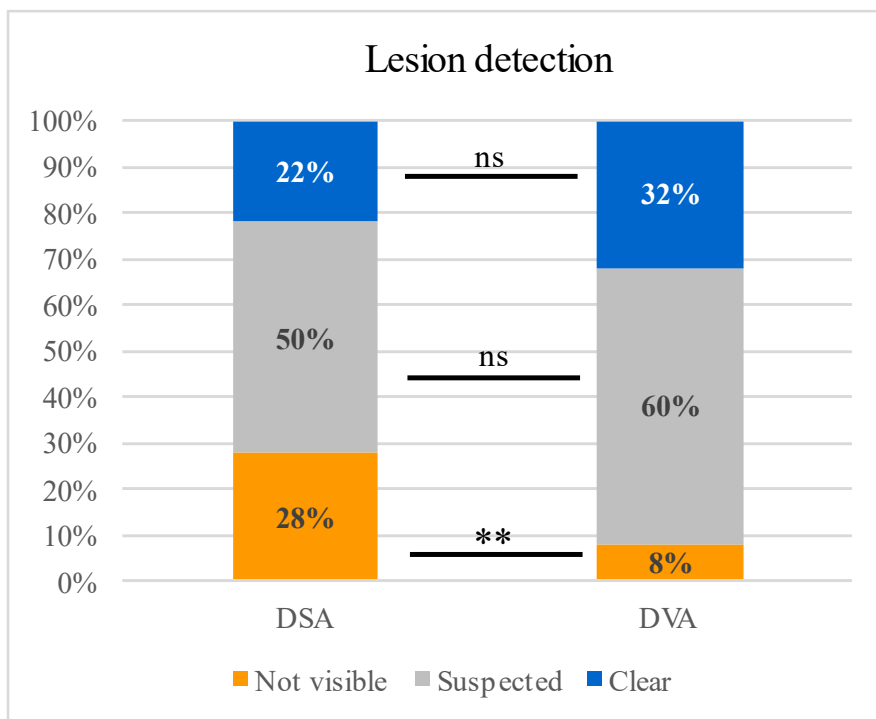
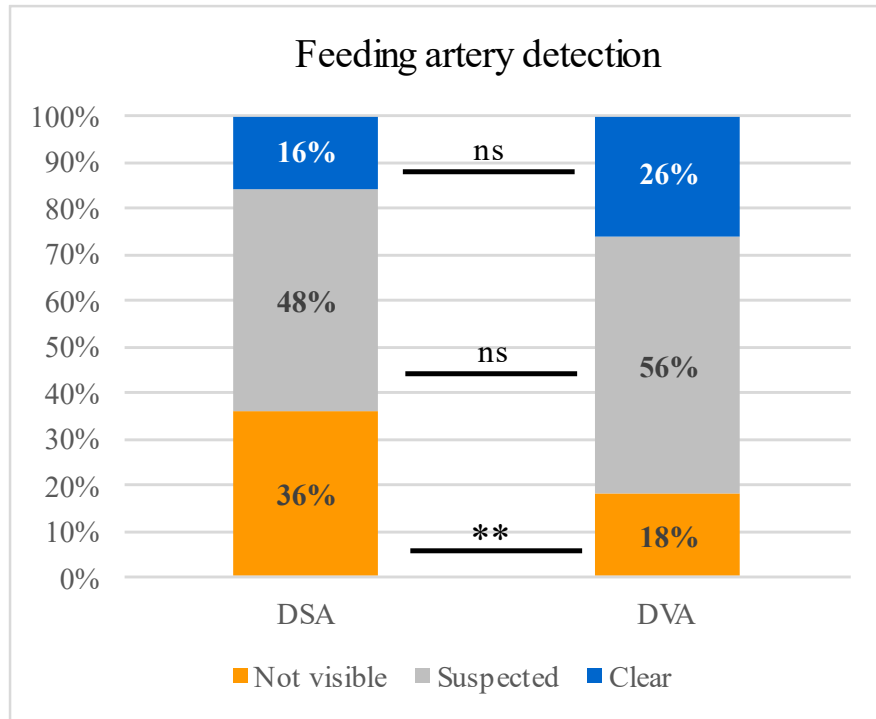


**Figure 6. A and B. Comparison of the diagnostic value of DSA and DVA. Readers classified each image based on the ability to identify structures (feeding arteries (A) and lesion (B)) being critically important in TACE interventions. Two-sided Z test was used for the statistical comparison of percentage data (\*p < 0.05, \*\*p < 0.01). TACE: transarterial chemoembolisation; DSA: digital subtraction angiography and DVA: digital variance angiography. (Source: Lucatelli et al., 2023) [60].**

Finally, since a blinded and randomised paired comparison was also performed, image type preference could be evaluated. In 80% of the responses, DVA was preferred over DSA. The median difference in image scores was 1.60 (IQR 2.4), which was significantly different from 0 (as we determined as a null hypothesis, see Materials and Methods section), according to the one-sample Wilcoxon's test ( $p < 0.001$ ). As previously reported, the inter-rater agreement was also tested with Kendall's W test, resulting in a significant agreement score indicating strong agreement ( $W = 0.575$ ,  $p < 0.001$ ). Results are shown in Figure 7. Representative DSA and DVA images are shown in Figure 8.

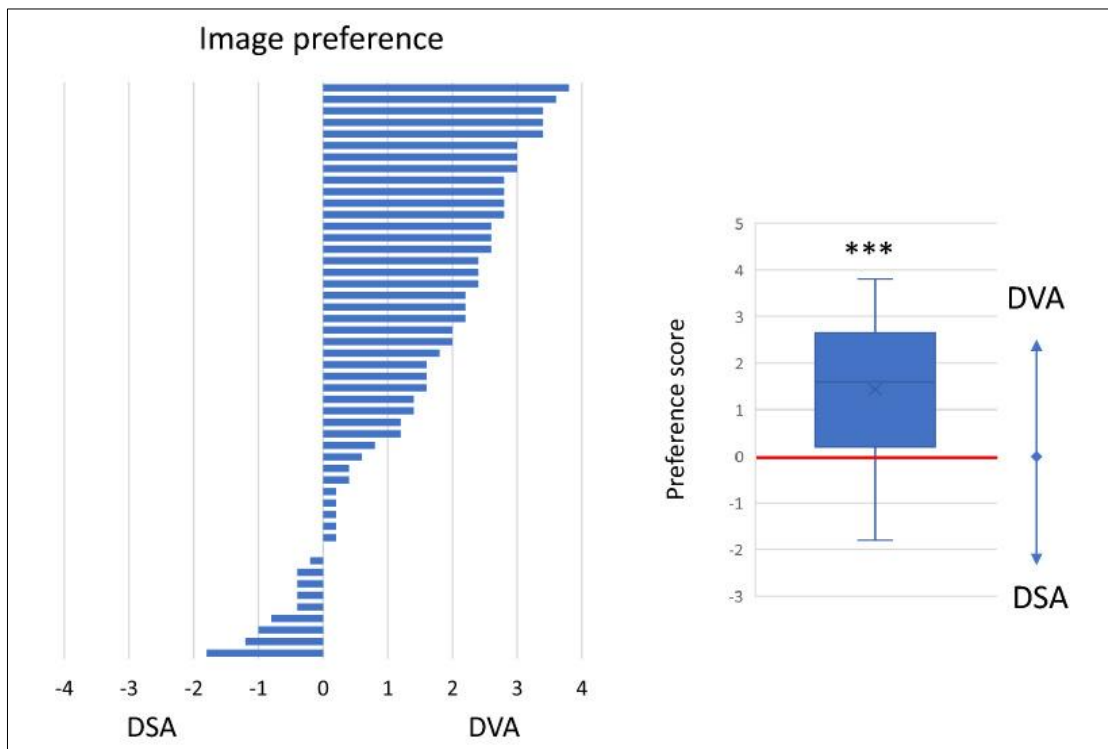


**Figure 7. Paired comparison of DSA and DVA images. Readers compared the image quality and diagnostic value of image pairs in a blinded, randomized manner, and expressed their image preference using a 5-grade preference scale. The left panel shows the distribution of the average preference scores of individual image pairs. The box and whiskers plot shows the mean (x), median (line), interquartile range (box) and internal fences (whiskers) of the complete image set. The 0 line represents the theoretical equal quality level. Data were analysed by the one-sample Wilcoxon test (\*\* $p < 0.001$ ). DSA: digital subtraction angiography and DVA: digital variance angiography. (Source: Lucatelli et al., 2023) [60].**

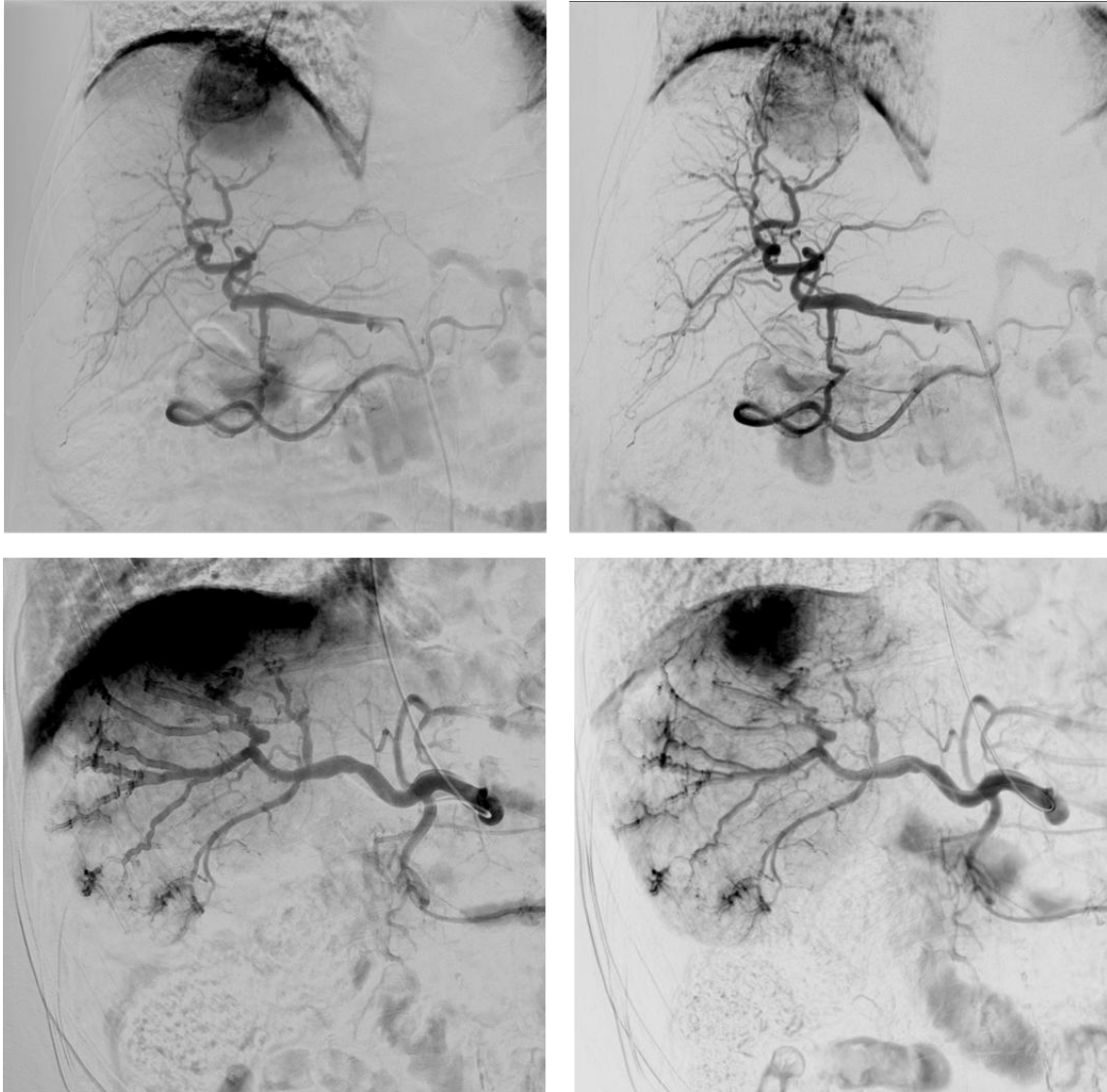


**Figure 8. Comparison of a representative DSA (left panels) and DVA (right panels) image pairs. The DSA and DVA images were generated from the same unsubtracted image series using the Siemens Syngo or the Kinect Medical Imaging Tool software, respectively. (Source: Lucatelli et al., 2023) [60].**

## **V/2. PAE study**

CNR measurements were performed on 108 DSA and DVA image pairs created from image data of 30 male patients (aged  $68.0 \pm 8.9$  years). CNR samples were taken from a total of 1418 locations (ROI pairs). The median DSA CNR was 7.33 (IQR: 6.40) and 29.99 (IQR: 25.93) for DVA. The median R-value (DVA CNR divided by the corresponding DSA CNR) was 4.11 (IQR: 1.72). The Wilcoxon signed-rank test verified a significant increase in the CNR provided by DVA ( $p < 0.001$ ) [39].

The first part of the visual evaluation, the single-image assessment of 108 DSA and 108 DVA images, was performed according to what was previously detailed in the previous section (Materials and Methods, “PAE Study”). DVA images’ median score reached 4.50 (IQR 0.75), while DSA images received 3.39 (median IQR: 1.00), which was significantly lower, according to Wilcoxon’s signed rank test ( $p < 0.001$ ). The inter-rater agreement was high in both groups (87% for DSA and 92% for DVA), which was determined to be significant, although moderate agreement was observed by Kendall’s W test (DVA  $W = 0.38$ , DSA  $W = 0.53$ ). Results are visualized in Figure 9.

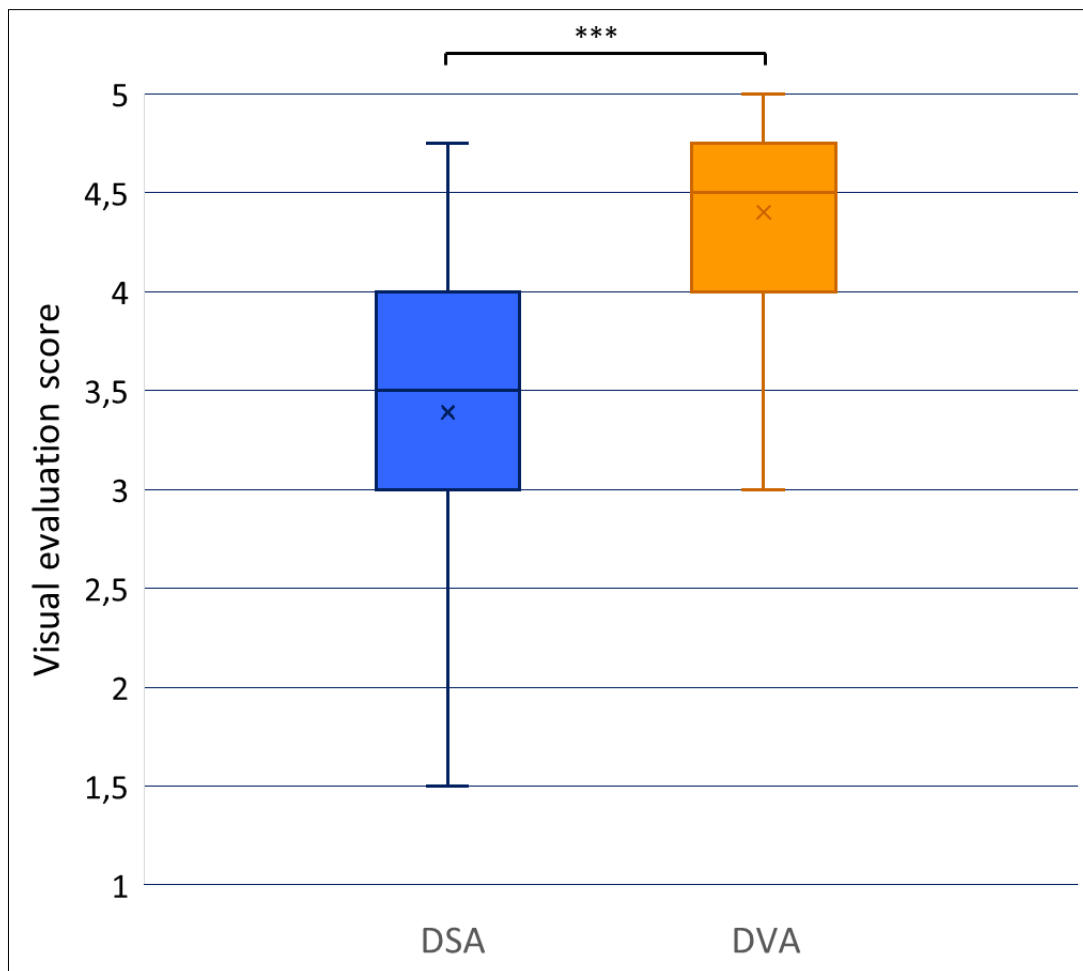


**Figure 9. Visual evaluation of digital subtraction angiography (DSA) and digital variance angiography (DVA) images. The box and whisker plots show the mean (x), median (line), interquartile range (box) and internal fences (whiskers) of the 5-grade Likert scale scores in each group. The paired data were analysed by the Wilcoxon signed rank test (\*\*\*)  $p < 0.001$ . (Source: Alizadeh et al., 2023) [39].**

The second part of the visual evaluation (paired comparison) showed a significantly higher preference for color-coded DVA images over DSA in all evaluated categories (visibility of large vessels, small vessels, feeding artery, and tissue blush) according to the binomial test ( $p < 0.01$ ). This meant an 89% preference for DVA for tissue blush visibility, 79% for small vessel visibility, 79% for feeding artery visibility, and 63% for large vessel visibility. The inter-rater agreement was between 58% and 79%, which was slight but significant in the three categories according to Fleiss' kappa test. For large vessels, agreement was not statistically significant. Results are shown in Figure 10. To illustrate the differences of DSA and ccDVA, an example is shown in Figure 11.

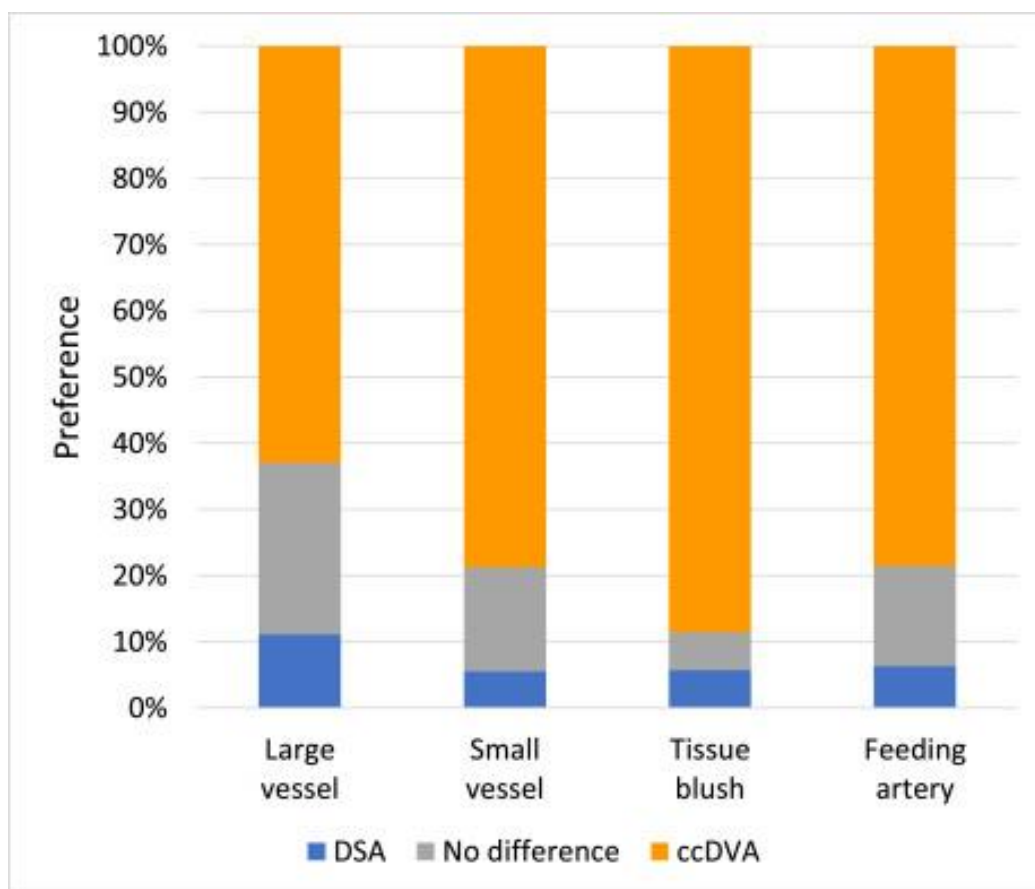


**Figure 10. Comparison of digital subtraction angiography (DSA) and color-coded digital variance angiography (ccDVA) images. Readers performed a paired comparison, and evaluated the visibility of large and small vessels, tissue blush and feeding arteries. In these categories there was also a ‘no difference’ option, and for the tissue blush and feeding artery an additional ‘not relevant’ option, to exclude those images where the structures were not visible. The ccDVA preference over the cumulated ‘DSA’ or ‘no difference’ options was significantly higher in all categories using the binomial test. (Source: Alizadeh et al., 2023) [39].**

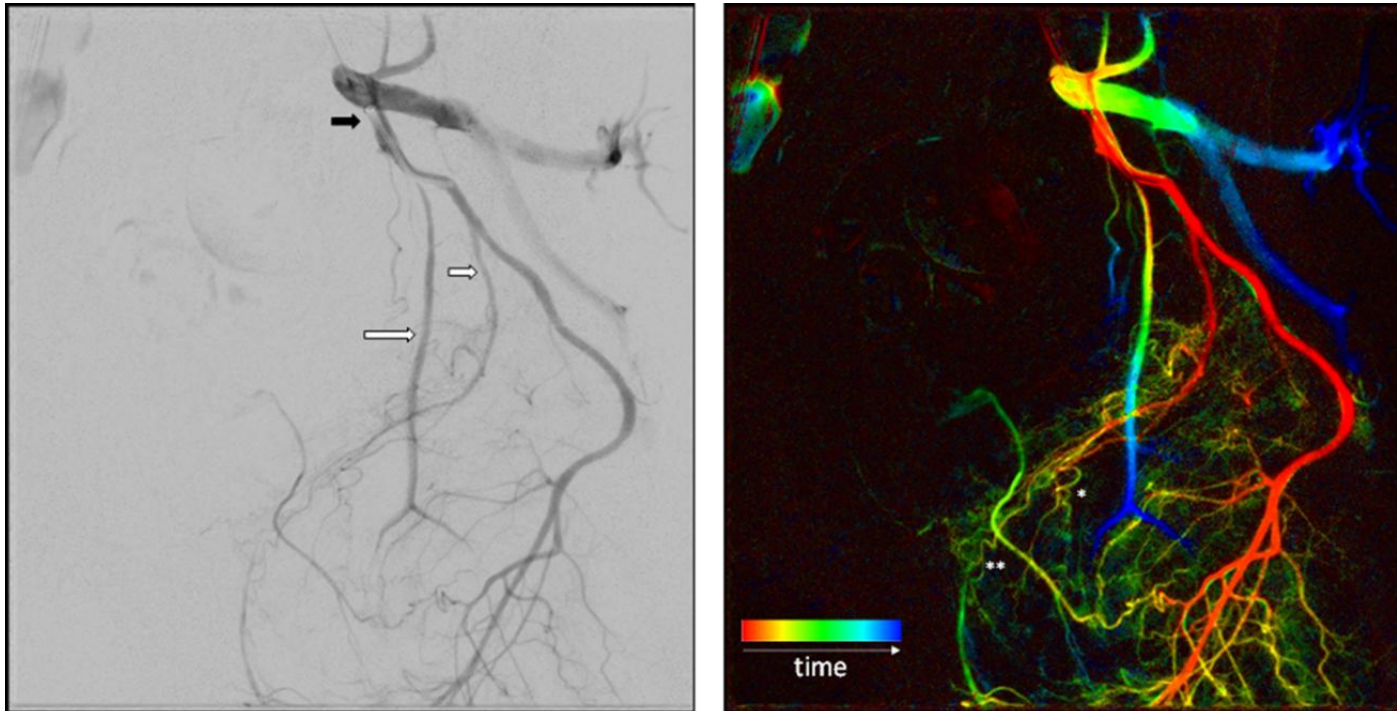


**Figure 11. Representative example of digital subtraction angiography (DSA) and color-coded digital variance angiography (ccDVA) images in a 63 year-old patient. Left: Application of 6 ml contrast agent (3 ml Vispaque 320 and 3 ml NaCl 0.9% solution) in the left pudendal artery (PuA) at the origin from the distal internal iliac artery (black arrow). The prostatic artery (short white arrow) is visible as a direct branch from the PuA. Proximal of the origin of the PuA the inferior vesical artery (IVA) is visible (long white arrow), with a proximal smaller lumen, suspicious for a stenosis. Right: The colors represent the time elapsed until the appearance of the contrast media in a specific blood vessel segment. In the IVA, color progression from orange to blue is visible, indicating a slower flow. Smaller vessels, like the characteristic corkscrew pattern (\*) or the collateralization of dominant prostatic artery to the pudendal areas (\*\*), have a higher visibility, and parenchymal blush is visible as greenish diffuse attenuation. (Source: Alizadeh et al., 2023) [39].**

### V/3. CcDVA study

A total of twenty-two pre- and post-interventional color-coded DSA images and the same number of color-coded DVA images were created in a previously detailed process. The data were divided by acquisition rates, resulting in the “4 FPS” and the “7.5 FPS” groups. Table 4 shows demographic data of patient population and Table 5 shows the distribution of image acquisition settings. Total procedural contrast agent dose per patient was 69,9 (+- 35,2) ml (mean +- SD).

**Table 4. Demographic data of patients. (Source: Góg et al. 2024) [61].**

Sex	Number of patients	Age <sup>1</sup> (years)	BMI <sup>1</sup>	GFR <sup>1</sup> (ml/min/1.73m <sup>2</sup> )
Male	8	69.6 ± 7.0	25.0 ± 4.5	65.3 ± 26.7
Female	11	67.9 ± 8.8	26.6 ± 4.6	55.8 ± 26.2

<sup>1</sup> All data are mean ± SD. BMI: Body Mass index. GFR: Glomerular Filtration Rate

**Table 5. Distribution of image acquisition protocol. (Source: Góg et al. 2024) [61].**

FPS (1/sec)		Flow (ml/s)			Contrast agent volume per image (ml)			
	N.o. of patients	N.o. of images		N.o. of patients	N.o. of images		N.o. of patients	N.o. of images
4/sec	13	14	2 ml/s	12	13	3 ml	10	12
7,5/sec	6	8	3 ml/s	3	4	4 ml	2	2
			4 ml/s	1	1	5 ml	3	4
			6 ml/s	3	3	6 ml	2	2
						8 ml	2	2

The analysis of 22 pre- and post-angioplasty image pairs resulted in the selection of 53 pre- and post-angioplasty ROI pairs in the “4 FPS” group and 32 pairs in the “7,5 FPS” group. When we compared the change in passage time, only those image pairs were used, where four ROIs were present for the reason that this way, the data collection seemed more homogenous, as in cases where only three ROIs per image were selected, the distance from the site of treatment varied highly.

In the analysis of the relationship between the TTP parameter and different imaging protocols, the correlation was found to be very high regardless of the acquisition settings. Pearson’s  $r$  value was 0.99 ( $p < 0.0001$ ) and  $R^2$  was 0.98 in both FPS groups. For visual representation, see Figure 12.

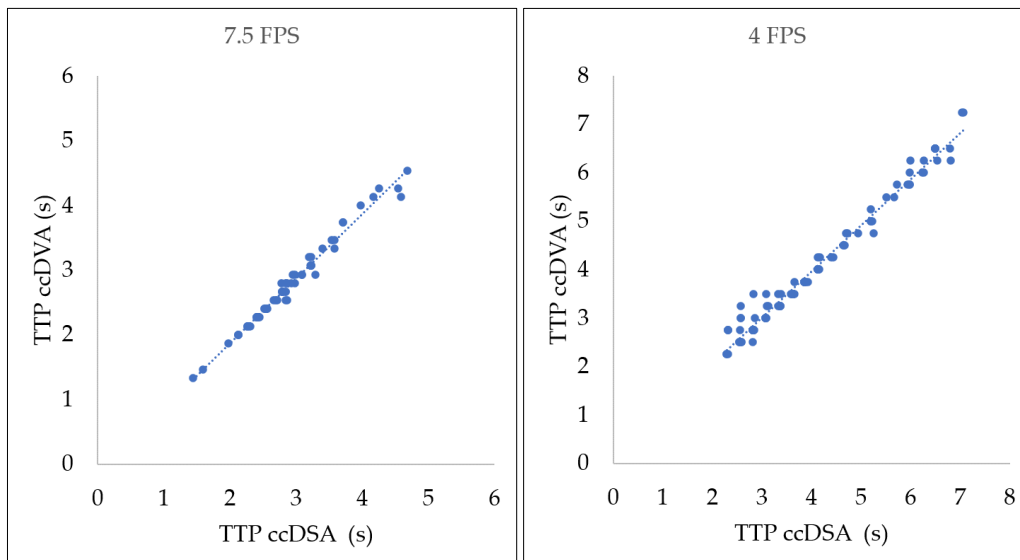


**Figure 12. Correlation of TTP values calculated by ccDSA and ccDVA in different acquisition protocols. Right panel: correlation of 106 ROI pairs in 4 FPS acquisitions. Left panel: correlation of 64 ROI pairs in 7.5 FPS acquisitions. (Source: Góg et al., 2024) [61].**

To investigate the relationship between different ROI positions and TTP parameters, a similar correlation testing was performed, and the resulting  $r$  and  $R^2$  values showed a very high correlation ( $r = 0.99$ ,  $p < 0.0001$ ,  $R^2 = 0.98$ ) in all ROI positions (not shown).

The change in passage time was also calculated, as we hypothesised that it could represent the change in haemodynamic conditions in the surveyed area. This passage time was

obtained by subtracting the TTP measured in the 1st ROI from the TTP of the 4<sup>th</sup> ROI. Change in passage time was obtained by subtracting post-interventional passage time from pre-interventional passage time. Correlation analysis showed that this parameter was measured likewise by both imaging software ( $r = 0.98$ ,  $p < 0.0001$ ,  $R^2 = 0.96$ ). Overall results are collected in Table 6.

**Table 6. Pearson correlation analysis of time-related parameters. TTP: Time-to-Peak; ROI: Region of In-terest; n: the number of ROI pairs included in the analysis, FPS: frame per second. (Source: Góg et al. 2024) [61].**

Correlation group (n)	Pearson r	95% confidence interval	R <sup>2</sup>	Two-tailed p
TTP 4 FPS (106)	0.9889	0.9837 - 0.9924	0.9779	< 0.0001
TTP 7.5 FPS (64)	0.9917	0.9864 - 0.9950	0.9835	< 0.0001
TTP ROI1 (44)	0.9899	0.9814 - 0.9845	0.9799	< 0.0001
TTP ROI2 (44)	0.9903	0.9822 - 0.9947	0.9807	< 0.0001
TTP ROI3 (44)	0.9902	0.9819 - 0.9947	0.9804	< 0.0001
TTP ROI4 (38)	0.9904	0.9814 - 0.9950	0.9808	< 0.0001
TTP all ROI (170)	0.9905	0.9871 - 0.9930	0.9811	< 0.0001
$\Delta$ passage time <sup>1</sup> (19)	0.9806	0.9491 - 0.9927	0.9615	< 0.0001

<sup>1</sup>. The change of passage time ( $\Delta$ ) was calculated as the difference of ( $TTP_{ROI4} - TTP_{ROI1}$ ) before and after intervention.

Results regarding change of passage time comparison is show in Figure 13.

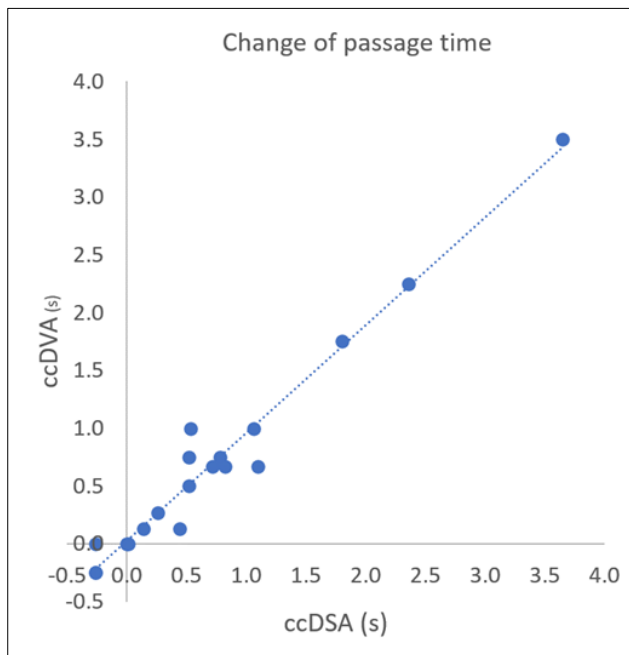


**Figure 13. Correlation of the change passage time calculated from TTP data of ccDSA and ccDVA. We could not place the 4th ROI in 3 interventions. Therefore, only 19 ROI pairs were used in the analysis. The change of passage time was calculated as the difference of ( $TTP_{ROI4} - TTP_{ROI1}$ ) before and after intervention. (Source: Góg et al. 2024) [61].**

## **VI. DISCUSSION**

In two retrospective studies, we have examined the capabilities of DVA to visualize vessels during visceral embolization and we compared it to the gold standard DSA. In the second embolization study, we also introduced color-coded DVA as a supplementary imaging modality. Results indicated a significant advantage for both DVA and color-coded DVA over DSA; however, due to the limitations of these studies (as detailed in the following sections), further conclusions regarding the actual clinical benefits of DVA and color-coded DVA can only be drawn from larger scale, prospective investigations. The most important limitation is the lack of validation for color-coded DVA, which we wished to surpass by performing a third retrospective analysis, in which we compared colour-coded DVA to Siemens iFlow, an already marketed, potentially useful decision-support tool in the field of peripheral and neurointerventions. The presented results support the claim that color-coded DVA is able to produce the same time-derived parameters as iFlow, which is the first step in the direction of color-coded DVA validation studies.

### **VI/1. TACE study**

The primary objective of this study was to evaluate the effectiveness of DVA in liver TACE procedures. Although previous research has shown DVA's quality in angiography of the lower extremities [9,14,15] and carotid arteries [13], the abdominal region presents unique challenges. Unlike these areas, the abdomen has less prominent bone shadows but is affected by intestinal gas and movement artefacts. Both objective and subjective measures of image quality were used in the present study: CNR and visual comparison, respectively. Furthermore, we evaluated the diagnostic value of different image types.

Our research revealed a notably higher CNR in DVA than in DSA. However, the absolute CNR DVA values were lower than those reported in other DVA applications. This discrepancy may be attributed to various factors. First, the previously mentioned motion artefacts originating from breathing, cardiac pulsations, and bowel gas can cause a lower CNR by lowering the image contrast. Second, the abdominal region tends to have higher attenuation than the extremities. Therefore, angiographies performed in this region usually require higher radiation doses to achieve a sufficient image quality. As the institutional protocols for abdominal and extremity angiographies were not compared, it may also be possible that the institution applies lower radiation doses overall (as the image quality threshold can be lower depending on the specialist's preference).

Despite the lower absolute CNR value, DVA technology still demonstrated an advantage over standard DSA, as the results of visual comparison showed that DVA produced superior image quality compared to DSA, although interrater agreement was somewhat higher for DSA images, likely due to readers' familiarity with this image type. Regarding diagnostic features, the quality advantage of DVA showed improved lesion visibility (DVA 32% vs. DSA 22%) and fewer cases in which angiography failed to detect any lesions (DVA 8% vs. DSA 28%). Furthermore, the DVA technology significantly outperformed standard DSA in the detection of feeder vessels. A blinded comparison of paired DVA and DSA images further emphasised DVA's superiority in terms of overall diagnostic value, as in DVA was the preferred image in 80% of cases. These findings clearly demonstrate the substantial clinical benefits of DVA technology by enabling operators to visualise more lesions and better identify feeding vasculature during liver embolisation procedures. DVA may prove particularly valuable in challenging TACE cases in which standard DSA imaging struggles to identify and characterise lesions. This may be the case in patients in whom tumours are hypovascularized or located in the uppermost parts of the right lobe [60].

The main conclusion of this study is that the demonstrated quality reserve of DVA could potentially be utilised to minimise radiation exposure for patients and medical staff during TACE. Additionally, the volume of contrast medium used could also be lowered, as previously shown in our study regarding carotid angiographies. This potential could be particularly significant in TACE, considering that patients often have compromised renal function and, more importantly, typically require multiple treatment sessions. Of course, validating these assertions requires further clinical trials, but this research provides a good basis for initiating prospective dose management studies in the future.

There were certain limitations to this study. The patient sample size was relatively small, in keeping with the design of a small cohort proof-of-concept study, although the number of images evaluated fully complies with FDA guidelines for testing X-ray imaging devices. Breathing artefacts and intestinal gases inevitably affected DVA performance, as mentioned previously. Another limitation was that image processing was conducted retrospectively, although DVA technology can operate in near real-time. This capability also supports the feasibility of a prospective study regarding DVA, ccDVA and TACE.

## **VI/2. PAE study**

The objective of this study was to evaluate the image quality of DVA compared with DSA in the context of PAE. We sought to determine whether the previously found superiority of DVA in endovascular lower-limb procedures was extended to prostatic interventions. Our findings indicate that DVA delivers a more than fourfold increase in CNR compared with DSA. This quantitative advantage is mirrored in qualitative assessments, with DVA images scoring one point higher on the Likert scale than DSA images. These results clearly demonstrate the quality advantages of the digital variance method [39].

A comparison of DSA and ccDVA images demonstrated that color-coded technology offers enhanced visualisation of the small arteries, tissue perfusion, and feeding vessels. These structures are critically important in the PAE procedure. Therefore, ccDVA might be a very useful tool to avoid complications, such as the most feared non-target embolization of important collaterals [69–72]; judge the efficacy of embolization during the intervention, shorten intervention time and, thereby, improve clinical outcome. It is also important, that since parametric imaging usually requires higher acquisition rates and consequently higher radiation dose, the use of ccDVA might also decrease the radiation load of these procedures, which could enhance the wider acceptance of color-coded angiography.

Despite the promising results, it must be noted that the quantitative aspect of color-coded angiography was not utilised in this study, as time-to-peak parametric maps were used for visual analysis, but no time measurement was performed. In future studies, quantitative measurements should also be utilised to compare changes in tissue blush before and after embolisation.

This study had several other limitations. As this was a small-cohort proof-of-concept retrospective study, the patient sample population was relatively small, although the number of analysed images allowed us to deduce statistically valid conclusions. In addition, all DVA and ccDVA images were generated retrospectively from unsubtracted acquisitions, preventing their use as real-time assistance for the medical staff during interventions. Future clinical investigations should use real-time data processing with a DVA workstation installed in the operating room.

### **VI/3. CcDVA study**

Another important question is whether the DVA-based color coded imaging provides reliable time-related parameters. In the “ccDVA study,” Time-to-peak (TTP) comparison demonstrated that ccDVA can accurately replicate the TTP parameters of the Syngo iFlow software, regardless of the frame rate or ROI positioning. We also compared the change in passage time, a time-based derived parameter that was nearly identical between ccDVA and iFlow. It has been hypothesised that change in the passage time may be a relevant parameter for the assessment of clinical outcomes [61]. However, this cannot be confirmed from retrospective data. To determine a proper assessment parameter, ccDVA must be compared with an already established tool, such as duplex ultrasound, preferably in a prospective manner. Nevertheless, the high reproducibility of iFlow TTP values by ccDVA validates the reliability of ccDVA imaging.

The concept of parametric angiography is not novel, with major manufacturers having developed their own methods to display the temporal progression of contrast media in blood vessels by using a single composite image [22,45]. In these images, different colours represent the time taken for the contrast medium to reach specific vessel segments. Although emerging evidence supports the usefulness of parametric imaging techniques in understanding haemodynamic conditions, it is at the expense of a higher radiation dose caused by the high frame rate (4–7.5 fps) requirement for good time resolution [59]. This may be a major factor limiting the widespread adoption of color-coded angiography. As ccDVA is based on DVA technology, it may significantly reduce radiation exposure owing to its dose management capabilities. Decreased radiation exposure for both patients and medical personnel, as well as the potentially reduced amount of contrast medium used, has been previously demonstrated in other clinical contexts. While these claims need validation through further clinical trials, our results provide a good foundation for initiating prospective dose management studies in procedures involving color-coded DVA.

Our “ccDVA” retrospective study had some limitations, which also occurred in similar studies, specifically the lack of standardised injection rates and catheter placement. In our study, we even struggled to use standardized image acquisition rates, which is the reason we were forced to divide an already small sample size into two groups during statistical analysis. However, the total number of measurement points enhanced the statistical power

and was adequate for drawing conclusions. Besides the relatively small patient sample, another limitation was that data collection was performed retrospectively. In addition to standardizing the image acquisition parameters, other factors should be considered, such as immobilising the patient's leg using specialised equipment [25,45] to reduce motion artefacts that could distort the results. The most obvious limitation is the lack of validation for color-coded angiographic methods in general. Since ultrasound is the gold standard method for flow measurements, we propose that either non-invasive or invasive ultrasound studies should be performed to validate color-coded angiographic data. Although non-invasive duplex ultrasound is able to give functional data of superficial vessels, such as the common and superficial femoral arteries or carotid arteries, which can be compared to data measured with color-coded angiography; with the availability of invasive IVUS, the validation of time-parameters can be performed in any region of the circulatory system. IVUS studies may generate higher expenses but may provide more reliable data for the sake of proper validation.

## VII. CONCLUSIONS

To conclude our results, we made the following thesis statements:

1. Concerning the usefulness and potential benefits of DVA in other indication: using contrast-to-noise measurements and visually comparing the quality and diagnostic value of DSA-DVA image pairs, we demonstrated that DVA has superior image quality and diagnostic value in PAE and liver TACE procedures. Thereby, we provided evidence that the advantages of DVA can be observed not only in lower limb but also in abdominal and pelvic interventions.
2. Concerning the qualitative advantages of color-coded DVA in other therapeutic indications: by visually comparing DSA and ccDVA, we have found evidence that ccDVA has the potential to augment PAE interventions by delivering more detailed information on small arteries, feeding arteries and tissue blush. All these structures are critically important in the embolization procedure, therefore their better visibility might improve the safety and efficacy of PAE interventions.
3. Concerning the reliability of time-related parameters provided by the ccDVA technology: by measuring and comparing time-to-peak values of paired ccDVA and iFlow images, we demonstrated the equivalence between the two parametric angiographic method regarding TTP measurement, which suggests DVA's utility as an alternative decision-support tool in endovascular interventions. The lower radiation load required by DVA technology might help to increase the use and significance of color-coded parametric imaging in minimally invasive endovascular interventions.

## VIII. SUMMARY

In this thesis, we introduced the concept of vascular imaging, Digital Subtraction Angiography (DSA), Digital Variance Angiography (DVA) and color-coded angiography. For research objectives, we have set to assess the effect of DVA on image quality in liver TACE and PAE, to find potential benefits in using ccDVA during PAE and to compare ccDVA with Siemens' Syngo iFlow technology. In order to complete objectives, three retrospective analysis was performed, in which SNR measurements revealed a 24 percent increase in SNR favouring DVA in the case of TACE and a four-fold increase in SNR also favouring DVA in the case of PAE. From these results it is deductible, that the quality advantage could potentially be utilised to manage both radiation and contrast media doses in the future for both PAE and liver TACE procedures. Visual survey results implied the preference of using DVA over DSA for small vessel and feeding artery detection in the case of both PAE and TACE procedures. In TACE, raters preferred DVA for tumor detection also. Single image evaluations regarding general diagnostic image quality also resulted in higher image scores for DVA in both liver TACE and PAE studies. In PAE, evidence regarding the benefit of using color-coded DVA over greyscale DSA was also found, as visual comparison revealed a preference of ccDVA for large and small vessel, tissue blush and feeding artery detection also. This benefit may enhance the efficiency of embolization procedures by limiting nontarget embolization.

In the retrospective comparison of DVA and Siemens' Syngo iFlow (in lower-limb interventions), the reproducibility of the time-to-peak (TTP) parameter was very high, which indicated that in lower-limb flow analysis, ccDVA could be just as reliable as iFlow. Considering our previous findings, this also means that with ccDVA, low-dose color-coded angiography is potentially achievable. Since parametric imaging requires higher acquisition rates and, therefore, higher radiation dosage but provides benefits presented in the "PAE" study, the use of color-coded DVA should be encouraged during these types of procedures. Nevertheless, additional larger scale, prospective clinical studies are needed to confirm these findings.

## IX. REFERENCES

1. Busch U. Claims of priority – The scientific path to the discovery of X-rays. *Z Med Phys.* 2023 May 1;33(2):230–242.
2. Van Tiggelen R. The Rise of Contrast-enhanced Roentgenology: An Illustrated and Chronological Overview. *J Belg Soc Radiol.* 2016;100(1):102.
3. Hafiani H, Saibari RC, Morsad N, Rami A. Sven Ivar Seldinger (1921-1998): The Founding Father of Interventional Radiology. *Cureus.* 2024 May 16;16(5):e60397.
4. Murphy TP, Soares GM. The Evolution of Interventional Radiology. *Semin Intervent Radiol.* 2005 Mar;22(1):6.
5. Reimer P, Landwehr P. Non-invasive vascular imaging of peripheral vessels. *Eur Radiol.* 1998;8(6):858–872.
6. Harrington DP, Boxt LM, Murray PD. Digital subtraction angiography: overview of technical principles. *AJR Am J Roentgenol.* 1982;139(4):781–786.
7. Szigeti K, Máthé D, Osváth S. Motion based X-ray imaging modality. *IEEE Trans Med Imaging.* 2014;33(10):2031–2038.
8. Góg István. Kinetikus képalkotás az angiográfiában: modellezés és klinikai vizsgálat. [Budapest]: Semmelweis University; 2019.
9. Gyánó M, Góg I, Óriás VIVI, Ruzsa Z, Nemes B, Csobay-Novák C, Oláh Z, Nagy Z, Merkely B, Szigeti K, Osváth S, Sótónyi P. Kinetic Imaging in Lower Extremity Arteriography: Comparison to Digital Subtraction Angiography. *Radiology.* 2018;290(1):172927.
10. Óriás VI, Góg I, Gyánó M, Dávid S, Dániel V, Nagy Z, Csobay-Novák C, Oláh Z, János K, Szigeti K, Osváth S, Ruzsa Z, Sótónyi P. Digital Variance Angiography as a paradigm shift in carbon-dioxide angiography. *Invest Radiol.* 2019;54(7):428–436.

11. Bastian MB, König AM, Viniol S, Gyánó M, Szöllősi D, Góg I, Kiss JP, Osvath S, Szigeti K, Mahnken AH, Thomas RP. Digital Variance Angiography in Lower-Limb Angiography with Metal Implants. *Cardiovasc Intervent Radiol*. 2020;
12. Thomas RP, Bastian MB, Viniol S, König AM, Amin SS, Eldergash O, Schnabel J, Gyánó M, Szöllősi D, Góg I, Kiss JP, Osváth S, Szigeti KP, Mahnken AH. Digital Variance Angiography in Selective Lower Limb Interventions. *J Vasc Interv Radiol*. 2022 Feb 1;33(2):104–112.
13. Óriás VI, Szöllősi D, Gyánó M, Veres DS, Nardai S, Csobay-Novák C, Nemes B, Kiss JP, Szigeti K, Osváth S, Sótonyi P, Ruzsa Z. Initial evidence of a 50% reduction of contrast media using digital variance angiography in endovascular carotid interventions. *Eur J Radiol Open*. 2020 Jan 1;7.
14. Gyánó M, Berczeli M, Csobay-Novák C, Szöllősi D, Óriás VI, Góg I, Kiss JP, Veres DS, Szigeti K, Osváth S, Pataki Á, Juhász V, Oláh Z, Sótonyi P, Nemes B. Digital variance angiography allows about 70% decrease of DSA-related radiation exposure in lower limb X-ray angiography. *Sci Rep*. 2021 Dec 1;11(1).
15. Sótonyi P, Gyánó M, Berczeli M, Csobay-Novák C, Szöllősi D, Óriás VI, Góg I, Kiss JP, Veres DS, Szigeti K, Osváth S, Pataki Á, Juhász V, Oláh Z, Nemes B. Digital variance angiography allows about 70% decrease of DSA-related radiation exposure in lower limb X-ray angiography. *Sci Rep*. 2021 Dec 1;11(1).
16. Ruedinger KL, Schafer S, Speidel MA, Strother CM. 4D-DSA: Development and Current Neurovascular Applications. *AJNR Am J Neuroradiol*. 2021 Feb 1;42(2):214–220.
17. Verschuur AS, Groot Jebbink E, Lo-A-Njoe PE, van Weel V. Clinical validation of 2D perfusion angiography using Syngo iFlow software during peripheral arterial interventions. *Vascular*. 2021 Jun 1;29(3):380–386.
18. Simgen A, Mayer C, Kettner M, Mühl-Benninghaus R, Reith W, Yilmaz U. Retrospective analysis of intracranial aneurysms after flow diverter treatment including color-coded imaging (syngo iFlow) as a predictor of aneurysm occlusion. *Interventional Neuroradiology*. 2022 Apr 1;28(2):190–200.

19. Fang K, Zhao J, Luo M, Xue Y, Wang H, Ye L, Zhang X, Zheng L, Shu C. Quantitative analysis of renal blood flow during thoracic endovascular aortic repair in type B aortic dissection using syngo iFlow. *Quant Imaging Med Surg.* 2021 Aug 1;11(8):3726–3734.
20. Ng JJ, Papadimas E, Dharmaraj RB. Assessment of Flow after Lower Extremity Endovascular Revascularisation: A Feasibility Study Using Time Attenuation Curve Analysis of Digital Subtraction Angiography. *EJVES Short Rep.* 2019 Jan 1;45:1–6.
21. Hinrichs JB, Murray T, Akin M, Lee M, Brehm MU, Wilhelmi M, Wacker FK, Rodt T. Evaluation of a novel 2D perfusion angiography technique independent of pump injections for assessment of interventional treatment of peripheral vascular disease. *International Journal of Cardiovascular Imaging.* 2017 Mar 1;33(3):295–301.
22. Tang M, Zeng F, Chang X, He M, Fang Q, Xue L, Luo X, Yin S. Feasibility study of Syngo iFlow in predicting hemodynamic improvement post-endovascular procedure in peripheral artery disease. *BMC Cardiovasc Disord.* 2024 Dec 1;24(1):1–10.
23. Jens S, Marquering HA, Koelemay MJW, Reekers JA. Perfusion Angiography of the Foot in Patients with Critical Limb Ischemia: Description of the Technique. *Cardiovasc Intervent Radiol.* 2015 Dec 13;38(1):201–205.
24. Murray T, Rodt T, Lee MJ. Two-dimensional perfusion angiography of the foot: Technical considerations and initial analysis. *Journal of Endovascular Therapy.* 2016 Feb 1;23(1):58–64.
25. Reekers JA, Koelemay MJW, Marquering HA, van Bavel ET. Functional Imaging of the Foot with Perfusion Angiography in Critical Limb Ischemia. *Cardiovasc Intervent Radiol.* 2016 Feb 1;39(2):183–189.
26. Donaldson C, O'Neill AH, Slater LA, Chong W, Lai LT, Chandra R V. Feasibility of Real-Time Angiographic Perfusion Imaging in the Treatment of Cerebral Vasospasm. *Interv Neurol.* 2017;6(3–4):163–169.

27. Ipema J, Heinen SGH, Janssens AJB, Potters FH, Ünlü Ç, de Vries JPPM, van den Heuvel DAF. Repeatability, and Intra-Observer and Interobserver Agreement of Two Dimensional Perfusion Angiography in Patients with Chronic Limb Threatening Ischaemia. *European Journal of Vascular and Endovascular Surgery*. 2021;61(6):980–987.
28. Kawarada O. Color coded circulation in the field of infrapopliteal intervention. *Cardiovasc Interv Ther*. 2021 Jan 1;36(1):131–133.
29. Maruyama M, Hiroya A, Araki H, Yoshida R, Ando S, Nakamura M, Yoshizako T, Kaji Y. Color-coded circulation for visualizing swirling flow with a 3-dimensional helical stent in the superficial femoral artery. *Radiol Case Rep*. 2024 Nov 1;19(11):4814–4817.
30. Ma GMY, Dmytriw AA, Patel PA, Shkumat N, Krings T, Shroff MM, Muthusami P. Quantitative color-coded digital subtraction neuroangiography for pediatric arteriovenous shunting lesions. *Child's Nervous System*. 2019 Dec 1;35(12):2399–2403.
31. Huang TC, Wu TH, Lin YH, Guo WY, Huang WC, Lin CJ. Quantitative flow measurement by digital subtraction angiography in cerebral carotid stenosis using optical flow method. *J Xray Sci Technol*. 2013;21(2):227–235.
32. Wisniewski AG, Shiraz Bhurwani MM, Sommer KN, Monteiro A, Baig AA, Davies JM, Siddiqui AH, Ionita CN. Quantitative angiography prognosis of intracranial aneurysm treatment failure using parametric imaging and distal vessel analysis. *Proc SPIE Int Soc Opt Eng*. 2022 Mar 30;12036:15.
33. Simgen A, Mayer C, Kettner M, Mühl-Benninghaus R, Reith W, Yilmaz U. Retrospective analysis of intracranial aneurysms after flow diverter treatment including color-coded imaging (syngo iFlow) as a predictor of aneurysm occlusion. *Interventional Neuroradiology*. 2021 Jun 9;28(2):190–200.
34. Fang K, Zhao J, Luo M, Xue Y, Wang H, Ye L, Zhang X, Zheng L, Shu C. Quantitative analysis of renal blood flow during thoracic endovascular aortic repair in type B aortic dissection using syngo iFlow. *Quant Imaging Med Surg*. 2021 Aug 1;11(8):3726–3734.

35. Thurner A, Augustin AM, Bley TA, Kickuth R. 2D-perfusion angiography for intra-procedural endovascular treatment response assessment in chronic mesenteric ischemia: a feasibility study. *BMC Med Imaging*. 2022 Dec 1;22(1):1–12.
36. Class 2 Device Recall SmartPerfusion [Internet]. [cited 2024 Nov 15]. Available from:  
<https://www.accessdata.fda.gov/scripts/cdrh/cfdocs/cfres/res.cfm?id=198920>
37. Saito A, Inoue M, Kon H, Imaruoka S, Basaki K, Midorikawa H, Sasaki T, Nishijima M. Effectiveness of intraarterial administration of fasudil hydrochloride for preventing symptomatic vasospasm after subarachnoid hemorrhage. *Acta Neurochir Suppl*. 2015;120:297–301.
38. Kawarada O. Color coded circulation in the field of infrapopliteal intervention. *Cardiovasc Interv Ther*. 2021 Jan 1;36(1):131–133.
39. Alizadeh LS, Gyánó M, Góg I, Szigeti K, Osváth S, Kiss JP, Yel I, Koch V, Grünwald LD, Vogl TJ, Booz C. Initial Experience Using Digital Variance Angiography in Context of Prostatic Artery Embolization in Comparison with Digital Subtraction Angiography. *Acad Radiol*. 2023 Apr 1;30(4):689–697.
40. Simgen A, Mayer C, Kettner M, Mühl-Benninghaus R, Reith W, Yilmaz U. Retrospective analysis of intracranial aneurysms after flow diverter treatment including color-coded imaging (syngo iFlow) as a predictor of aneurysm occlusion. *Interventional Neuroradiology*. 2022 Apr 1;28(2):190–200.
41. Brunozzi D, Shakur SF, Charbel FT, Alaraj A. Intracranial contrast transit times on digital subtraction angiography decrease more in patients with delayed intraparenchymal hemorrhage after Pipeline. *Interventional Neuroradiology*. 2018 Apr 1;24(2):140–145.
42. Gupta V, Chinchure S, Goel G, Jha AN, Gupta A, Narang KS. Coil embolization of intracranial aneurysms with ipsilateral carotid stenosis: Technical considerations. *Turk Neurosurg*. 2014;24(4):587–592.

43. Chen CW, Hsu LS, Weng JC, Weng HH, Ye YL, Hsu SL, Lin WM. Assessment of small hepatocellular carcinoma: Perfusion quantification and time-concentration curve evaluation using color-coded and quantitative digital subtraction angiography. *Medicine (United States)*. 2018 Nov 1;97(48).
44. Lin EY, Lee RC, Guo WY, Wu FCH, Gehrisch S, Kowarschik M. Three-Dimensional Quantitative Color-Coding Analysis of Hepatic Arterial Flow Change during Chemoembolization of Hepatocellular Carcinoma. *Journal of Vascular and Interventional Radiology*. 2018 Oct 1;29(10):1362–1368.
45. Jens S, Marquering HA, Koelemay MJW, Reekers JA. Perfusion Angiography of the Foot in Patients with Critical Limb Ischemia: Description of the Technique. *Cardiovasc Intervent Radiol*. 2015 Dec 13;38(1):201–205.
46. Yoneyama F, Osaka M, Sato F, Sakamoto H, Hiramatsu Y. Efficacy of Two-Dimensional Perfusion Angiography for Evaluations after Infrapopliteal Bypass Surgery for Critical Limb Ischemia. *Ann Vasc Dis*. 2018 Jun 25;11(2):248.
47. Strother CM, Bender F, Deuerling-Zheng Y, Royalty K, Pulfer KA, Baumgart J, Zellerhoff M, Aagaard-Kienitz B, Niemann DB, Lindstrom ML. Parametric color coding of digital subtraction angiography. *AJNR Am J Neuroradiol*. 2010 May;31(5):919–924.
48. Wen WL, Fang Y Bin, Yang PF, Zhang YW, Wu YN, Shen H, Ge JJ, Xu Y, Hong B, Huang QH, Liu JM. Parametric Digital Subtraction Angiography Imaging for the Objective Grading of Collateral Flow in Acute Middle Cerebral Artery Occlusion. *World Neurosurg*. 2016;88:119–125.
49. Göllitz P, Struffert T, Lücking H, Rösch J, Knossalla F, Ganslandt O, Deuerling-Zheng Y, Doerfler A. Parametric color coding of digital subtraction angiography in the evaluation of carotid cavernous fistulas. *Clin Neuroradiol*. 2013;23(2):113–120.
50. Göllitz P, Muehlen I, Gerner ST, Knossalla F, Doerfler A. Ultraearly assessed reperfusion status after middle cerebral artery recanalization predicting clinical outcome. *Acta Neurol Scand*. 2018 Jun 1;137(6):609–617.

51. Kostrzewa M, Kara K, Pilz L, Mueller-Muertz H, Rathmann N, Schoenberg SO, Diehl SJ. Treatment Evaluation of Flow-Limiting Stenoses of the Superficial Femoral and Popliteal Artery by Parametric Color-Coding Analysis of Digital Subtraction Angiography Series. *Cardiovasc Intervent Radiol*. 2017 Aug 1;40(8):1147–1154.
52. Tinelli G, Minelli F, De Nigris F, Vincenzoni C, Filipponi M, Bruno P, Massetti M, Flex A, Iezzi R. The potential role of quantitative digital subtraction angiography in evaluating type B chronic aortic dissection during TEVAR: Preliminary results. *Eur Rev Med Pharmacol Sci*. 2018;22(2):516–522.
53. Chen Y, Xu W, Liu J, Zhao C, Cao X, Wang R, Feng D, Zhang R, Zhou X. Color-coded parametric imaging support display of vessel hemorrhage—an in vitro experiment and clinical validation study. *Front Cardiovasc Med*. 2024;11:1387421.
54. Badar W, Anitescu M, Ross B, Wallace S, Uy-Palmer R, Ahmed O. Quantifying Change in Perfusion after Genuicular Artery Embolization with Parametric Analysis of Intraprocedural Digital Subtraction Angiograms. *J Vasc Interv Radiol*. 2023 Dec 1;34(12):2190–2196.
55. Meine TC, Maschke SK, Kirstein MM, Jaeckel E, Lena BS, Werncke T, Dewald CLA, Wacker FK, Meyer BC, Hinrichs JB. Evaluation of perfusion changes using a 2D Parametric Parenchymal Blood Flow technique with automated vessel suppression following partial spleen embolization in patients with hypersplenism and portal hypertension. *Medicine (United States)*. 2021 Feb 19;100(7):E24783.
56. Rivera R, Sordo JG, Echeverria D, Badilla L, Pinto C, Merino-Osorio C. Quantitative evaluation of arteriovenous malformation hemodynamic changes after endovascular treatment using parametric color coding: A case series study. *Interv Neuroradiol*. 2017 Dec 1;23(6):650–655.
57. Gölitz P, Struffert T, Rösch J, Ganslandt O, Knossalla F, Doerfler A. Cerebral aneurysm treatment using flow-diverting stents: in-vivo visualization of flow alterations by parametric colour coding to predict aneurysmal occlusion: preliminary results. *Eur Radiol*. 2015 Feb 1;25(2):428–435.

58. Hussein AE, Shownkeen M, Thomas A, Stapleton C, Brunozzi D, Nelson J, Naumgart J, Linninger A, Atwal G, Alaraj A. 2D parametric contrast time-density analysis for the prediction of complete aneurysm occlusion at six months' post-flow diversion stent. *Interventional Neuroradiology*. 2020 Aug 1;26(4):468.
59. Whitehead JF, Hoffman CA, Wagner MG, Periyasamy S, Meram E, Keller ME, Speidel MA, Laeseke PF. Quantitative Digital Subtraction Angiography Measurement of Arterial Velocity at Low Radiation Dose Rates. *Cardiovasc Intervent Radiol*. 2024 Aug 1;47(8):1119–1126.
60. Lucatelli P, Rocco B, Ciaglia S, Teodoli L, Argirò R, Guiu B, Saba L, Vallati G, Spiliopoulos S, Patrone L, Gyánó M, Góg I, Osváth S, Szigeti K, Kiss JP, Catalano C. Possible use of Digital Variance Angiography in Liver Transarterial Chemoembolization: A Retrospective Observational Study. *Cardiovasc Intervent Radiol*. 2023 May 1;46(5):635.
61. Góg I, Sótonyi P, Nemes B, Kiss JP, Szigeti K, Osváth S, Gyánó M. Quantitative Comparison of Color-Coded Parametric Imaging Technologies Based on Digital Subtraction and Digital Variance Angiography: A Retrospective Observational Study. *J Imaging*. 2024, Vol 10, Page 260. 2024 Oct 18;10(10):260.
62. Rose A. The sensitivity performance of the human eye on an absolute scale. *J Opt Soc Am*. 1948;38(2):196–208.
63. Rose A. A unified approach to the performance of photographic film, television pickup tubes, and the human eye. *Journal of the Society of Motion Picture Engineers*. 1946;47(4)
64. Rose A. *Vision: Human and Electronic*. Wolfe WL, editor. New York - London: Plenum Press; 1973.
65. Rose A. Quantum and noise limitations of the visual process. *J Opt Soc Am*. 1953;43(9):715–716.
66. Burgess AE. The Rose model, revisited. *J Opt Soc Am*. 1999;16(3):633.
67. Wagner RF, Brown DG. Unified SNR analysis of medical imaging systems. *Phys Med Biol*. 1985;30(6):489–518.

68. Cunningham IA, Model AR. Signal-to-noise optimization of medical imaging systems 2 . IMAGE QUALITY : ROSE MODEL TO NOISE-EQUIVALENT NUMBER OF QUANTA. America (NY). 1999;16(3):9–11.
69. Ierardi AM, Pesapane F, Hörer T, Reva V, Carrafiello G. Embolization and its Limits: Tips and Tricks. J Endovasc Resusc Trauma Manag. 2019 Oct 28;3(3):120–130.
70. Liu J, Gong YY, Ran C, Liu HJ, Zeng DS, Feng YG. Case report of avascular necrosis of the glans penis after PAE embolization. BMC Urol. 2023 Dec 1;23(1).
71. Cornelis FH, Barral M, Jenoudet H, Boutault JR, Zurlinden O. Successful conservative management of non-targeted embolization of the penile glans after prostate artery embolization. Diagn Interv Imaging. 2020 Sep 1;101(9):617–618.
72. Sédat J, Arnoffi P, Poirier F, Jamjoom M, Raffaelli C, Colomb F, Chau Y. Non-target embolic events during prostatic embolization with ethylene vinyl alcohol copolymer (EVOH). CVIR Endovasc. 2023 Dec 1;6(1):1–8.

## **X. BIBLIOGRAPHY OF THE CANDIDATE'S PUBLICATIONS**

### **Publications that are the subject of the doctoral thesis:**

Alizadeh LS, Gyánó M, **Góg I**, Szigeti K, Osváth S, Kiss JP, Yel I, Koch V, Grünwald LD, Vogl TJ, Booz C. Initial Experience Using Digital Variance Angiography in Context of Prostatic Artery Embolisation in Comparison with Digital Subtraction Angiography. *Acad Radiol*. 2023 Apr 1;30(4):689–697.

Lucatelli P, Rocco B, Ciaglia S, Teodoli L, Argirò R, Guiu B, Saba L, Vallati G, Spiliopoulos S, Patrone L, Gyánó M, **Góg I**, Osváth S, Szigeti K, Kiss JP, Catalano C. Possible use of Digital Variance Angiography in Liver Transarterial Chemoembolisation: A Retrospective Observational Study. *Cardiovasc Intervent Radiol*. 2023 Apr 19;46(5):635–642.

**Góg I**, Sótonyi P, Nemes B, Kiss JP, Szigeti K, Osváth S, Gyánó M. Quantitative Comparison of Color-Coded Parametric Imaging Technologies Based on Digital Subtraction and Digital Variance Angiography: A Retrospective Observational Study. *J Imaging*. 2024 Oct 18.

### **Other publications related to the topics mentioned in this thesis**

Gyánó M, **Góg I**, Óriás VI, Ruzsa Z, Nemes B, Csobay-Novák C, Oláh Z, Nagy Z, Merkely B, Szigeti K, Osváth S, Sótonyi P. Kinetic Imaging in Lower Extremity Arteriography: Comparison to Digital Subtraction Angiography. *Radiology*. 2018 Oct 16;290(1):246–253.

Óriás VI, Gyánó M, **Góg I**, Szöllősi D, Veres DS, Nagy Z, Csobay-Novák C, Zoltán O, Kiss JP, Osváth S, Szigeti K, Zoltán R, Sótonyi P. Digital Variance Angiography as a Paradigm Shift in Carbon Dioxide Angiography. *Invest Radiol*. 2019 Mar 1;54(7):428–436.

Gyánó M, Csobay-Novák C, Berczeli M, **Góg I**, Kiss JP, Szigeti K, Osváth S, Nemes B. Initial Operating Room Experience with Digital Variance Angiography in Carbon Dioxide-Assisted Lower Limb Interventions: A Pilot Study. *Cardiovasc Intervent Radiol*. 2020 May 31;43(8):1226–1231.

Bastian MB, König AM, Viniol S, Gyánó M, Szöllősi D, **Góg I**, Kiss JP, Osvath S, Szigeti K, Mahnken AH, Thomas RP. Digital Variance Angiography in Lower-Limb Angiography with Metal Implants. *Cardiovasc Intervent Radiol*. 2020 Nov 3;44(3):452–459.

Gyánó M, Berczeli M, Csobay-Novák C, Szöllősi D, Óriás VI, **Góg I**, Kiss JP, Veres DS, Szigeti K, Osváth S, Pataki Á, Juhász V, Oláh Z, Sótonyi P, Nemes B. Digital variance angiography allows about 70% decrease of DSA-related radiation exposure in lower limb X-ray angiography. *Sci Rep*. 2021 Nov 8;11(1).

Thomas RP, Bastian MB, Viniol S, König AM, Amin SS, Eldergash O, Schnabel J, Gyánó M, Szöllősi D, **Góg I**, Kiss JP, Osváth S, Szigeti KP, Mahnken AH. Digital Variance Angiography in Selective Lower Limb Interventions. *J Vasc Interv Radiol*. 2021 Oct 13;33(2):104–112.

Sótonyi P, Berczeli M, Gyánó M, Legeza P, Mihály Z, Csobay-Novák C, Pataki Á, Juhász V, **Góg I**, Szigeti K, Osváth S, Kiss JP, Nemes B. Radiation Exposure Reduction by Digital Variance Angiography in Lower Limb Angiography: A Randomized Controlled Trial. *J Cardiovasc Dev Dis*. 2023 Apr 30;10(5):198.

**Góg I**, Sótonyi P, Kiss JP, Szigeti K. Application of Color-coded Digital Variance Angiography in Endovascular Interventions. *Scientia et Securitas*. 2024 Aug 5;4(4):240–248

#### **Publications unrelated to this thesis**

Jávor P, Hanák L, Hegyi P, Csonka E, Butt E, Horváth T, **Góg I**, Lukacs A, Soós A, Rumbus Z, Pákai E, Toldi J, Hartmann P. Predictive value of tachycardia for mortality in trauma-related haemorrhagic shock: a systematic review and meta-regression. *BMJ Open*. 2022 Oct 1;12(10):e059271.

## **XI. FUNDING STATEMENT**

The presented studies have been funded by the European Union's Horizon 2020 EIC Accelerator Program under grant agreement "No 968430 KMIT-ACC", by the Ministry of Innovation and Technology of Hungary from the National Research, Development and Innovation Fund (NKFI) under grant agreements "NVKP-16-1-2016-0017 National Heart Program", "2020-1.1.5-GYORSÍTÓSÁV-2021-00018", "Thematic Excellence Program 2020-4.1.1.-TKP2020".

This project (n.o. 1007190) has also been supported by the Ministry of Culture and Innovation of Hungary from the National Research, Development and Innovation Fund, financed under the „NKFI KDP-2020” funding scheme (recipient Góg I.).

## **XII. ACKNOWLEDGEMENTS**

I wish to express my profound gratitude to my supervisors, Dr Péter Sótonyi, Dr János Kiss and Dr Krisztián Szigeti for their unwavering support and insightful critiques throughout my research journey. I am also deeply thankful to my colleagues at Kinepict Health Ltd., especially Dr Szabolcs Osváth, for letting me be part of their team. I extend my appreciation to Dr Marcell Gyánó from the Department of Interventional Radiology at the Heart and Vascular Center of Semmelweis University, whose expertise in interventional radiology was crucial for my experiments. I am equally thankful for Dr Pierleone Lucatelli from the University Hospital “Policlinico Umberto I” (Rome) and Dr Leona Alizadeh from Goethe University Frankfurt for letting me take part in their research. My appreciation also goes to the faculty and staff in the Department of Vascular Surgery at the Heart and Vascular Center of Semmelweis University, whose resources and assistance have been invaluable. I am also very grateful for the honest critique received from my opponents during the home defence process, Dr Tímea Hevér and Dr Zsuzsanna Mihály, as their insights and comments helped me to greatly improve the quality of my dissertation.

# Possible use of Digital Variance Angiography in Liver Transarterial Chemoembolization: A Retrospective Observational Study

Pierleone Lucatelli<sup>1</sup>  · Bianca Rocco<sup>1</sup> · Simone Ciaglia<sup>1</sup> · Leonardo Teodoli<sup>1</sup> · Renato Argirò<sup>2</sup> · Boris Guiu<sup>3</sup> · Luca Saba<sup>4</sup> · Giulio Vallati<sup>5</sup> · Stavros Spiliopoulos<sup>6</sup> · Lorenzo Patrone<sup>7</sup> · Marcell Gyánó<sup>8,9</sup> · István Góg<sup>8,10</sup> · Szabolcs Osváth<sup>9,11</sup> · Krisztian Szigeti<sup>9,11</sup> · János P. Kiss<sup>9</sup> · Carlo Catalano<sup>1</sup>

Received: 26 December 2022 / Accepted: 11 March 2023 / Published online: 19 April 2023  
© The Author(s) 2023

## Abstract

**Purpose** Digital variance angiography (DVA), a recently developed image processing technology, provided higher contrast-to-noise ratio (CNR) and better image quality (IQ) during lower limb interventions than digital subtraction angiography (DSA). Our aim was to investigate whether this quality improvement can be observed also during liver transarterial chemoembolization (TACE).

**Materials and Methods** We retrospectively compared the CNR and IQ parameters of DSA and DVA images from 25 patients (65% male, mean  $\pm$  SD age: 67.5  $\pm$  11.2 years) underwent TACE intervention at our institute. CNR was calculated on 50 images. IQ of every image set was evaluated by 5 experts using 4-grade Likert scales. Both single image evaluation and paired image comparison were performed in a blinded and randomized manner. The diagnostic value was evaluated based on the possibility to identify lesions and feeding arteries.

**Results** DVA provided significantly higher CNR (mean  $CNR_{DVA}/CNR_{DSA}$  was 1.33). DVA images received

significantly higher individual Likert score (mean  $\pm$  SEM 3.34  $\pm$  0.08 vs. 2.89  $\pm$  0.11, Wilcoxon signed-rank  $p < 0.001$ ) and proved to be superior also in paired comparisons (median comparison score 1.60 [IQR:2.40], one sample Wilcoxon  $p < 0.001$  compared to equal quality level). DSA could not detect lesion and feeding artery in 28 and 36% of cases, and allowed clear detection only in 22% and 16%, respectively. In contrast, DVA failed only in 8 and 18% and clearly revealed lesions and feeding arteries in 32 and 26%, respectively.

**Conclusion** In our study, DVA provided higher quality images and better diagnostic insight than DSA; therefore, DVA could represent a useful tool in liver TACE interventions.

**Level of evidence** III Non-consecutive study.

**Keywords** Digital variance angiography (DVA) · Digital subtraction angiography (DSA) · Transarterial chemoembolization (TACE) · Image quality (IQ) · Contrast-to-noise ratio (CNR)

✉ Bianca Rocco  
biancarocco.br@gmail.com

Pierleone Lucatelli  
pierleone.lucatelli@gmail.com

<sup>1</sup> University Hospital “Policlinico Umberto I, Sapienza University of Rome, Rome, Italy

<sup>2</sup> Department of Interventional Radiology, University of Rome Tor Vergata, Rome, Italy

<sup>3</sup> Montpellier University Hospital, Montpellier, France

<sup>4</sup> Department of Medical Sciences, University of Cagliari, Cagliari, Italy

<sup>5</sup> Interventional Radiology Unit of “IRCCS Istituto Nazionale Tumori Regina Elena”, Rome, Italy

<sup>6</sup> Department of Radiology, Interventional Radiology Unit, National and Kapodistrian University of Athens, Athens, Greece

<sup>7</sup> West London Vascular and Interventional Centre, Northwick Park Hospital, London, UK

<sup>8</sup> Department of Interventional Radiology, Heart and Vascular Center, Semmelweis University, Budapest, Hungary

<sup>9</sup> Kinect Health Ltd, Budapest, Hungary

<sup>10</sup> Department of Vascular and Endovascular Surgery, Heart and Vascular Center, Semmelweis University, Budapest, Hungary

<sup>11</sup> Department of Biophysics and Radiation Biology, Semmelweis University, Budapest, Hungary

## Introduction

Transarterial chemoembolization (TACE) represents the standard of care for early or intermediate stage liver cancer [1] and hepatic metastases from colorectal cancer in patients not suitable for surgery/ablation [2]. The updated guideline documents clearly indicate the need of advanced imaging modality to guide such interventions, thus allowing a better clinical response. Patients selected for TACE, may need multiple sessions of treatment, depending on the total tumour burden. In this respect, radiation exposure and contrast media administration throughout the procedure should be kept at the minimum [3].

Digital variance angiography (DVA), a recently developed image processing technology, might address these problems. The method is based on the principles of kinetic imaging [4]. In contrast with digital subtraction angiography (DSA), DVA does not use a mask image, but calculates standard deviation for each pixel in an unsubtracted image series. This statistical analysis enhances the contrast agent-generated signal and suppresses the noise, therefore provides a higher contrast-to-noise ratio (CNR) and an improved image quality (IQ). This excess quality, also termed as quality reserve, has already been demonstrated in lower limb angiography using either iodinated contrast media (ICM) [5–7] or carbon dioxide (CO<sub>2</sub>) [8, 9] as a contrast agent. The quality reserve of DVA provides opportunity for dose management solutions [10, 11], which could be beneficial not only in lower limb procedures but also, and even more, in a wide range of endovascular interventions, particularly the ones involving visceral vessels which usually require higher radiation exposure to the patient and the operator.

The aim of the present study is to compare the performance of DSA and DVA in liver TACE procedures. For this reason, we compared the CNR and IQ of the two image processing technologies, and also their specific diagnostic value to identify and characterise liver tumours and feeding arteries of lesions in patients with hepatocellular cancer.

## Materials and Methods

In our single-centre observational study, angiographical image series of 25 patients affected by hepatocarcinoma and who underwent TACE, were retrospectively collected and processed. All procedures were in accordance with the ethical standards of the institutional and/or national research committee and with the 1964 Helsinki Declaration and its later amendments. Because of the retrospective nature of the study, informed consent was not required. All indications for TACE treatment were decided by a

multidisciplinary tumour board (composed by a surgeon, oncologist, hepatologist and body radiology).

## Study Design

Two pre-embolization acquisitions (a frontal and an oblique view) were included in the study from each patient. The same unsubtracted series was used to generate DSA and DVA images using the Siemens Syngo and the Kinepict Medical Imaging Tool software, respectively. The CNR values and the ratio were calculated for each image pair, and the IQ was evaluated by 4-grade Likert scales in blinded and randomized surveys. The visual evaluation included single image scoring and paired image comparison (for details see below). The diagnostic value was evaluated by the ability of the readers to identify lesions and their feeding arteries.

## Image Acquisition

TACE procedures were performed by two interventional radiologists with more than 13 years of experience according to the standardized institutional protocol. Following femoral or radial access under local anaesthesia, a diagnostic catheter (Simmons 1, Cordis, Hialeah, FL, USA) was introduced in the common hepatic artery, and two angiograms (an anteroposterior and 25° right anterior oblique) were acquired at 3 FPS on a Siemens Artis Zee system and a Syngo XWP VB21N workstation (Siemens Healthcare). A Medrad Avanta Mark V ProVis automated injector (Bayer) was used for injecting 12–15 ml/injection contrast media (Ultravist 370, Bayer) at 3–5 ml/s flowrate from a 4 Fr catheter positioned in proper hepatic artery. A cone-beam CT was also acquired to obtain the liver tumour vascularization map and lesion's feeders detection. On the basis of these two imaging modalities, the best location to perform embolization by microcatheter (Progreat, Terumo, Tokyo, Japan) was identified, and the embolization was occurred using LifePearl (Terumo, Japan) 100 µm or DC beads M1 (Boston Scientific) microspheres.

## Image Processing

Stacked DSA images were generated using the opacification function, and the brightness/contrast was optimised on the Syngo XWP VB21N workstation (Siemens Healthineers AG, Erlangen, Germany). The raw unsubtracted acquisitions were exported from the Siemens workstation, and the corresponding DVA images were generated and

post-processed retrospectively from the same unsubtracted raw series using the Kinect Medical Imaging Tool v.5.0 (Kinect Health, Budapest, Hungary). The post-processed DSA and DVA images were saved in DICOM format and were used for CNR calculations and visual evaluation.

### CNR Analysis

For CNR measurements, regions of interest (ROI) were defined on vessels and background regions by using Image J (v.2.0.0-rc-68/1.52e, Creative Common License, NIH) Rueden [12]. The vascular and adjacent background ROI were placed in pairs. The same ROI sets were used on all corresponding DSA and DVA images. ROI positions were adjusted when patient positioning or pixel shifting caused slight geometric differences. CNR values were calculated for all ROI pairs individually according to the following formula, wherein  $Mean_v$  and  $Mean_b$  referred to mean pixel intensity values of the vascular and background ROI, respectively, and  $Std_b$  being the background standard deviation (Rose) [13]

$$CNR = \frac{|Mean_v - Mean_b|}{Std_b}$$

$CNR_{DVA}/CNR_{DSA}$  ratios ( $R$ ) for each corresponding DVA and DSA ROIs were calculated.

### Visual Evaluation

Visual evaluation was performed by five interventional radiologist experts in the field of liver catheter-based treatments with at least 15 years of experience. The readers were not involved in the treatment of the enrolled patients.

In the single image evaluation only one, randomly selected DSA or DVA image was visible at a time. The readers, blinded to the processing modality, evaluated the IQ using the following 4-grade Likert scale:

1. Poor IQ, vascular structures are not distinguishable
2. Low IQ, good visualization of lobar vessels only
3. Medium IQ, good visualization of lobar and segmental vessels
4. Good IQ, good visualization of lobar, segmental and subsegmental vessels

The diagnostic value was evaluated in this survey as the readers had to judge the visibility of lesions and feeding arteries using the following options:

1. Not visible
2. Suspected but not definitive
3. Clear identification

The IQ and diagnostic value were also evaluated in a paired comparison, when a DSA and the corresponding DVA image were shown simultaneously (but the image type was undisclosed). The readers had to select a preferred image and compare the IQ and diagnostic value based on the visibility of small vessels, lesions and feeding arteries. The following 5-grade preference scale was used:

1. No difference
2. Slightly better
3. Moderate differences
4. Major differences
5. Better in every aspect

The image type was never disclosed, and the order of image pairs (i.e. the appearance on the left or right side of the screen) or the appearance of single images was randomized. Thus, all rating scales were implemented in blinded and randomized web-based surveys, and the data were collected automatically in a database for later processing.

### Statistical Analysis

Calculations of CNR and  $R$  means, medians and interquartile ranges were performed using Excel 2016 (Microsoft, Redmond, WA). CNR values were compared by the Wilcoxon signed-rank test (Prism 8.4.2., GraphPad).

For visual evaluation scores, the mean and standard error of mean (SEM) were calculated. Because of the non-Gaussian distribution of data, the median and interquartile range (Q1–Q3) were also determined. The single image scores were compared by the Wilcoxon signed-rank test, the results of the paired image comparison were analysed by the one sample Wilcoxon test to investigate the relation of DSA and DVA images (equal quality or superiority), whereas the single image diagnostic results were analysed by the two-sided Z test. Kendall's  $W$  was calculated to describe interrater agreement. The level of significance was set at  $p < 0.05$  in all tests.

## RESULTS

### Patients

Patients ( $n = 25$ , 65% male, mean  $\pm$  SD age:  $67.5 \pm 11.2$  years) with previously diagnosed hepatocarcinoma nodules received TACE treatment between January 2021 and June 2021 at the University Hospital 'Policlinico Umberto I', and were retrospectively enrolled for image analysis in a consecutive manner.

**Table 1** Contrast-to-noise ratio (CNR) analysis. Data are expressed as mean  $\pm$  standard error of mean (SEM), and as median and interquartile range (IQR). Wilcoxon signed-rank test was used for

statistical comparison, significance level was set at  $p < 0.05$ . DVA: digital variance angiography and DSA: digital subtraction angiography

	CNR		R	Wilcoxon signed-rank test
	DSA	DVA		
Mean $\pm$ SEM	15.01 $\pm$ 0.30	20.14 $\pm$ 0.58	1.34 $\pm$ 0.02	$p < 0.001$
Median (IQR)	13.34 (9.21)	16.02 (14.89)	1.24 (0.69)	

## CNR Results

A total of 686 ROI pairs were measured on 50 images. Table 1 summarizes the results of the CNR measurements. The mean ( $\pm$  SEM) CNR of DVA images (20.14  $\pm$  0.58) was significantly higher than that of DSA images (15.02  $\pm$  0.31, Wilcoxon signed-rank  $p < 0.001$ ), the R (CNR<sub>DVA</sub>/CNR<sub>DSA</sub>) value was 1.34  $\pm$  0.04 (Fig. 1).

## Visual Evaluations Results

Readers evaluated 50 DSA and 50 DVA images in blinded, randomized manner. In the single image evaluation (when only one image appeared on the screen), DVA images received significantly higher Likert score (mean  $\pm$  SEM DVA 3.34  $\pm$  0.08 vs. DSA 2.89  $\pm$  0.11, Wilcoxon signed-rank  $p < 0.001$ ), and similar difference was seen in the median and IQR values (DSA 3.0, IQR 1.2 vs. DVA 3.4, IQR 0.55) (Fig. 2). The Kendall W values showed substantial agreement for DSA (0.610,  $p < 0.001$ ) and moderate agreement for DVA (0.423  $p < 0.001$ ).

The diagnostic value was also evaluated during the single image survey. Readers evaluated the visibility of lesions and feeding arteries. DVA failed to visualize these critically important structures in significantly less images than DSA (8 vs. 28% for lesions, two-sided Z  $p < 0.01$ ; and 16 vs. 32% for feeding arteries,  $p < 0.05$ ). There was no significant difference in the proportion of suspected and clearly visualized structures, although DVA showed a tendency to enhance visualization, as it increased by 45 and 63% the number of images with clear lesion and feeding artery identification, respectively (Fig. 3). The interrater agreement was moderate for both feeding artery (Kendall's W value: DSA 0.541,  $p < 0.001$ , DVA 0.551,  $p < 0.001$ ) and lesion detection (Kendall's W value: DSA 0.564,  $p < 0.001$ , DVA 0.561,  $p < 0.001$ ).

The paired comparison allowed a side-by-side evaluation of DSA and DVA images in a blinded and randomized manner. DVA was the preferred image in 80% of comparisons (Fig. 4, left panel), and the average score (mean  $\pm$  SEM) of the whole image set was 1.44  $\pm$  0.21,

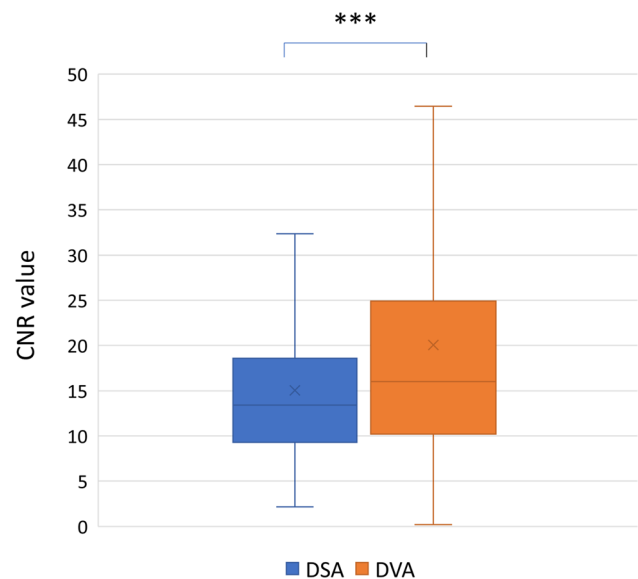


**Fig. 1** Contrast-to-noise ratio (CNR) results. The box and whisker plots show the median (line), mean (x), interquartile range (box) and internal fences (whiskers) of CNR values in each group. Data sets were analysed by the Wilcoxon signed-rank test (\*\* $p < 0.001$ ). DVA: digital variance angiography and DSA: digital subtraction angiography

the median score was 1.60 (IQR 2.4), significantly different from 0 (one-sample Wilcoxon  $p < 0.001$ ), which represented the equal quality level, indicating the superiority of DVA images (Fig. 4, right panel). The interrater agreement was also significant (Kendall's W value: 0.575,  $p < 0.001$ ). Representative image pairs are shown on Fig. 5.

## Discussion

The major aim of our study was to compare the performance of DSA and DVA in liver TACE intervention. Although the quality reserve of DVA has already been demonstrated in lower limb [5–8] and carotid [10] angiography, these anatomical regions are very different from the abdominal area, where bone shadow is less emphasized but bowel gas and intestinal movement artefacts might be significant. We have analysed the CNR, an

objective predictor, and visual evaluation, a subjective descriptor of image quality. In addition, the diagnostic value of the image types was also assessed.

In our study, CNR was significantly higher in DVA than DSA imaging. In terms of absolute values, the CNR DVA values were lower than those reported in other DVA applications: in lower extremity regions [5–8] and endovascular carotid interventions [10]. This may be due to

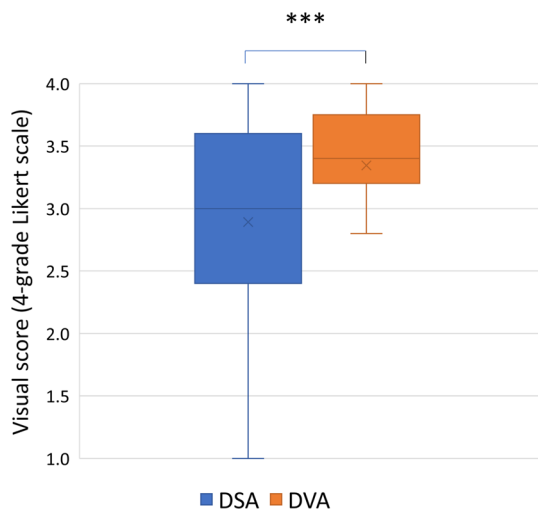


**Fig. 2** Single image evaluation results. A 4-grade Likert score was used in the blinded, randomized survey (see Materials and Methods) to evaluate the image quality of DSA and DVA images. The box and whisker plots show the median (line), mean (x), interquartile range (box) and internal fences (whiskers) of single image scores values in each group. Data sets were analysed by the Wilcoxon signed-rank test (\*\* $p < 0.001$ ). DVA: digital variance angiography and DSA: digital subtraction angiography

several factors that may have influenced the final results. During TACE procedures, motion artefacts may occur due to breathing, cardiac pulsations, and bowel gas may cause a loss of important information [14]. Regardless the fact that the obtained absolute CNR value was lower than in other anatomical regions, this was sufficient to provide an advantage of DVA technology over standard DSA in visual and diagnostic evaluation. Further DVA development, currently under investigation, may compensate movement artefact and eliminate bowel gases, thus potentially further ameliorating diagnostic performance even in the liver field of application.

The visual evaluation results showed that DVA provides higher image quality than DSA (Fig. 2), even if the inter-rater agreement was higher for the DSA images (probably, because this is the usual image type, the readers met before). Due to this quality advantage, DVA was able to improve the percentage of visible lesions (DVA 32% vs. DSA 22%) (Fig. 3) and to reduce the number of cases, in which angiography did not depict any lesion (DVA 8% vs. DSA 28%). Moreover, in terms of feeder vessel detection, readers evaluation also revealed a significant advantage of DVA technology over standard DSA. The blinded comparison of corresponding DVA and DSA images shows even more evidently the superiority of DVA in terms of overall diagnostic value. These data clearly demonstrate, how DVA technology may provide a major clinical benefit by allowing the operator to see more lesions and to better identify feeding vasculature during liver embolization procedure. DVA may be valuable also during more challenging TACE interventions (e.g. in case of hypo-vascular lesions or for tumours located high in the dome), when the

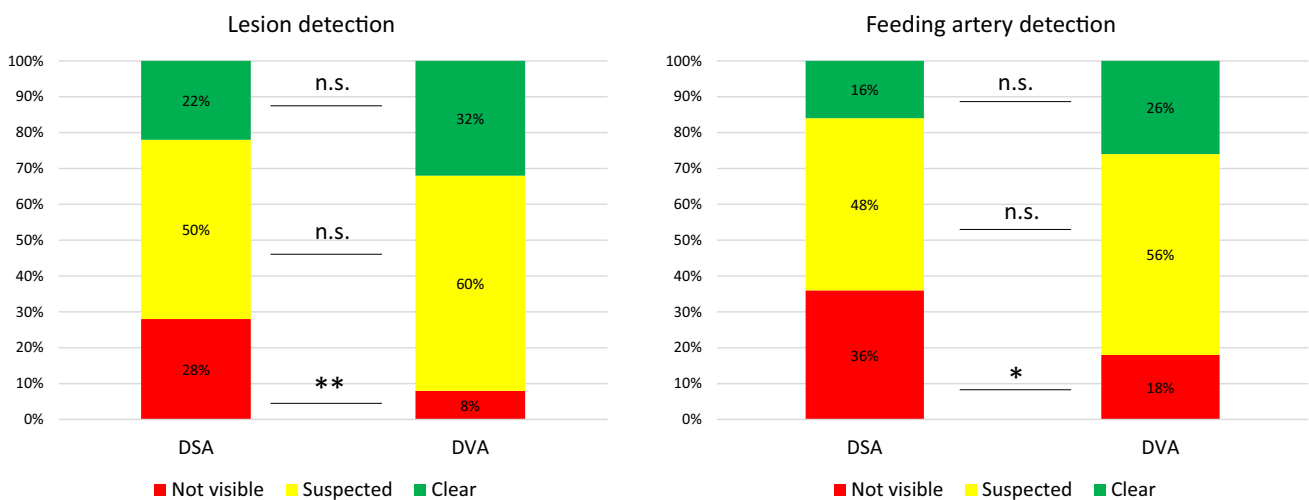


**Fig. 3** Comparison of the diagnostic value of DSA and DVA. Readers classified each image based on the ability to identify structures (lesion and feeding arteries) being critically important in TACE interventions. Two-sided Z test was used for the statistical

comparison of percentage data ( $*p < 0.05$ ,  $**p < 0.01$ ). TACE: TransArterial ChemoEmbolization; DSA: digital subtraction angiography and DVA: digital variance angiography



identification and characterization of lesions by standard imaging is more difficult, and consequently, their endovascular treatment is more complicated.

Our results might have further clinical implications. The observed quality reserve of DVA might be used to reduce the radiation exposure to patients and operators, and the amount of contrast medium administered, as already demonstrated earlier in other clinical settings: This technology allowed 50% reduction of contrast media in carotid angiography [10] and 70% reduction of radiation dose in lower limb angiography [11] without compromising the image quality and diagnostic value of stationary acquisitions. The possibility to reduce contrast medium and/or radiation dose administered during TACE interventions might be especially important, if we consider that patients selected for transarterial intervention may have impaired renal function and usually need more than one treatment session. Obviously, validation of these claims requires further clinical trials, but this study provides a rationale for the initiation of prospective dose management trials in TACE.

The study has some limitations. The number of patients is relatively low, in line with the design of a small cohort proof-of-concept study, even though the number of evaluated images fully complies with the recommendations of an FDA guideline on the testing X-ray imaging devices [15]. The breathing artefacts and bowel gases obviously impair the performance of DVA, which was reflected also by the smaller difference in CNR values between DSA and DVA. The quality reserve of DVA is clearly demonstrated even under the current conditions, and we are confident that new compensatory algorithms currently under development (which will reduce or eliminate these disturbing factors) will increase even more the gap between the two diagnostic modalities. Another possible limitation of this study is that the image processing was done off-line in a retrospective manner as the raw data were exported from the angiography computer. Nevertheless, the technology can be operated in quasi real-time, as the transfer and data processing take usually less than 2 s. Thus, the DVA image appears on the operating room monitor almost immediately. Of course, due to these circumstances, the technology cannot be used in fluoroscopy, but otherwise the 1–2 s delay is tolerable for stationary acquisitions. The advantages of DVA in real-time operation has already been validated in a previous study on CO<sub>2</sub>-assisted lower limb interventions [9], but the possible benefits in TACE interventions should be investigated in the future in a live setting, when the technology is fully integrated with the angiography system and DVA images are available in real time in the operating room.

## Conclusion

The results of this study present the application of digital variance angiography (DVA) in liver embolization procedures. Our data indicate that DVA provides better image quality and more diagnostic information than DSA; therefore, it might be a useful new tool in TACE procedures for the treatment of liver tumours. The observed quality reserve of DVA might be used for radiation dose and contrast agent reduction in TACE; however, these claims need validation by further prospective clinical studies.

**Acknowledgements** The study was supported by the European Union's Horizon 2020 EIC Accelerator program (968430 KMIT-ACC), and by the National Research, Development and Innovation Office of Hungary (2020-1.1.5-GYORSÍTÓSÁV-2021-00018).

**Funding** Open access funding provided by Università degli Studi di Roma La Sapienza within the CRUI-CARE Agreement.

## Declarations

**Conflict of interest** MG and IG are part-time, JPK is full-time employee of Kinepict Health Ltd. KS and SO are the owners and founders of Kinepict Health Ltd.

**Ethical Approval** All procedures performed in studies involving human participants were in accordance with the ethical standards of the institutional and/or national research committee and with the 1964 Helsinki Declaration and its later amendments or comparable ethical standards. For this type of study, formal consent is not required.

**Open Access** This article is licensed under a Creative Commons Attribution 4.0 International License, which permits use, sharing, adaptation, distribution and reproduction in any medium or format, as long as you give appropriate credit to the original author(s) and the source, provide a link to the Creative Commons licence, and indicate if changes were made. The images or other third party material in this article are included in the article's Creative Commons licence, unless indicated otherwise in a credit line to the material. If material is not included in the article's Creative Commons licence and your intended use is not permitted by statutory regulation or exceeds the permitted use, you will need to obtain permission directly from the copyright holder. To view a copy of this licence, visit <http://creativecommons.org/licenses/by/4.0/>.

## References

1. Forner A, Reig ME, Rodriguezde Lope C, Bruix J. Current strategy for staging and treatment: the bclc update and future prospects. *Semin Liver Dis.* 2010;30:61–74. <https://doi.org/10.1055/s-0030-1247133>.
2. Narayanan G, Barbery K, Suthar R, Guerrero G, Arora G. Transarterial chemoembolization using DEBIRI for treatment of hepatic metastases from colorectal cancer. *Anticancer Res.* 2013;33:2077–83.
3. Lucatelli P, Burrel M, Guiu B, de Rubeis G, van Delden O, Helmlinger T. CIRSE standards of practice on hepatic transarterial chemoembolisation. *Cardiovasc Intervent Radiol.* 2021;44:1851–67. <https://doi.org/10.1007/s00270-021-02968-1>.

4. Szigeti K, Máthé D, Osváth S. Motion based X-ray imaging modality. *IEEE Trans Med Imaging*. 2014;33:2031–8. <https://doi.org/10.1109/TMI.2014.2329794>.
5. Gyánó M, Góg I, Óriás VI, Ruzsa Z, Nemes B, Csobay-Novák C, Oláh Z, Nagy Z, Merkely B, Szigeti K, Osváth S, Sótónyi P. Kinetic imaging in lower extremity arteriography: comparison to digital subtraction angiography. *Radiology*. 2019;290:246–53. <https://doi.org/10.1148/radiol.2018172927>.
6. Bastian MB, König AM, Viniol S, Gyánó M, Szöllősi D, Góg I, Kiss JP, Osváth S, Szigeti K, Mahnken AH, Thomas RP. Digital variance angiography in lower-limb angiography with metal implants. *Cardiovasc Intervent Radiol*. 2021;44:452–9. <https://doi.org/10.1007/s00270-020-02697-x>.
7. Thomas RP, Bastian MB, Viniol S, König AM, Amin SS, Eldergash O, Schnabel J, Gyánó M, Szöllősi D, Góg I, Kiss JP, Osváth S, Szigeti KP, Mahnken AH. Digital variance angiography in selective lower limb interventions. *J Vasc Interv Radiol*. 2022;33:104–12. <https://doi.org/10.1016/j.jvir.2021.09.024>.
8. Óriás VI, Gyánó M, Góg I, Szöllősi D, Veres DS, Nagy Z, Csobay-Novák C, Zoltán O, Kiss JP, Osváth S, Szigeti K, Zoltán R, Sótónyi P. Digital variance angiography as a paradigm shift in carbon dioxide angiography. *Invest Radiol*. 2019;54:428–36. <https://doi.org/10.1097/RLI.0000000000000555>.
9. Gyánó M, Csobay-Novák C, Berczeli M, Góg I, Kiss JP, Szigeti K, Osváth S, Nemes B. Initial operating room experience with digital variance angiography in carbon dioxide-assisted lower limb interventions: a pilot study. *Cardiovasc Intervent Radiol*. 2020;43:1226–31. <https://doi.org/10.1007/s00270-020-02530-5>.
10. Óriás VI, Szöllősi D, Gyánó M, Veres DS, Nardai S, Csobay-Novák C, Nemes B, Kiss JP, Szigeti K, Osváth S, Sótónyi P, Ruzsa Z. Initial evidence of a 50% reduction of contrast media using digital variance angiography in endovascular carotid interventions. *Eur J Radiol Open*. 2020;17:100288. <https://doi.org/10.1016/j.ejro.2020.100288>.
11. Gyánó M, Berczeli M, Csobay-Novák C, Szöllősi D, Óriás VI, Góg I, Kiss JP, Veres DS, Szigeti K, Osváth S, Pataki Á, Juhász V, Oláh Z, Sótónyi P, Nemes B. Digital variance angiography allows about 70% decrease of DSA-related radiation exposure in lower limb X-ray angiography. *Sci Rep*. 2021;11:21790. <https://doi.org/10.1038/s41598-021-01208-3>.
12. Rueden CT, Schindelin J, Hiner MC, DeZonia BE, Walter AE, Arena ET, Eliceiri KW. ImageJ2: ImageJ for the next generation of scientific image data. *BMC Bioinformatics*. 2017;18:529. <https://doi.org/10.1186/s12859-017-1934-z>.
13. Rose A. Quantum and noise limitations of the visual process. *J Opt Soc Am*. 1953;43:715–6. <https://doi.org/10.1364/josa.43.000715>.
14. Becker LS, Dewald CLA, von Falck C, Werncke T, Maschke SK, Kloeckner R, Wacker FK, Meyer BC, Hinrichs JB. Effectuality study of a 3D motion correction algorithm in C-arm CTs of severely impaired image quality during transarterial chemoembolization. *Cancer Imaging*. 2022;22:37. <https://doi.org/10.1186/s40644-022-00473-3>.
15. FDA Center for Devices and Radiological Health. Guidance for the submission of 510(k)s for solid state X-ray imaging devices. 2016, Docket number: FDA-1997-N-0389

**Publisher's Note** Springer Nature remains neutral with regard to jurisdictional claims in published maps and institutional affiliations.



# Initial Experience Using Digital Variance Angiography in Context of Prostatic Artery Embolization in Comparison with Digital Subtraction Angiography

Leona S. Alizadeh, MD, Marcell Gyánó, MD, PhD, István Góg, MD, Krisztián Szigeti, PhD, Szabolcs Osváth, PhD, János P. Kiss, MD, PhD, DSc, Ibrahim Yel, MD, Vitali Koch, MD, Leon D. Grünwald, MD, Thomas J. Vogl, MD, Christian Booz, MD

**Rationale and Objectives:** In previous clinical studies digital variance angiography (DVA) provided higher contrast-to-noise ratio (CNR) and better image quality in lower extremity angiography than digital subtraction angiography (DSA). Our aim was to investigate whether DVA has similar quality reserve in prostatic artery embolization (PAE). The secondary aim was to explore the potential advantages of the color-coded DVA (ccDVA) technology in PAE.

**Material and Methods:** This retrospective study evaluated 108 angiographic acquisitions from 30 patients (mean  $\pm$  SD age  $68.0 \pm 8.9$ , range 41-87) undergoing PAE between May and October 2020. DSA and DVA images were generated from the same unsubtracted acquisition, and their CNR was calculated. Visual evaluation of DVA and DSA image quality was performed by four experienced interventional radiologists in a randomized, blinded manner. The diagnostic value of DSA and ccDVA images was also evaluated using clinically relevant criteria (visibility of small [ $< 2.5$  mm] and large arteries [ $> 2.5$  mm], feeding arteries and tissue blush) in a paired comparison. Data were analysed by the Wilcoxon signed rank test or the binomial test, the interrater agreement was determined by the Kendall W or Fleiss Kappa analysis.

**Results:** DVA provided 4.11 times higher median CNR than DSA (IQR: 1.72). The visual score of DVA images ( $4.40 \pm 0.05$ ) was significantly higher than that of DSA ( $3.39 \pm 0.07$ ,  $p < 0.001$ ). The Kendall W analysis showed moderate but significant agreement ( $W_{DVA} = 0.38$ ,  $W_{DSA} = 0.53$ ). The preference of ccDVA images was significantly higher in all criteria (63-89%) with an interrater agreement of 58-79%. The Fleiss Kappa range was 0.02-0.18, significant in all criteria except large vessels.

**Conclusion:** Our data show that DVA provides higher CNR and better image quality in PAE. This quality reserve might be used for dose management (reduction of radiation dose and contrast agent volume), and ccDVA technology has also a high potential to assist PAE interventions in the future.

**Key Words:** Angiography, Digital Subtraction, Diagnostic Imaging, Image Enhancement, Subtraction Technique.

© 2022 The Association of University Radiologists. Published by Elsevier Inc. This is an open access article under the CC BY license (<http://creativecommons.org/licenses/by/4.0/>)

**Abbreviations:** (BPH) Benign Prostatic Hyperplasia, (ccDVA) Color-Coded Digital Variance Angiography, (CNR) Contrast-to-Noise Ratio, (DSA) Digital Subtraction Angiography, (DVA) Digital Variance Angiography, (ICM) Iodinated Contrast Media, (LUTS) Lower Urinary Tract Symptoms, (NICE) National Institute for Health and Care Excellence, (PAE) Prostatic Artery Embolization, (ROI) Region Of Interest, (SEM) standard error of mean, (TURP) Transurethral Resection of the Prostate

Acad Radiol 2023; 30:689–697

From the The Institute for Interventional and Diagnostic Radiology, University Hospital Frankfurt, Germany (L.S.A., I.Y., V.K., L.D.G., T.J.V., C.B.); The Heart and Vascular Center, Semmelweis University, Budapest, Hungary (M.G., I.G.); Research Department, Kinect Health Ltd, Budapest, Hungary (M.G., I.G., K.S., S.O., J.P.K.); The Department of Biophysics and Radiation Biology, Semmelweis University, Budapest, Hungary (K.S., S.O.); The Department of Vascular Surgery, Hungarian Defence Forces Medical Centre, Budapest, Hungary (I.G.). Received March 12, 2022; revised May 11, 2022; accepted May 11, 2022. **Summary statement:** Digital Variance Angiography (DVA) and color-coded DVA provide better image quality and more information in prostatic artery embolization (PAE) than digital subtraction angiography, therefore these technologies might improve PAE procedures. Address correspondence to: L. S. A. e-mail: [leona.alizadeh@outlook.de](mailto:leona.alizadeh@outlook.de)

© 2022 The Association of University Radiologists. Published by Elsevier Inc. This is an open access article under the CC BY license (<http://creativecommons.org/licenses/by/4.0/>)  
<https://doi.org/10.1016/j.acra.2022.05.007>

## INTRODUCTION

**B**enign Prostatic Hyperplasia (BPH) is one of the most common and frequently treated diseases in elderly men. Prostatic artery embolization (PAE) is a new therapeutic approach for lower urinary tract symptoms (LUTS) associated with BPH (1). The positive effect of PAE on BPH-associated symptoms was first observed by Demerritt et al. in 2000 (2). Since then, PAE has been described as an effective and safe method (3,4) and since 2018 been recommended by the British guideline of the National Institute for Health and Care Excellence (NICE) (5). Increasing patient numbers indicate that PAE is gradually accepted as a treatment alternative to traditional transurethral resection of the prostate (TURP), mainly due to the minimally invasive one-day surgery approach, the lack of general anaesthesia, and a low complication rate (5,6).

PAE is usually performed in an angiography room under sterile conditions with C-arm image guidance using digital subtraction angiography (DSA) and fluoroscopy. The interventional radiologist has to identify the dominant feeding artery of the hyperplastic prostate region, then this artery has to be embolized in order to reduce blood supply of the target region without embolizing other important arteries (like pudendal arteries). Pre-existing conditions of elderly patients, such as atherosclerosis, arterial hypertension, or complex vascular anatomy complicate intravascular navigation of catheters and anatomical orientation and sometimes bilateral puncture or a two-stage procedure is required (3,5). During these steps a large number of DSA acquisitions are prepared, which can be accounted for the majority (80%–90%) of the total procedural radiation load. Due to this complexity of PAE interventions, high radiation exposures and amounts of contrast agent are needed (7), increasing the risk of radiation injury, nephropathy and loss of renal function (7–9).

A recently developed new image processing technology, digital variance angiography (DVA) might provide dose management solutions in PAE. DVA is based on the principles of kinetic imaging (10). While DSA records a native image before the injection of contrast media, and subtracts this mask from every subsequent contrasted image frame, DVA does not use a mask, but calculates the standard deviation of pixel intensities in an unsubtracted image series for each pixel. This mathematical algorithm extracts more information from the raw data than DSA, because it enhances the signal generated by contrast agents, but suppresses image noise. These features result in higher image quality, which has been verified in multiple clinical studies on lower limb angiography using either iodinated contrast media (ICM) (11–13) or carbon dioxide (14,15). This quality reserve might provide opportunity for the reduction of radiation exposure (16) or contrast media (17). Our primary aim was to compare the performance of DVA and DSA in terms of CNR and image quality, in order to investigate whether the precondition of dose management, the quality reserve of DVA can be observed

also in PAE. An additional aim was to investigate the potential advantages of color-coded DVA (ccDVA) – a recently developed DVA image modality suitable for the visualization of certain hemodynamic information – in the visibility of small [ $< 2.5$  mm] and large arteries [ $> 2.5$  mm], feeding arteries and tissue blush, as the recognition of these structures is critically important in PAE.

## MATERIALS AND METHODS

In our observational study image series were retrospectively collected from patients undergoing PAE at **\*\*\*BLINDED\*\*\***. Ethical approval was obtained from the Institutional Review Board (IRB no. 467-17) with a waiver for informed consent.

### Patients

Between May and October 2020, a total of 32 patients were screened for study inclusion. After exclusion of two patients due to incomplete PAE intervention (the patients could not collaborate to follow instructions, therefore the intervention could not be completed), 30 male patients were included consecutively. The number of patients was determined on the basis of an FDA Guideline developed for the concurrence testing of X-ray imaging devices (18). None of the patients underwent previous TURP, and 72% of patients received alpha-1-inhibitors (Prazosin, Tamsulosin) prior to the PAE treatment, but they were classified as therapy refractory or showed progredient LUTS under medication. Table 1 shows the detailed demographic data.

### Study Design

Each patient received a regular PAE-intervention with commonly used fluoroscopy and DSA image-guidance. DSA, DVA and ccDVA images were retrospectively generated from the stored unsubtracted acquisitions. As primary outcomes, the contrast-to-noise ratio (CNR) and the visual evaluation scores of DSA and DVA images were compared. An additional paired comparison was performed between DSA and ccDVA images. Fig. 1 shows the flow chart of the study.

### PAE Procedure

PERFECTED PAE technique (19) was applied, using unilateral puncture of the right femoral artery in Seldinger technique. To avoid false embolization and to avoid collaterals, the prostatic artery (PA) was reached superselectively with 2.4F microcatheters (Progreat; Terumo, Tokyo, Japan). The PA was embolized as distally as possible aiming for complete stasis. Bilateral embolization was performed in all treatments using 100–300  $\mu$ m embolizing spheres. PAE was planned on an outpatient basis so that all patients were discharged on the same day. No severe complications were observed.

**TABLE 1. Demographic Table. Patient Demographics: n Number of Patients. Values are Mean ± Standard Deviation (range); p < 0.05 Indicates a Significant Difference Between Pre- and Post-PAE Values. IPSS, International Prostate Symptom Score; QoL, Quality of Life; IIEF, International Index of Erectile Function; PAE, Prostate Artery Embolization; PV Prostate Volume**

Patient Demographic n = 30	
Age, y	68.0 ± 8.9 (41-87)
PSA [ng / ml]	1.80 ± 0.09 (0.01-2.10)
IPSS score (possible range 0-35)	20.74 ± 7.00 (17-34)
pre-PAE	11.33 ± 6.03 (5-18)
post-PAE	< 0.001
p-value	QoL score (possible range 0-5)
pre-PAE	4.06 ± 1.29 (3-5)
post-PAE	2.13 ± 1.32 (1-4)
p-value	< 0.001
	IIEF (possible range 1-30)
pre-PAE	21.50 ± 10.15 (9-28)
post-PAE)	24.00 ± 10.38 (9-28)
p-value	0.216
	PV, [ml]
pre-PAE	75.4 ± 49.1 (35.3-107.2)
post-PAE	55.5 ± 13.2 (28.9-87.3)
p-value	0.032

**Image Acquisition**

PAE was performed on a latest generation angiography suite (ARTIS pheno®; Siemens Healthineers, Forchheim,

Germany) using fluoroscopy and DSA image-guidance. Standard, pre-installed image acquisition protocols protocols (CARE aorta, CARE pelvis) were used for DSA image acquisition (1.17 µGy/frame, 2 fps). A Medrad Mark 7 Arterion (Bayer AG, Leverkusen, Germany) automatized injector was used for injecting 15-30 ml/injection ICM (Ultravist 370, Bayer) at 3-10 ml/s flowrate. Cumulative radiation dose measurements for the procedures resulted in a mean dose are product (DAP) of 19203.24 µGy·m2 ( ± 8293.2, [1028-59234]). Mean entrance dose (RP) was reported with 272.29 mGy ( ± 328.19,[110-1006]) and an average of n = 14 ( ± 9,[6-40]) image series was acquired. Mean fluoroscopy time was 21.43 minutes ( ± 11.21,[5.3-47.0]).

All images were retrieved from the angiography suite as unsubtracted raw-data (DICOM-files). DSA images (common cumulative OPAC files) were exported without compression. Mask images were manually chosen by the discretion of an experienced interventional radiologist with over 20 years of experience. DVA and ccDVA images were retrospectively generated on a dedicated local workstation (Kinepict Medical Imaging Tool, v4.0) using the same raw DICOM file as for DSA images.

**CNR Calculation**

As described earlier (11), regions of interest (ROI) were defined on vessels and background regions by using Image J (v.2.0.0-rc-68/1.52e, Creative Common License, NIH). The vascular and adjacent background ROI were placed in pairs. ROI positions

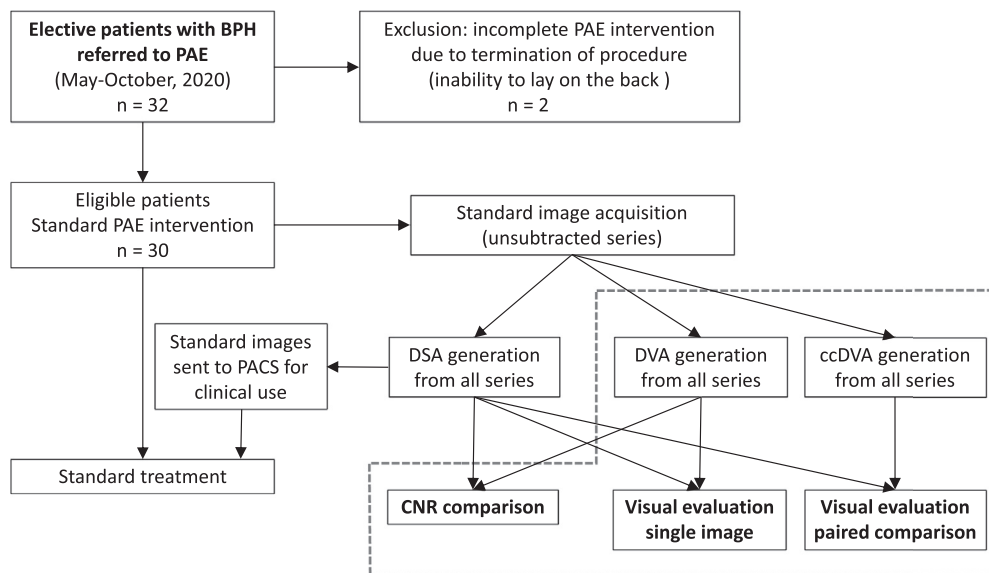


**Figure 1.** Flow chart of the study. Elective patients with benign prostatic hyperplasia (BPH), referred to our institute for prostatic artery embolization (PAE) between May and October 2020, were screened for inclusion. Patients with completed PAE were added in a consecutive manner. All patients received standard treatment, and the observational study was performed retrospectively (dashed rectangle). Digital subtraction angiography (DSA) images were prepared during the intervention by the Siemens Syngo workstation, whereas digital variance angiography (DVA) images (both normal and color-coded [ccDVA]) were generated later by the Kinepict Medical Imaging Tool from the same unsubtracted series as DSA images. Contrast-to-noise ratio (CNR) and single image visual score was determined for DSA and DVA images, whereas ccDVA images were compared to DSA images in another blinded and randomised survey.

were adjusted when patient positioning or pixel shifting caused slight geometric differences. CNR values were calculated for all ROI pairs individually according to the following formula (20), wherein  $Mean_v$  and  $Mean_b$  referred to mean pixel intensity values of the vascular and background ROI respectively and  $Std_b$  being the background standard deviation

$$CNR = \frac{|Mean_v - Mean_b|}{Std_b}$$

$CNR_{DVA}/CNR_{DSA}$  ratios (R) for each corresponding DVA and DSA ROIs were calculated (Table 2).

### Visual Evaluation

A blinded evaluation of images was done by four interventional radiologists (the number after the initials represent the relevant experience in years: AA 5, BB 7, CC 25, DD 6). DVA and DSA images were evaluated using the following 5-grade rating scale:

- (1) Non-diagnostic
- (2) Low
- (3) Medium
- (4) Good
- (5) Outstanding

For further details see Fig. 3. The rating scale was implemented in a blinded and randomized web-based survey and data were collected automatically in a data base for later processing.

DSA and ccDVA images were evaluated in a paired comparison, where the experts had to choose between the DSA

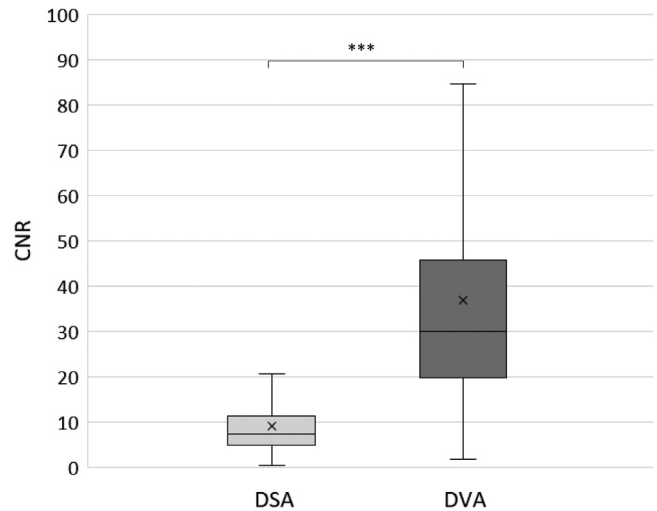


**Figure 2.** Contrast-to-noise ratio (CNR) results. The box and whisker plots show the mean (x), median (line), interquartile range (box) and internal fences (whiskers) of CNR values in each group. The paired data were analysed by the Wilcoxon signed rank test (\*\* $p < 0.001$ ). Abbreviations: DVA: digital variance angiography; DSA digital subtraction angiography.

and corresponding ccDVA image in terms of visibility of small

[ $< 2.5$  mm] and large arteries [ $> 2.5$  mm], feeding artery and tissue blush. There were four options: DVA is better, DSA is better, no difference, and in case of tissue blush and feeding artery an additional option (not relevant) was available, for indicating that the structure was not visible on the image. Only those images were included in the statistical analysis, where all four readers recognized the given structure. In the

**TABLE 2. Comparison of Digital Subtraction Angiography (DSA) and Color-coded Digital Variance Angiography (ccDVA) Images. Readers Evaluated four Subcategories (visibility of large and small vessels, tissue blush, feeding artery), Where They Had Three Options DSA Is Better, ccDVA Is Better, or No Difference. As Tissue Blush and Feeding Arteries Were Not Present in All Images, in These Categories There Was a Fourth Option (not relevant). Only Those Images Were Included in the Final Analysis, Where All four Readers Recognized and Rated the Given Structure (see Eq). The Image Was Rated as 'ccDVA', if at least three readers selected ccDVA, 'equal' if Exactly Two Readers Selected ccDVA, and 'DSA' if Maximum One Reader Voted for ccDVA. For Further Details, See the Materials and Methods Section. The Significance of Preference Values Was Evaluated by the Binomial Test. Interrater Agreement Was Analysed by the Fleiss Kappa Test, and Included Only Those Images Where All Readers Recognized the Given Structure**

Category	DSA (a)	Equal (b)	ccDVA (c)	Not Relevant (d)	Total Images (e = a+b+c+d)	DVA Preference (f = 100*c/[e-d])	Binomial Test p	Interrater Agreement (image number)	Fleiss Kappa	Kappa p
Large vessel	12	28	68	-	108	63 % (68/108)	$< 0.005$	58 % (373/648) (n = 108)	0.02	0.61
Small vessel	6	17	85	-	108	79 % (85/108)	$< 0.001$	70 % (452/648) (n = 108)	0.13	0.001
Tissue blush	4	4	62	38	108	89 % (62/70)	$< 0.001$	79 % (332/420) (n = 70)	0.18	$< 0.001$
Feeding artery	5	12	62	29	108	79 % (62/79)	$< 0.001$	65 % (306/474) (n = 79)	0.07	$< 0.001$

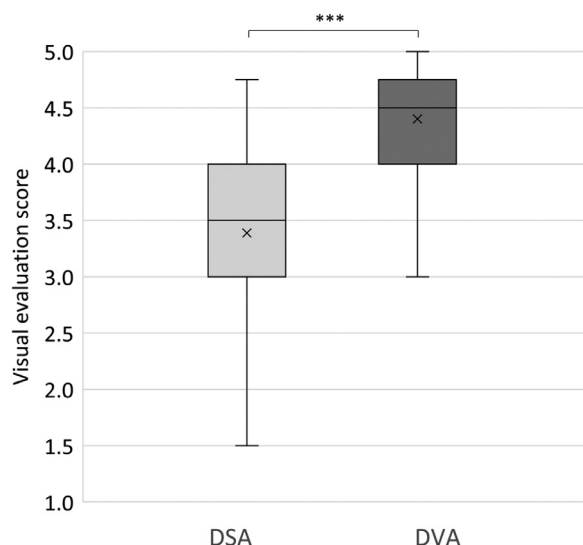


**Figure 3.** Visual evaluation of digital subtraction angiography (DSA) and digital variance angiography (DVA) images. The box and whisker plots show the mean (x), median (line), interquartile range (box) and internal fences (whiskers) of the 5-grade Likert scale scores in each group. (1) Non-diagnostic: unsuitable for diagnosis (2) Low: main vessels are distinguishable but not examinable. (3) Medium: sufficient for diagnosis in the main arteries, but smaller vessels and collateralization are not examinable. (4) Good: both smaller and the main vessels are examinable, suitable for everyday use (5) Outstanding: much richer in details compared to the everyday routine, makes decision-making easier. The paired data were analysed by the Wilcoxon signed rank test (\*\* $p < 0.001$ ).

final analysis the ‘DSA is better’ and ‘equal’ judgments were cumulated and compared to the ‘DVA is better’ option. For any image, ‘DVA is better’ was the final judgement if at least three readers selected the DVA image, and ‘equal’ if exactly two readers voted for DVA. In any other cases the outcome was ‘DSA is better’. For further details see Fig. 5 and Table 2.

### Statistical Analysis

Calculations of CNR and R medians and interquartile ranges were performed using Excel 2016 (Microsoft, Redmond, WA). CNR values were compared by the Wilcoxon signed rank test (Prism 8.4.2., GraphPad).

For visual evaluation scores, the mean and standard error of mean (SEM), and because of the non-Gaussian distribution of data, the median and interquartile range (IQR) were also calculated. The visual scores of the corresponding DSA and DVA images, generated from the same unsubtracted image series, were compared by the Wilcoxon signed rank test. The level of significance was set at  $p < 0.05$  in all tests. The interrater agreement was analyzed by the Kendall’s W test.

For the DSA–ccDVA comparison the binomial test was used. Interrater agreement was analysed by the Fleiss kappa test. In the tissue blush and feeding artery categories only those images were included in the analysis, where all readers recognized the evaluated structure.

## RESULTS

Our retrospective observational study included 30 male patients undergoing PAE (mean  $\pm$  SD age  $68.0 \pm 8.9$ , range 41–87) at our institute. Table 1 shows the detailed demographic data. Patients were enrolled in a consecutive manner. The exclusion criteria and the flow chart are shown on Fig. 1.

### CNR Calculations

CNR data were calculated on 108 DSA and DVA image pairs using 1418 ROI pairs. The median CNR for DSA images was 7.33 (IQR: 6.40), whereas for DVA it was 29.99 (IQR: 25.93), thus DVA provided a significantly higher (Wilcoxon signed rank  $p < 0.001$ ), more than 4-fold CNR than DSA (Fig 2), the median R value was 4.11 (IQR: 1.72).

### Visual Evaluation I: Single-image Evaluation of DSA and DVA Images

The visual evaluation of 108 DSA and 108 DVA images was performed in a blinded and randomized manner by four readers using a 5-grade Likert scale. DVA images received a significantly higher visual score (Mean  $\pm$  SEM was  $4.40 \pm 0.05$ , Wilcoxon signed rank  $p < 0.001$ ) than DSA images ( $3.39 \pm 0.07$ ). Score values showed a highly asymmetric distribution (Fig 3), therefore the median and IQR values were also calculated, yielding a similar difference between DVA (4.50, IQR: 0.75) and DSA (3.50, IQR: 1.00) images. The interrater agreement was 87% and 92% in the DSA and DVA groups, respectively. The Kendall W analysis showed a moderate but significant agreement in both groups (DVA  $W = 0.38$ , DSA  $W = 0.53$ ). Fig. 4 shows representative DSA and DVA images for comparison.

### Visual Evaluation II: Paired Comparison of DSA and ccDVA Images

For the paired evaluation, the readers had to compare DSA and corresponding ccDVA images regarding different clinically important aspects, such as the visibility of large vessels, small vessels, feeding artery and tissue blush. The preference of ccDVA images was significantly higher in all evaluated categories (binomial test  $p < 0.01$ ). The best performance was observed in the visibility of tissue blush (89%), the preference was slightly lower in the small vessels (preference 79%) and in the feeding artery category (79%), whereas the least advantage was observed regarding the visualisation of large vessels (63%) (Fig 5). As feeding arteries and tissue blush were not visible in all image pairs, only those answers were included in the statistical analysis, where all readers recognized and judged these structures (70 and 79 images in the tissue blush and feeding artery categories, respectively). The interrater agreement ranged between 58% and 79%, the Fleiss Kappa analysis showed slight agreement in all categories ranging from 0.02 (large vessels) to 0.18 (tissue blush), which was significant in

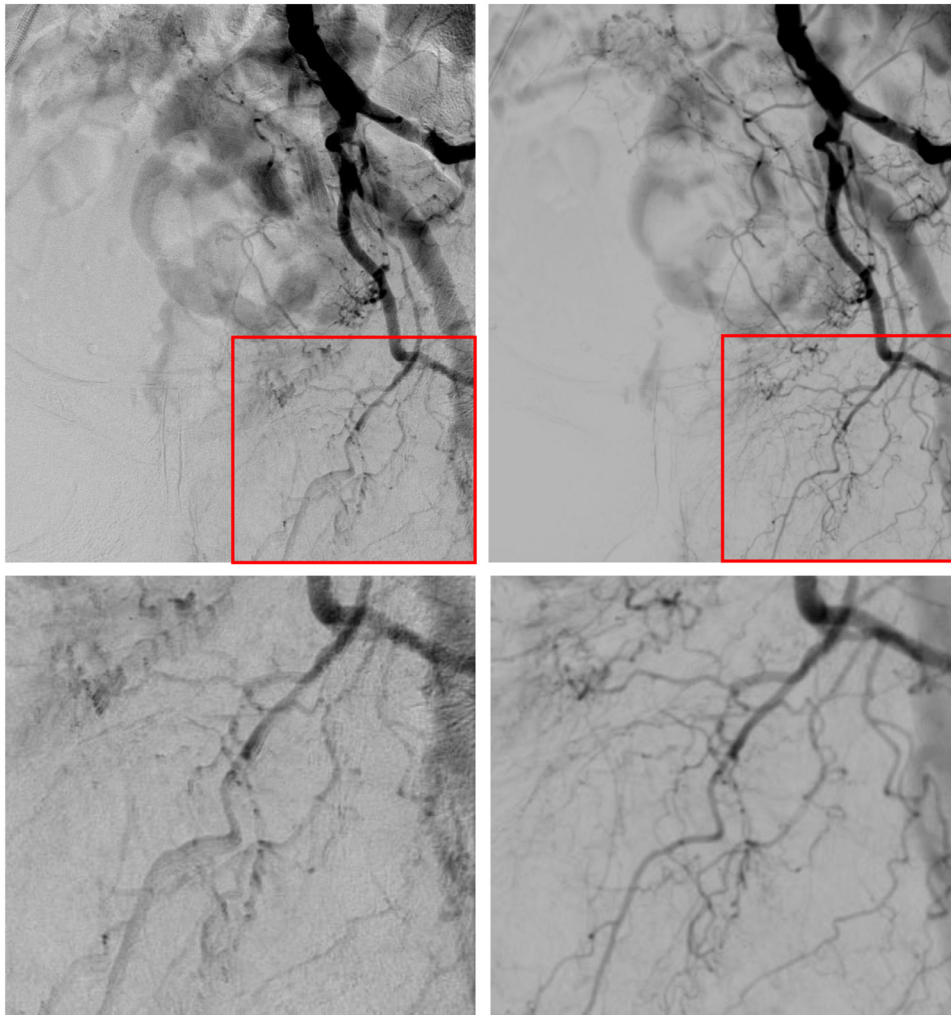


**Figure 4.** Representative digital subtraction angiography (DSA, left side) and digital variance angiography (DVA, right side) images of the common iliac artery after manual application of 8ml contrast agent bolus (4 ml Vispaque 320 and 4 ml NaCl 0.9% solution) through a pigtail catheter in a 78 year-old patient receiving PAE. Little difference can be observed at the level of large vessels, but small arteries have sharper contour and the overall background noise is lower in DVA images. The lower panels show the magnification of the marked segments of upper images. (Color version of figure is available online.)

small vessels, tissue blush and feeding artery visibility. The detailed results with statistical evaluation are shown in [Table 2](#). [Fig. 6](#) shows a representative DSA-ccDVA image pair.

## DISCUSSION

Our aim was to compare the image quality of DVA to that of DSA in context of PAE. The primary question was whether the previously observed quality advantage of DVA, described in endovascular lower limb procedures (11–14,16), also exists in prostatic interventions. Our data show that DVA provides more than four-times higher CNR than the traditionally used DSA and this objective advantage is reflected also in subjective visual evaluation, as the Likert score of DVA images was one unit higher than that of DSA images. These data clearly verify the quality reserve of DVA in PAE. A secondary aim was to compare the performance of ccDVA with DSA. The visual comparison data show that ccDVA provides a

better insight in the clinically relevant domains, as it particularly improves the visualization of tissue blush (DVA preference 89%) small vessels (DVA preference 79%), and feeding arteries (DVA preference 79%). These structures are critically important in PAE procedure, therefore ccDVA might be a very useful tool to avoid complications (such as non-target embolization of important collaterals), judge the efficacy of embolization during intervention, shorten intervention time and, thereby of all, improve clinical outcome. These potential benefits, however, have to be verified in carefully designed prospective studies.

Our data might have major clinical implications. Previous studies have shown that the quality reserve of DVA can be effectively used for dose management. DVA allowed 50% reduction of contrast media without compromising the image quality in carotid angiography (17). A recent report has shown that 70% reduction of the dose/frame value in lower limb angiography yielded 68% reduction of the DSA-related

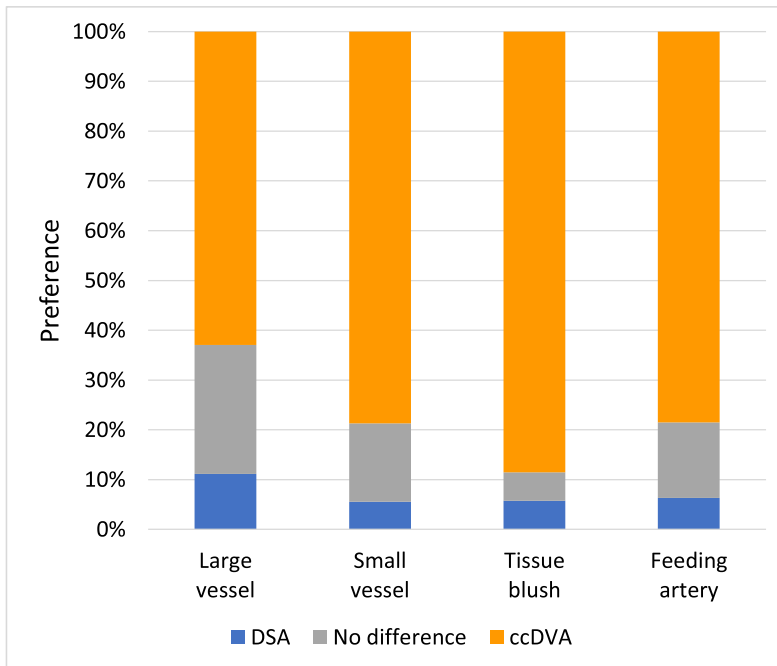


**Figure 5.** Comparison of digital subtraction angiography (DSA) and color-coded digital variance angiography (ccDVA) images. Readers performed a paired comparison, and evaluated the visibility of large and small vessels, tissue blush and feeding arteries. In these categories there was also a 'no difference' option, and for the tissue blush and feeding artery an additional 'not relevant' option, to exclude those images where the structures were not visible. For further details, see the Materials and Methods section and Table 2. The ccDVA preference over the cumulated 'DSA' or 'no difference' options was significantly higher in all categories using the binomial test. (Color version of figure is available online.)

dose-area-product, and DVA with reduced radiation dose provided non-inferior image quality in the abdominal and femoral regions, and superior image quality in the crural region compared to full dose DSA images (16). As PAE has been reported as effective as TURP in improving subjective symptom scores, with fewer complications and shorter hospitalization times (6), the procedure will play an increasing role in the treatment of BPH. The associated radiation burden,

however, might be a risk for the patients (7–9) and also for the medical staff (8,21,22), and the contrast agents used might increase the risk of renal impairments (17,23,24). Thus, the dose management efforts might be crucial in PAE, and DVA has the potential to address these problems. The dose management capabilities of DVA in PAE have to be validated in further clinical studies.

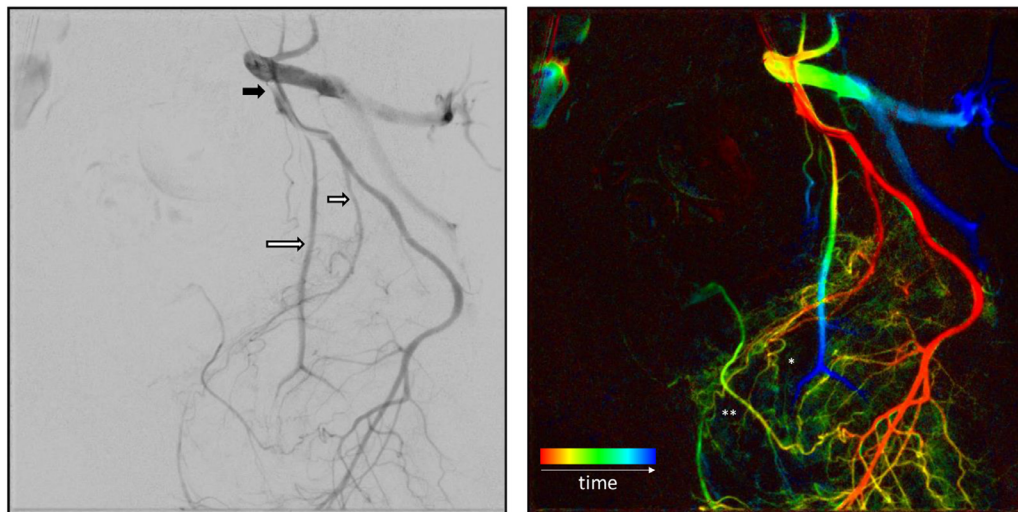


**Figure 6.** Representative example of digital subtraction angiography (DSA) and color-coded digital variance angiography (ccDVA) images in a 63 year-old patient. Left: Application of 6 ml contrast agent (3 ml Vispaque 320 and 3 ml NaCl 0.9% solution) in the left pudendal artery (PuA) at the origin from the distal internal iliac artery (black arrow). The prostatic artery (short white arrow) is visible as a direct branch from the PuA. Proximal of the origin of the PuA the inferior vesical artery (IVA) is visible (long white arrow), with a proximal smaller lumen, suspicious for a stenosis. Right: The colors represent the time elapsed until the appearance of the contrast media in a specific blood vessel segment. In the IVA, color progression from orange to blue is visible, indicating a slower flow. Smaller vessels, like the characteristic corkscrew pattern (\*) or the collateralization of dominant prostatic artery to the pudendal areas (\*\*) have a higher visibility, and parenchymal blush is visible as greenish diffuse attenuation. (Color version of figure is available online.)

The comparison of DSA and ccDVA images clearly show, that the color-coded technology provides more information on small arteries, tissue blush and feeding arteries. The idea of color-coded imaging is not new. Major manufacturers have already developed their own solutions (25,26) to visualize the temporal appearance of contrast media in blood vessels in a single composite image, where the different colors represent the time elapsed until the contrast media reaches a specific vessel segment. This parametric imaging can help the understanding of hemodynamic conditions. Nevertheless, it requires a high frame rate (4–7.5 fps) to obtain good time resolution and a relatively long acquisition time (8–10 s) to also visualize the venous phase, therefore the method is not widespread because of the required high radiation dose. As ccDVA is based on the DVA technology, it might substantially reduce the radiation burden because of its dose management capabilities, thereby it might help the use of parametric imaging by reducing the associated risks.

Our study has several limitations. First, as it was designed as a small-cohort proof-of-concept retrospective study, the number of patients is relatively low, nevertheless, the number of analysed images allows to reach statistically valid conclusions. Second, all DVA and ccDVA images were generated in a retrospective manner from the unsubtracted acquisitions, therefore they could not serve any help for the medical staff during the interventions. As the DVA workstation has already been installed in the operating room, our future clinical investigations will use real-time data processing (14). Third, the color-coded imaging is a parametric technology, which requires a quantitative analysis, but in our case we have used only a qualitative evaluation. In further studies we will use the parametric ccDVA tool, which provides quantitative information on the hemodynamic conditions.

## CONCLUSION

In conclusion, our study demonstrated that DVA can provide higher CNR and better visual image quality in PAE than DSA. This quality reserve might be used for dose management of radiation and contrast media amount. The qualitative evaluation of ccDVA suggests that the technology might help the decision-making process during PAE interventions. The verified quality reserve of DVA and the advantages of ccDVA provide a basis for further prospective clinical studies in the field of PAE and possibly other embolization settings.

## FUNDING

The study was supported by the European Commission EIC Accelerator Pilot grant (968430 KMIT-ACC), the National Research, Development and Innovation Office of Hungary (NKFI; NVKP-16-1-2016-0017 National Heart Program, and 2020-1.1.5-GYORSÍTÓSAV-2021-00018) and by the Thematic Excellence Program (2020-4.1.1.-TKP2020) of the Ministry of Innovation and Technology of Hungary,

within the framework of the BIOImaging Excellence program at Semmelweis University.

## REFERENCES

1. Maclean D, Harris M, Drake T, et al. Factors predicting a good symptomatic outcome after prostate artery embolisation (PAE). *Cardiovasc Intervent Radiol* 2018; 41(8):1152–1159.
2. DeMeritt JS, Elmasri FF, Esposito MP, et al. Relief of benign prostatic hyperplasia-related bladder outlet obstruction after transarterial polyvinyl alcohol prostate embolization. *J Vasc Intervent Radiol* 2000; 11(6):767–770.
3. McWilliams JP, Bilhim TA, Carnevale FC, et al. Society of interventional radiology multisociety consensus position statement on prostatic artery embolization for treatment of lower urinary tract symptoms attributed to benign prostatic hyperplasia: from the society of interventional radiology, the cardiovascular and interventional radiological society of europe, société française de radiologie, and the british society of interventional radiology. *J Vasc Intervent Radiol* 2019; 30(5):627–637. .e1.
4. Malling B, Røder MA, Brasso K, et al. Prostate artery embolisation for benign prostatic hyperplasia: a systematic review and meta-analysis. *Eur Radiol* 2019; 29(1):287–298.
5. Powell J. Prostate artery embolisation for lower urinary tract symptoms caused by benign prostatic hyperplasia: Interventional procedures guidance [IPG611]. (2018).
6. Xiang P, Guan D, Du Z, et al. Efficacy and safety of prostatic artery embolization for benign prostatic hyperplasia: a systematic review and meta-analysis of randomized controlled trials. *Eur Radiol* 2021; 31(7):4929–4946.
7. Andrade G, Khoury HJ, Garzón WJ, et al. Radiation exposure of patients and interventional radiologists during prostatic artery embolization: a prospective single-operator study. *J Vasc Intervent Radiol* 2017; 28(4):517–521.
8. Garzón WJ, Andrade G, Dubourcq F, et al. Prostatic artery embolization: radiation exposure to patients and staff. *J Radiol Prot* 2016; 36(2):246–254.
9. Laborda A, De Assis AM, Ioakeim I, et al. Radiodermatitis after prostatic artery embolization: case report and review of the literature. *Cardiovasc Intervent Radiol* 2015; 38(3):755–759.
10. Szigeti K, Mathe D, Osvath S. Motion based x-ray imaging modality. *IEEE Trans Med Imaging* 2014; 33(10):2031–2038.
11. Gyánó M, Góg I, Óriás VI, et al. Kinetic imaging in lower extremity arteriography: comparison to digital subtraction angiography. *Radiology* 2019; 290(1):246–253.
12. Bastian MB, König AM, Viniol S, et al. Digital variance angiography in lower-limb angiography with metal implants. *Cardiovasc Intervent Radiol* 2021; 44(3):452–459.
13. Thomas RP, Bastian MB, Viniol S, et al. Digital variance angiography in selective lower limb interventions. *J Vasc Intervent Radiol* 2022; 33(2):104–112.
14. Gyánó M, Csobay-Novák C, Berczeli M, et al. Initial operating room experience with digital variance angiography in carbon dioxide-assisted lower limb interventions: a pilot study. *Cardiovasc Intervent Radiol* 2020; 43(8):1226–1231.
15. Óriás VI, Gyánó M, Góg I, et al. Digital variance angiography as a paradigm shift in carbon dioxide angiography. *Invest Radiol* 2019; 54(7):428–436.
16. Gyánó M, Berczeli M, Csobay-Novák C, et al. Digital variance angiography allows about 70% decrease of DSA-related radiation exposure in lower limb X-ray angiography. *Sci Rep* 2021; 11(1):21790.
17. Óriás VI, Szöllösi D, Gyánó M, et al. Initial evidence of a 50% reduction of contrast media using digital variance angiography in endovascular carotid interventions. *Eur J Radiol Open* 2020; 7:100288.
18. Pritchard Jr, William F, Ronald F. Carey, US Food and Drug Administration and regulation of medical devices in radiology. *Radiology* 1997; 205(1):27–36.
19. Carnevale FC, Moreira AM, Antunes AA, et al. The “PerFecTED Technique”: proximal embolization first, then embolize distal for benign prostatic hyperplasia. *Cardiovasc Intervent Radiol* 2014; 37(6):1602–1605.
20. Rose A. Quantum and noise limitations of the visual process. *J Opt Soc Am* 1953; 43:715–716.

21. Bernier M-O, Journy N, Villoing D, et al. Cataract risk in a Cohort of U.S. radiologic technologists performing nuclear medicine procedures. *Radiology* 2018; 286(2):592–601.
22. Roguin A, Goldstein J, Bar O, et al. Brain and neck tumors among physicians performing interventional procedures. *Am J Cardiol* 2013; 111(9):1368–1372.
23. Davenport MS, Perazella MA, Yee J, et al. Use of intravenous iodinated contrast media in patients with kidney disease: consensus statements from the American College of Radiology and the National Kidney Foundation. *Radiology* 2020; 294(3):660–668.
24. Nijssen EC, Nelemans PJ, Rennenberg RJ, et al. evaluation of safety guidelines on the use of iodinated contrast arterial: conundrum continued. *Invest Radiol* 2018; 53(10):616–622.
25. Jens S, Marquering HA, Koelemay MJW, et al. Perfusion angiography of the foot in patients with critical limb ischemia: description of the technique. *Cardiovasc Intervent Radiol* 2015; 38(1):201–205.
26. Strother CM, Bender F, Deuerling-Zheng Y, et al. Parametric color coding of digital subtraction angiography. *AJNR Am J Neuroradiol* 2010; 31(5):919–924.

Communication

# Quantitative Comparison of Color-Coded Parametric Imaging Technologies Based on Digital Subtraction and Digital Variance Angiography: A Retrospective Observational Study

István Góg<sup>1,2</sup> , Péter Sótónyi<sup>1</sup>, Balázs Nemes<sup>3</sup> , János P. Kiss<sup>2</sup> , Krisztián Szigeti<sup>4</sup>, Szabolcs Osváth<sup>2,4</sup> and Marcell Gyánó<sup>2,3,\*</sup>

- <sup>1</sup> Department of Vascular and Endovascular Surgery, Heart and Vascular Center, Semmelweis University, Városmajor utca 68, 1122 Budapest, Hungary; gogistvan@gmail.com (I.G.); sotonyi.peter1@semmelweis.hu (P.S.)
- <sup>2</sup> Kinepict Health Ltd., Szilágyi Erzsébet fasor 31, 1027 Budapest, Hungary; janos.kiss@kinepict.com (J.P.K.); szabolcs.osvath@kinepict.com (S.O.)
- <sup>3</sup> Department of Interventional Radiology, Heart and Vascular Center, Semmelweis University, Városmajor utca 68, 1122 Budapest, Hungary; nemes.balazs@semmelweis.hu
- <sup>4</sup> Department of Biophysics and Radiation Biology, Semmelweis University, Tűzoltó u. 37-47, 1094 Budapest, Hungary; szigeti.krisztian@semmelweis.hu
- \* Correspondence: gyano.marcell@semmelweis.hu or mgyanostb@gmail.com

**Abstract:** The evaluation of hemodynamic conditions in critical limb-threatening ischemia (CLTI) patients is inevitable in endovascular interventions. In this study, the performance of color-coded digital subtraction angiography (ccDSA) and the recently developed color-coded digital variance angiography (ccDVA) was compared in the assessment of key time parameters in lower extremity interventions. The observational study included 19 CLTI patients who underwent peripheral vascular intervention at our institution in 2020. Pre- and post-dilatational images were retrospectively processed and analyzed by a commercially available ccDSA software (Kinepict Medical Imaging Tool 6.0.3; Kinepict Health Ltd., Budapest, Hungary) and by the recently developed ccDVA technology. Two protocols were applied using both a 4 and 7.5 frames per second acquisition rate. Time-to-peak (TTP) parameters were determined in four pre- and poststenotic regions of interest (ROI), and ccDVA values were compared to ccDSA read-outs. The ccDVA technology provided practically the same TTP values as ccDSA ( $r = 0.99$ ,  $R^2 = 0.98$ ,  $p < 0.0001$ ). The correlation was extremely high independently of the applied protocol or the position of ROI; the  $r$  value was 0.99 ( $R^2 = 0.98$ ,  $p < 0.0001$ ) in all groups. A similar correlation was observed in the change in passage time ( $r = 0.98$ ,  $R^2 = 0.96$ ,  $p < 0.0001$ ). The color-coded DVA technology can reproduce the same hemodynamic data as a commercially available DSA-based software; therefore, it has the potential to be an alternative decision-supporting tool in catheter labs.



**Citation:** Góg, I.; Sótónyi, P.; Nemes, B.; Kiss, J.P.; Szigeti, K.; Osváth, S.; Gyánó, M. Quantitative Comparison of Color-Coded Parametric Imaging Technologies Based on Digital Subtraction and Digital Variance Angiography: A Retrospective Observational Study. *J. Imaging* **2024**, *10*, 260. <https://doi.org/10.3390/jimaging10100260>

Academic Editor: Manuel Curado

Received: 30 August 2024

Revised: 14 October 2024

Accepted: 15 October 2024

Published: 18 October 2024

**Keywords:** color-coded parametric imaging; digital subtraction angiography; digital variance angiography; time–density curve; peripheral artery disease; critical limb ischemia



**Copyright:** © 2024 by the authors. Licensee MDPI, Basel, Switzerland. This article is an open access article distributed under the terms and conditions of the Creative Commons Attribution (CC BY) license (<https://creativecommons.org/licenses/by/4.0/>).

## 1. Introduction

Minimally invasive endovascular interventions play an increasingly important role in the treatment of cardiovascular disorders and certain types of benign or malignant oncological states [1]. These procedures require a detailed visualization of blood vessels during the intervention. The reference standard method for this purpose is digital subtraction angiography (DSA), which subtracts a mask image from the subsequent contrast agent-enhanced image series, thereby allowing it to show the vasculature in the site of intervention without other disturbing anatomical structures [2].

The morphological analysis of key lesions can be performed by measuring the degree of stenosis; however, the visual evaluation of gray-scale DSA images gives two-dimensional

projected information of a three-dimensional structure, which can lead to misdiagnosis by evaluating a stenotic vascular segment as normal. Without a quantitative evaluation of hemodynamic conditions, the intraprocedural assessment of stenotic lesions can be subjective. In response to this medical need, a new quantitative technology, called color-coded parametric angiography (also termed as color-coded DSA, quantitative DSA, or two-dimensional perfusion angiography), has been developed [3–6]. The method creates a time–density (also called time–attenuation) curve and extracts time- and attenuation-related parameters from DSA acquisition. These parameters are used to create a color-coded image, where the colors represent the arrival time of the contrast agent at any point of the angiogram (the earliest is red, the latest is blue) and the brightness is proportional to the attenuation. Thus, this single image contains quantifiable spatiotemporal information on the blood flow and visualizes hemodynamic conditions in the target area.

Color-coded parametric imaging has been tested in a number of clinical studies over the last 15 years [5–18]. Certain ccDSA parameters showed strong correlation with the clinical outcome in stroke treatment [7,8] and helped the evaluation of carotid cavernous fistulas better than gray-scale DSA videos [9]. In comparison with DSA videos, color-coded images significantly improved diagnosis and treatment planning in cerebrovascular disorders, and the positive effect was greater for less experienced readers [5]. Parametric imaging proved to be useful in other endovascular procedures as well, including lower limb interventions [10,11], the intraprocedural evaluation of type B aorta dissections in thoracic endovascular aortic repair [12], the identification of bleeding points [13], the intraprocedural evaluation of genicular embolization [14], spleen embolization [15], the evaluation of hemodynamic changes during the endovascular treatment of brain arteriovenous malformations [16], and the prediction of brain aneurysm occlusion after embolization [17,18]. In spite of these promising results, the ccDSA technology did not become an everyday tool because of certain disadvantages (e.g., the high radiation load during ccDSA acquisitions).

Digital variance angiography (DVA) is a recently developed image processing alternative to DSA. The technology is based on the principles of kinetic imaging [19]. In contrast to DSA, DVA does not use a mask for subtraction. Instead, DVA calculates the standard deviation of changing pixel intensities for each pixel, which generates a standard deviation map, the so-called DVA image. The motion of the contrast agent creates high standard deviation values, while the stationary background and the background noise give low standard deviation values, resulting in high contrast and a greatly improved image quality. This quality advantage has been validated in lower limb interventions [20–23], carotid angiography [24], prostatic artery embolization [25], and the transarterial chemoembolization of liver tumors [26].

The quality reserve of DVA also provides opportunity for dose management [24,27,28]. As the technology can generate color-coded DVA (ccDVA) images, our hypothesis was that ccDVA could solve the problem of a high radiation dose of ccDSA, provided it can reliably reproduce the parametric data generated by ccDSA. This assumption is not evident as the algorithms of DSA and DVA are completely different. Our aim, therefore, was to compare the key time-related parameter, the time to peak (TTP), obtained with DVA, to the TTP values of a commercially available color-coded DSA software in the lower limb intervention of patients with critical limb-threatening ischemia (CLTI) in order to provide evidence for the validity of ccDVA measurements.

## 2. Materials and Methods

### 2.1. Patients

Our retrospective observational study prospectively enrolled 19 CLTI patients (mean  $\pm$  SD age  $68.6 \pm 8.0$  years, 42% male) (Fontaine stage III–IV) who underwent peripheral vascular intervention at the Heart and Vascular Center, Semmelweis University, between September and December of 2020. The detailed demographic data are shown in Table 1. All patients signed an informed consent and permitted the use of their anonymous acquisitions for

research purposes. There was no change in the interventional protocol recommended for color-coded imaging, and the standard of care was given to all subjects.

**Table 1.** Demographic data.

Sex	Number of Patients	Age <sup>1</sup> (Years)	BMI <sup>1</sup>	GFR <sup>1</sup> (mL/min/1.73 m <sup>2</sup> )
Male	8	69.6 ± 7.0	25.0 ± 4.5	65.3 ± 26.7
Female	11	67.9 ± 8.8	26.6 ± 4.6	55.8 ± 26.2

<sup>1</sup> All data are mean ± SD. BMI: body mass index. GFR: glomerular filtration rate.

## 2.2. Image Acquisition

Each procedure was performed from either a brachial or femoral access using the Seldinger technique and locoregional anesthesia. Image acquisition was made on a Siemens Artis Zee system (Siemens Healthineers, Erlangen, Germany), which included the parametric angiography software iFlow (Siemens Healthineers, Erlangen, Germany) with a Medrad Avanta automated injector (Bayer, Berlin, Germany). During the procedure, a pre-interventional angiogram was created by injecting 3–8 mL of iodinated contrast media (Ultravist 370, Bayer) at a 2–6 mL/s flowrate through a single endhole catheter placed selectively into the target artery, which was the superficial femoral artery in 45% ( $n = 10$ ), the popliteal artery in 27% ( $n = 6$ ), the common or external iliac artery in 18% ( $n = 4$ ), and the crural branches in 9% ( $n = 2$ ) of all cases ( $n = 22$ ). Image acquisition occurred at 4 or 7.5 frames per second (FPS). These higher rates are recommended for the generation of good quality color-coded images by the iFlow software (Syngo Workplace version VD11B, Siemens, Germany). The treatment of stenoses was conducted by “plain-old-balloon-angioplasty (POBA)” and/or by the placement of a self-expanding stent into the artery. Three patients had multiple level lesions, and they were treated in two sessions. These interventions were handled as separate cases.

## 2.3. Image Processing

Pre- and postinterventional color-coded images were generated retrospectively. The ccDSA images were prepared from the DSA acquisitions by the iFlow software package running on a Syngo workstation (XVP VD11B and VD11C; Siemens Healthineers, Erlangen, Germany), whereas the ccDVA images were calculated from the unsubtracted raw acquisition by the Kinect Medical Imaging Tool software (KMIT 6.0.3; Kinect Health, Budapest, Hungary) running on a separate computer. Each workstation allowed further postprocessing, such as pixel shift for motion correction and setting the brightness and contrast.

## 2.4. Data Collection

Each software allows the placement of regions of interests (ROIs), for which they can generate time–attenuation curves. These curves can be used to calculate the time-to-peak (TTP) parameter, which gives the time from the start of acquisition until the development of the maximum average contrast intensity in the given ROI (Figure 1).

Usually, 4 ROIs were placed on the images: the first being 5–10 cm proximally from the stenotic lesion; the second being at the beginning of the lesion; the third being at the end of the lesion; and the fourth being 5–10 cm distally from the lesion. (Figure 2). In three cases, the fourth ROI could not be placed due to anatomical reasons. Only the ROI1-ROI3 data were included in calculations for these patients, and they were excluded from passage time calculations (see below). The same ROI sets were used on the pre- and postinterventional images.

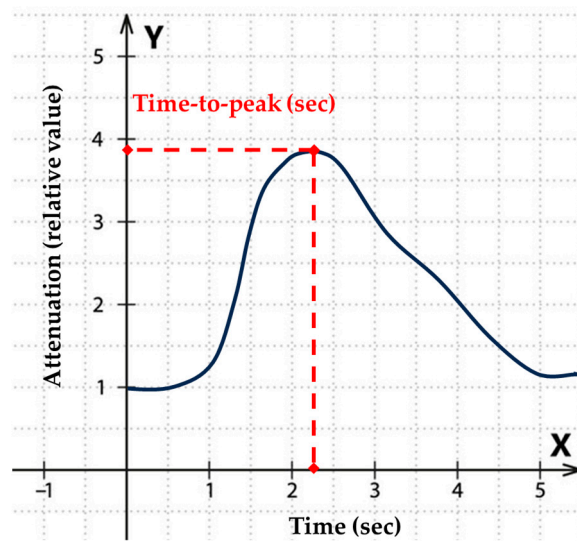


**Figure 1.** Calculation of the time-to-peak (TTP) parameter from the time–attenuation curve. The red dotted lines indicate the level of peak attenuation (vertical line) and the time at the peak (horizontal line).

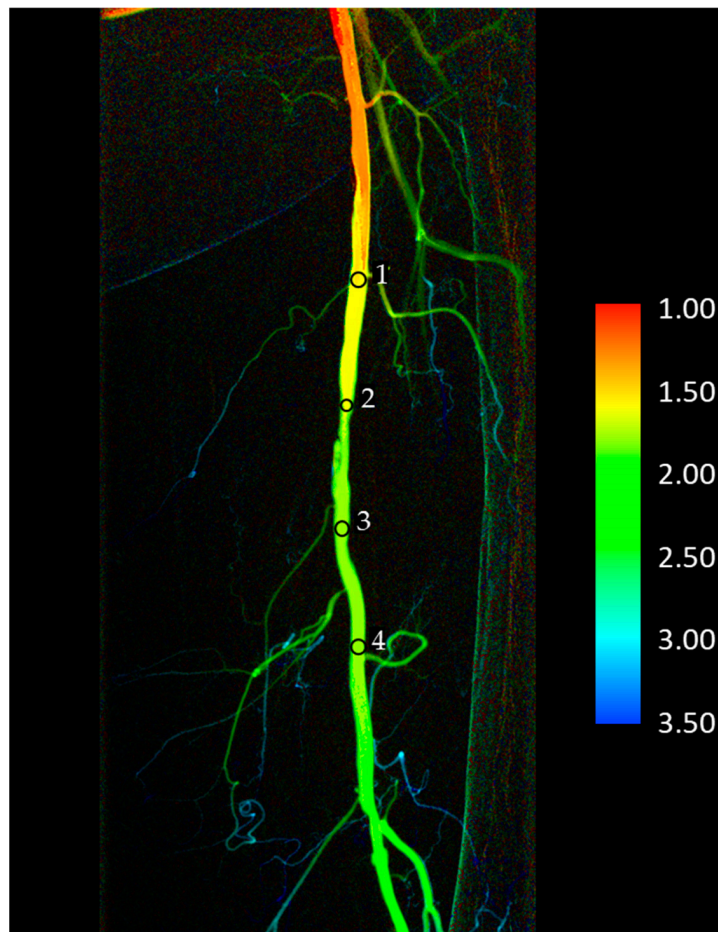


**Figure 2.** Typical placement of region of interests (ROIs) on a color-coded DVA image. The color bar shows the connection between the colors and the elapsed time (in seconds) measured from the injection of contrast media. In three cases (iliac and talocrural lesions), there was no space to place the fourth ROI. The ‘change in passage time’ calculations did not include these patients. The numbers besides the round shaped selections (ROIs) are serial numbers, indicating the sequence of ROI placement.

As our aim was to compare the performance of KMIT to iFlow, the placement of ROIs on DSA images defined the position of ROIs on DVA images. The analogous ROIs were placed at identical positions with identical sizes, with the help of an open-source mouse-position tracking software (MPos, version 0.5, Bluegrams, <https://github.com/Bluegrams>, accessed on 13 October 2024).

Passage time was defined as the difference between TTPROI4 and TTPROI1, i.e., the time necessary for the bolus to flow across the target area. The change in passage time is the difference between the passage time before and after intervention. This parameter is an indicator of treatment efficacy, and normally, a positive number being used as the passage should be accelerated due to angioplasty/stenting.

### 2.5. Data Analysis

TTP data were separately analyzed according to the acquisition protocol and the ROI position. The change in passage time was also compared between the two parametric imaging technologies. The TTP and passage time parameters calculated by iFlow and KMIT were compared using the Pearson correlation test. SPSS (version 28, IBM Corp Armonk, NY, USA) and Prism 8.4 (GraphPad, San Diego, CA, USA) were used for statistical analysis.

## 3. Results

Altogether twenty-two pre-interventional and twenty-two postinterventional acquisitions were processed from nineteen patients, as two independent interventions were included from three patients. Two different acquisition protocols (4 FPS and 7.5 FPS) and four ROI positions (ROI1-4) were tested, except for in three patients, where only three ROI positions (ROI1-3) could be placed. All these patients belonged to the 4 FPS group. When the change in passage time was investigated, only those patients who had four ROIs were included.

### 3.1. Correlation of TTP Parameters in Different Acquisition Protocols

The correlation was not dependent on the acquisition protocol and was extremely high in all cases (Figure 3). The Pearson correlation coefficient ( $r$ ) was 0.99 ( $p < 0.0001$ ) and the  $R^2$  was 0.98 in both the 4 FPS and the 7.5 FPS groups (Table 2).

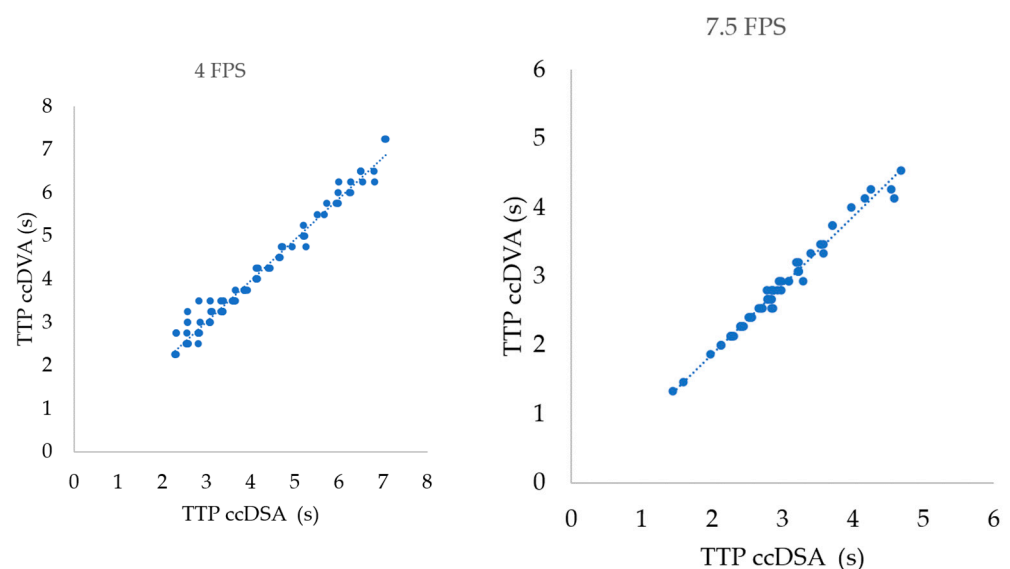


**Figure 3.** Correlation of TTP values calculated by ccDSA and ccDVA in different acquisition protocols. Left panel: correlation of 106 ROI pairs in 4 FPS acquisitions. Right panel: correlation of 64 ROI pairs in 7.5 FPS acquisitions.

**Table 2.** Pearson correlation analysis of time-related parameters. TTP: time to peak; ROI: region of interest; *n*: the number of ROI pairs included in the analysis, FPS: frame per second.

Correlation Group ( <i>n</i> )	Pearson <i>r</i>	95% Confidence Interval	R <sup>2</sup>	Two-Tailed <i>p</i>
TTP 4 FPS (106)	0.9889	0.9837–0.9924	0.9779	<0.0001
TTP 7.5 FPS (64)	0.9917	0.9864–0.9950	0.9835	<0.0001
TTP ROI1 (44)	0.9899	0.9814–0.9845	0.9799	<0.0001
TTP ROI2 (44)	0.9903	0.9822–0.9947	0.9807	<0.0001
TTP ROI3 (44)	0.9902	0.9819–0.9947	0.9804	<0.0001
TTP ROI4 (38)	0.9904	0.9814–0.9950	0.9808	<0.0001
TTP all ROI (170)	0.9905	0.9871–0.9930	0.9811	<0.0001
Δ passage time <sup>1</sup> (19)	0.9806	0.9491–0.9927	0.9615	<0.0001

<sup>1</sup> The change in passage time (Δ) was calculated as the differences in (TTP<sub>ROI4</sub>–TTP<sub>ROI1</sub>) before and after intervention.

### 3.2. Correlation of TTP Parameters in Different ROI Positions

The correlation was not dependent on the ROI position and was extremely high in all cases (Figure 4). The Pearson correlation coefficient (*r*) was 0.99 (*p* < 0.0001) and the R<sup>2</sup> was 0.98 in all ROI positions (Table 2).

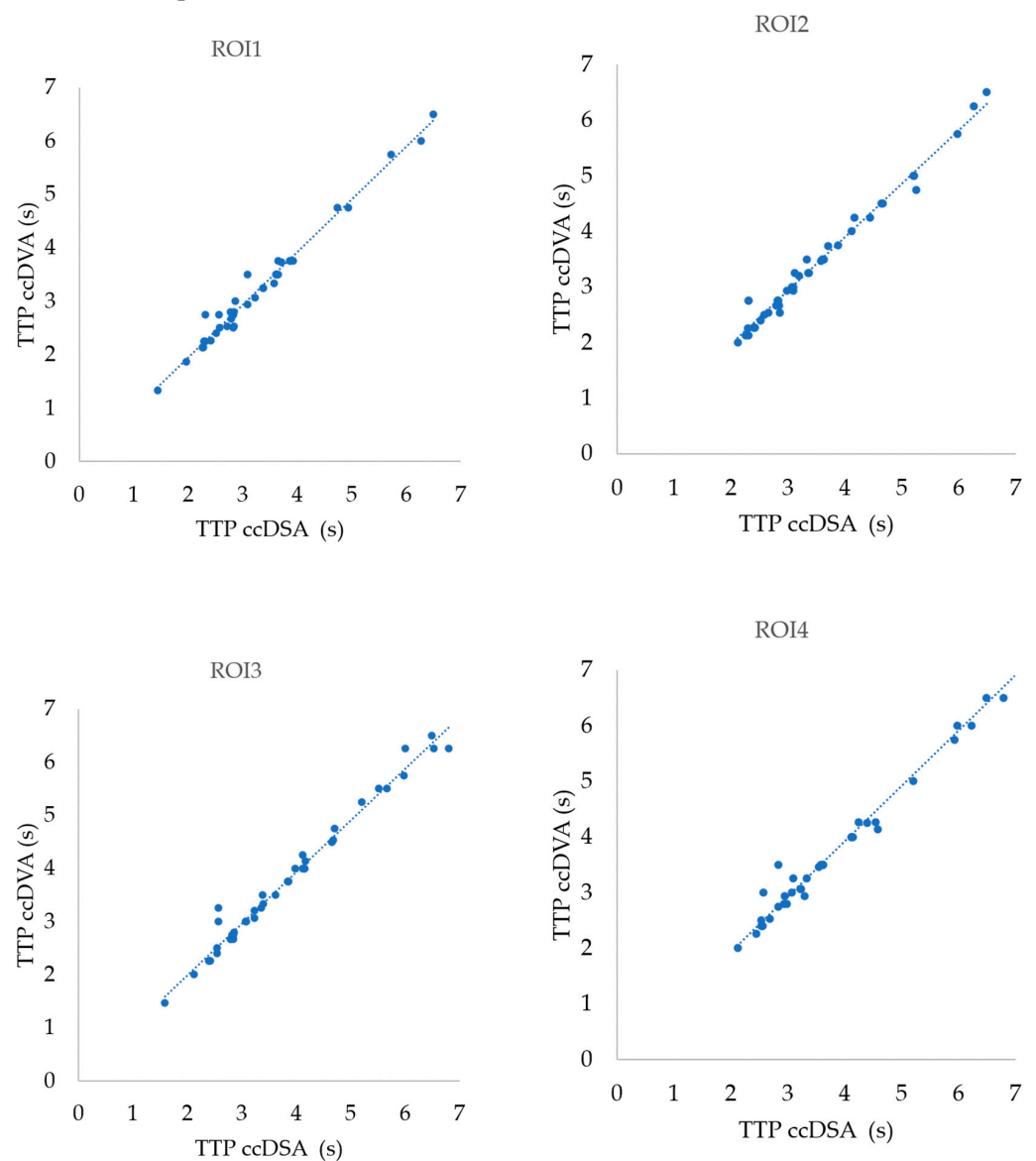


**Figure 4.** Correlation of TTP values calculated by ccDSA and ccDVA in different ROI positions. In all cases, 44 ROI pairs were included in the analysis except for ROI4, where only 38 ROI pairs were used.

### 3.3. Correlation of Change in Passage Time Following the Intervention

The passage time (for more details, see the ‘Material and Methods’ section) is an important parameter which characterizes the hemodynamic conditions of in the target area. Beyond the raw TTP data, our aim was to test the changes in this functional parameter that can reflect the efficacy of treatment. The change in passage time was detected very similarly by both technologies; the correlation was extremely high (Figure 5). The Pearson correlation coefficient ( $r$ ) was 0.98 ( $p < 0.0001$ ) and the  $R^2$  was 0.96 (Table 2).

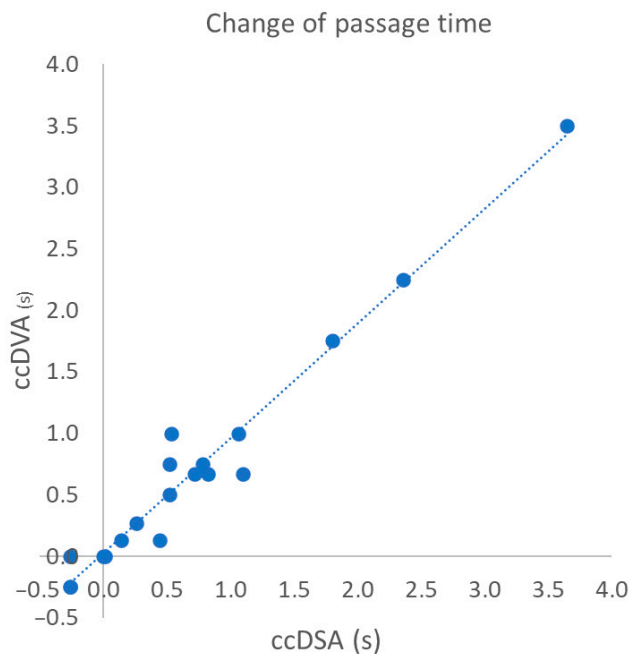


**Figure 5.** Correlation of the change in passage time calculated from TTP data of ccDSA and ccDVA. We could not place the 4th ROI in 3 interventions. Therefore, only 19 ROI pairs were used in the analysis. The change in passage time was calculated as the differences in  $(TTP_{ROI4} - TTP_{ROI1})$  before and after intervention.

## 4. Discussion

Our aim was to investigate the reliability of ccDVA to determine time-related parameters in lower limb interventions aiming to restore or improve the circulation in lower extremity arteries of CLTI patients. For this purpose, we compared the TTP values obtained by ccDVA to those obtained by a commercially available ccDSA software. The comparison was justified as the two technologies use different algorithms. The ccDSA software extracts data from the subtracted DSA acquisition, while the ccDVA software calculates parametric data from the raw unsubtracted series. The correlation analysis clearly shows that ccDVA reproduces the TTP parameters of the ccDSA software with high fidelity, and the performance is not dependent on the applied frame rate or the position of the ROIs. Another time-based parameter, the change in the passage time was also compared as this value might help to evaluate the efficacy of intervention. Again, the DVA-based software gave practically the same values as the DSA-based solution, indicating that the time parameters obtained with ccDVA are valid and can be used in clinical practice similarly to the commercially available comparator technology.

The principles of color-coded angiographic imaging emerged four decades ago [3,4], but the major angiography manufacturers introduced their own color-coded solutions only in the last 10–15 years. Although clinical studies indicated the potential usefulness of this technology [7–18], color-coded parametric imaging is not very widespread. There are several factors that make daily use difficult. It is essential to define strict clinical protocols for this type of imaging for the sake of reproducibility and for valid, clinically

useful measures. Besides image acquisition parameters, other circumstances should be considered, such as fixing the patient's leg with special equipment (footrest) to minimize motion artifacts, which may distort results and may not be eliminated by image registration algorithms. Nevertheless, perhaps the most severe problem is that good quality color-coded images require repeated longer acquisitions with higher frame rates (4 FPS and above) in order to obtain good time resolution and a clear picture on the hemodynamic conditions. This is a very significant radiation burden for the patients and for the medical staff as well.

**Clinical significance.** The recently developed DVA technology provides higher CNR and better image quality than DSA [20–26], and this quality advantage can be used for dose management. DVA allowed for the reduction in the dose/frame parameter by 70%, which resulted in a more than 60% reduction in the DSA-related DAP values without compromising the image quality of angiograms [27,28]. As the ccDVA technology proved to be a reliable substitute for the currently available DSA-based parametric imaging, it could solve the problem of high radiation burdens through its dose management capability and could help in the wide-spread use of color-coded parametric imaging.

**Limitations.** The study involved a relatively low number of patients. Nevertheless, the larger number of measurement points increased the power of calculation and was sufficient to reach a solid conclusion. Another limitation is that we have tested only the time-related parameters. Both software can also calculate attenuation-related parameters, like the area under curve or the peak attenuation. Nevertheless, these parameters have arbitrary units and are less indicative when small ROIs are used (like in our case), which includes only a blood vessel cross section. The reliability of these parameters could be investigated in perfusion-type interventions, where the judgment of tissue blush or the arteriovenous phase is more important. Based on the current positive results, we plan to perform such studies in the field of prostatic artery embolization, uterine fibroid embolization, or cerebral imaging after thrombectomy.

## 5. Conclusions

Our data clearly show that the color-coded DVA technology can reproduce the same time-related parameters as the commercially available DSA-based color-coded parametric imaging; therefore, ccDVA can be a potential alternative in clinical practice. The previously described quality reserve of DVA might allow for a very significant reduction in the radiation dose applied during color-coded imaging, which might help to increase the use and significance of parametric imaging in endovascular intervention. However, the validation of these claims requires further prospective clinical studies.

**Author Contributions:** Conceptualization, I.G., P.S., J.P.K., K.S., S.O. and M.G.; methodology, I.G., B.N., K.S., S.O. and M.G.; software, K.S. and S.O.; validation, J.P.K. and M.G.; formal analysis, I.G. and J.P.K.; investigation, B.N. and M.G.; resources, B.N., P.S., K.S. and S.O.; data curation, I.G. and J.P.K.; writing—original draft preparation, I.G. and J.P.K.; writing—review and editing, P.S., K.S., S.O. and M.G.; visualization, I.G., J.P.K. and M.G.; supervision, P.S., J.P.K. and K.S.; project administration, B.N., K.S., and S.O.; funding acquisition, J.P.K., K.S. and S.O. All authors have read and agreed to the published version of the manuscript.

**Funding:** This project has received funding from the European Union's Horizon 2020 research and innovation program under grant agreement No 968430. The study was supported by the Ministry of Innovation and Technology of Hungary from the National Research, Development and Innovation Fund (2020-1.1.5-GYORSÍTÓSÁV-2021-00018 and KDP-14-3/PALY-2021, project No C1007109, recipient I.G).

**Institutional Review Board Statement:** The study was conducted in accordance with the Declaration of Helsinki and approved by the Institutional Review Board of the Semmelweis University (SE RKEB 161/2020, 30 July 2020).

**Informed Consent Statement:** Although this clinical investigation was a retrospective observational study, informed consent was obtained from all enrolled patients concerning their consent to a later use of anonymous acquisitions for research purposes.

**Data Availability Statement:** Study protocols, ethical approval documents, fully anonymized images, and TTP read-outs are available on request at the Heart and Vascular Center and at the head office of Kinepict Health Ltd.

**Conflicts of Interest:** I.G. and M.G. were part-time employees and K.S. was a full-time employee of Kinepict Health Ltd. until 2023. J.P.K. and S.O. are full-time employees of Kinepict Health Ltd. K.S. and S.O. hold stocks of Kinepict Health Ltd. P.S. and B.N. declare no potential conflicts of interest.

## References

1. Arnold, M.J.; Keung, J.J.; McCarragher, B. Interventional Radiology: Indications and Best Practices. *Am. Fam. Physician* **2019**, *99*, 547–556. [[PubMed](#)]
2. Jeans, W.D. The development and use of digital subtraction angiography. *Br. J. Radiol.* **1990**, *63*, 161–168. [[CrossRef](#)] [[PubMed](#)]
3. Haendle, H.; Haendle, J.; Maass, W.; Finkler, K. Digitale Subtraktionsangiographie mit dynamischen Farbfunktionsbildern [Digital subtraction angiography with dynamic color function images]. *Digit. Bilddiagn.* **1984**, *4*, 153–157.
4. Hunter, G.J.; Hunter, J.V.; Brown, N.J. Parametric imaging using digital subtraction angiography. *Br. J. Radiol.* **1986**, *59*, 7–11. [[CrossRef](#)] [[PubMed](#)]
5. Strother, C.M.; Bender, F.; Deuerling-Zheng, Y.; Royalty, K.; Pulfer, K.A.; Baumgart, J.; Zellerhoff, M.; Aagaard-Kienitz, B.; Niemann, D.B.; Lindstrom, M.L. Parametric color coding of digital subtraction angiography. *AJNR Am. J. Neuroradiol.* **2010**, *31*, 919–924. [[CrossRef](#)]
6. Jens, S.; Marquering, H.A.; Koelemay, M.J.; Reekers, J.A. Perfusion angiography of the foot in patients with critical limb ischemia: Description of the technique. *Cardiovasc. Interv. Radiol.* **2015**, *38*, 201–205. [[CrossRef](#)]
7. Wen, W.L.; Fang, Y.B.; Yang, P.F.; Zhang, Y.W.; Wu, Y.N.; Shen, H.; Ge, J.J.; Xu, Y.; Hong, B.; Huang, Q.H.; et al. Parametric Digital Subtraction Angiography Imaging for the Objective Grading of Collateral Flow in Acute Middle Cerebral Artery Occlusion. *World Neurosurg.* **2016**, *88*, 119–125. [[CrossRef](#)]
8. Gölitz, P.; Muehlen, I.; Gerner, S.T.; Knossalla, F.; Doerfler, A. Ultraearly assessed reperfusion status after middle cerebral artery recanalization predicting clinical outcome. *Acta Neurol. Scand.* **2018**, *137*, 609–617. [[CrossRef](#)]
9. Gölitz, P.; Struffert, T.; Lücking, H.; Rösch, J.; Knossalla, F.; Ganslandt, O.; Deuerling-Zheng, Y.; Doerfler, A. Parametric color coding of digital subtraction angiography in the evaluation of carotid cavernous fistulas. *Clin. Neuroradiol.* **2013**, *23*, 113–120. [[CrossRef](#)]
10. Kostrzewa, M.; Kara, K.; Pilz, L.; Mueller-Muertz, H.; Rathmann, N.; Schoenberg, S.O.; Diehl, S.J. Treatment Evaluation of Flow-Limiting Stenoses of the Superficial Femoral and Popliteal Artery by Parametric Color-Coding Analysis of Digital Subtraction Angiography Series. *Cardiovasc. Interv. Radiol.* **2017**, *40*, 1147–1154. [[CrossRef](#)]
11. Ng, J.J.; Papadimas, E.; Dharmaraj, R.B. Assessment of Flow after Lower Extremity Endovascular Revascularisation: A Feasibility Study Using Time Attenuation Curve Analysis of Digital Subtraction Angiography. *EJVES Short. Rep.* **2019**, *45*, 1–6. [[CrossRef](#)] [[PubMed](#)]
12. Tinelli, G.; Minelli, F.; De Nigris, F.; Vincenzoni, C.; Filipponi, M.; Bruno, P.; Massetti, M.; Flex, A.; Iezzi, R. The potential role of quantitative digital subtraction angiography in evaluating type B chronic aortic dissection during TEVAR: Preliminary results. *Eur. Rev. Med. Pharmacol. Sci.* **2018**, *22*, 516–522. [[PubMed](#)]
13. Chen, Y.; Xu, W.; Liu, J.; Zhao, C.; Cao, X.; Wang, R.; Feng, D.; Zhang, R.; Zhou, X. Color-coded parametric imaging support display of vessel hemorrhage—an in vitro experiment and clinical validation study. *Front. Cardiovasc. Med.* **2024**, *11*, 1387421. [[CrossRef](#)] [[PubMed](#)]
14. Badar, W.; Anitescu, M.; Ross, B.; Wallace, S.; Uy-Palmer, R.; Ahmed, O. Quantifying Change in Perfusion after Genicular Artery Embolization with Parametric Analysis of Intraoperative Digital Subtraction Angiograms. *J. Vasc. Interv. Radiol.* **2023**, *34*, 2190–2196. [[CrossRef](#)] [[PubMed](#)]
15. Meine, T.C.; Maschke, S.K.; Kirstein, M.M.; Jaekel, E.; Lena, B.S.; Werncke, T.; Dewald, C.L.A.; Wacker, F.K.; Meyer, B.C.; Hinrichs, J.B. Evaluation of perfusion changes using a 2D Parametric Parenchymal Blood Flow technique with automated vessel suppression following partial spleen embolization in patients with hypersplenism and portal hypertension. *Medicine* **2021**, *100*, e24783. [[CrossRef](#)]
16. Rivera, R.; Sordo, J.G.; Echeverria, D.; Badilla, L.; Pinto, C.; Merino-Osorio, C. Quantitative evaluation of arteriovenous malformation hemodynamic changes after endovascular treatment using parametric color coding: A case series study. *Interv. Neuroradiol.* **2017**, *23*, 650–655. [[CrossRef](#)]
17. Gölitz, P.; Struffert, T.; Rösch, J.; Ganslandt, O.; Knossalla, F.; Doerfler, A. Cerebral aneurysm treatment using flow-diverting stents: In-vivo visualization of flow alterations by parametric colour coding to predict aneurysmal occlusion: Preliminary results. *Eur. Radiol.* **2015**, *25*, 428–435. [[CrossRef](#)]
18. Hussein, A.E.; Shownkeen, M.; Thomas, A.; Stapleton, C.; Brunozzi, D.; Nelson, J.; Naumgart, J.; Linninger, A.; Atwal, G.; Alaraj, A. 2D parametric contrast time-density analysis for the prediction of complete aneurysm occlusion at six months' post-flow diversion stent. *Interv. Neuroradiol.* **2020**, *26*, 468–475. [[CrossRef](#)]
19. Szigeti, K.; Mathe, D.; Osvath, S. Motion based X-ray imaging modality. *IEEE Trans. Med. Imaging* **2014**, *33*, 2031–2038. [[CrossRef](#)]

20. Gyánó, M.; Góg, I.; Óriás, V.I.; Ruzsa, Z.; Nemes, B.; Csobay-Novák, C.; Oláh, Z.; Nagy, Z.; Merkely, B.; Szigeti, K.; et al. Kinetic imaging in lower extremity arteriography: Comparison to digital subtraction angiography. *Radiology* **2019**, *290*, 246–253. [[CrossRef](#)]
21. Óriás, V.I.; Gyánó, M.; Góg, I.; Szöllősi, D.; Veres, D.S.; Nagy, Z.; Csobay-Novák, C.; Zoltán, O.; Kiss, J.P.; Osváth, S.; et al. Digital Variance Angiography as a Paradigm Shift in Carbon Dioxide Angiography. *Investig. Radiol.* **2019**, *54*, 428–436. [[CrossRef](#)] [[PubMed](#)]
22. Bastian, M.B.; König, A.M.; Viniol, S.; Gyánó, M.; Szöllősi, D.; Góg, I.; Kiss, J.P.; Osvath, S.; Szigeti, K.; Mahnken, A.H.; et al. Digital Variance Angiography in Lower-Limb Angiography with Metal Implants. *Cardiovasc. Interv. Radiol.* **2021**, *44*, 452–459. [[CrossRef](#)] [[PubMed](#)]
23. Thomas, R.P.; Bastian, M.B.; Viniol, S.; König, A.M.; Amin, S.S.; Eldergash, O.; Schnabel, J.; Gyánó, M.; Szöllősi, D.; Góg, I.; et al. Digital variance angiography in selective lower limb interventions. *J. Vasc. Interv. Radiol.* **2022**, *33*, 104–112. [[CrossRef](#)] [[PubMed](#)]
24. Óriás, V.I.; Szöllősi, D.; Gyánó, M.; Veres, D.S.; Nardai, S.; Csobay-Novák, C.; Nemes, B.; Kiss, J.P.; Szigeti, K.; Osváth, S.; et al. Initial evidence of a 50% reduction of contrast media using digital variance angiography in endovascular carotid interventions. *Eur. J. Radiol. Open* **2020**, *7*, 100288. [[CrossRef](#)] [[PubMed](#)]
25. Alizadeh, L.S.; Gyánó, M.; Góg, I.; Szigeti, K.; Osváth, S.; Kiss, J.P.; Yel, I.; Koch, V.; Grünwald, L.D.; Vogl, T.J.; et al. Initial experience using Digital Variance Angiography in context of Prostatic Artery Embolization in comparison with Digital Subtraction Angiography. *Acad. Radiol.* **2022**, *30*, 689–697. [[CrossRef](#)]
26. Lucatelli, P.; Rocco, B.; Ciaglia, S.; Teodoli, L.; Argirò, R.; Guiu, B.; Saba, L.; Vallati, G.; Spiliopoulos, S.; Patrone, L.; et al. Possible use of digital variance angiography in liver transarterial chemoembolization: A retrospective observational study. *Cardiovasc. Interv. Radiol.* **2023**, *46*, 635–642. [[CrossRef](#)]
27. Gyánó, M.; Berczeli, M.; Csobay-Novák, C.; Szöllősi, D.; Óriás, V.I.; Góg, I.; Kiss, J.P.; Veres, D.S.; Szigeti, K.; Osváth, S.; et al. Digital variance angiography allows about 70% decrease of DSA-related radiation exposure in lower limb X-ray angiography. *Sci. Rep.* **2021**, *11*, 21790. [[CrossRef](#)]
28. Sóttonyi, P.; Berczeli, M.; Gyánó, M.; Legeza, P.; Mihály, Z.; Csobay-Novák, C.; Pataki, Á.; Juhász, V.; Góg, I.; Szigeti, K.; et al. Radiation Exposure Reduction by Digital Variance Angiography in Lower Limb Angiography: A Randomized Controlled Trial. *J. Cardiovasc. Dev. Dis.* **2023**, *10*, 198. [[CrossRef](#)]

**Disclaimer/Publisher’s Note:** The statements, opinions and data contained in all publications are solely those of the individual author(s) and contributor(s) and not of MDPI and/or the editor(s). MDPI and/or the editor(s) disclaim responsibility for any injury to people or property resulting from any ideas, methods, instructions or products referred to in the content.